^{1}H NMR spectroscopic determination of deterioration marker compounds in fats and oils

Dissertation zur Erlangung des

naturwissenschaftlichen Doktorgrades

der Julius-Maximilians-Universität Würzburg

vorgelegt von

Christina Skiera

aus Karlsruhe

Würzburg 2013

Eingereicht am: 11.09.2013
bei der Fakultät für Chemie und Pharmazie

1. Gutachter: Frau Prof. Dr. Holzgrabe
2. Gutachter: Frau Prof. Dr. Wawer
der Dissertation

1. Prüfer: Frau Prof. Dr. Ulrike Holzgrabe
2. Prüfer: Frau Prof. Dr. Iwona Wawer
3. Prüfer: Herr Prof. Dr. Oliver Germershaus
des Öffentlichen Promotionskolloquiums

Tag des Öffentlichen Promotionskolloquiums: 18.12.2013

Doktorurkunde ausgehändigt am: .....

Der praktische Teil meiner Arbeit wurde im Zeitraum April 2010 bis November 2012 am Chemischen und Veterinäruntersuchungsamt (CVUA) Karlsruhe durchgeführt mit vorangegangener dreiwöchiger Einarbeitsphase in die NMR-Technik durch Herrn Dr. Bernd Diehl bei Spektral Service (Köln). Die Themenstellung erfolgte von Dr. Bernd Diehl in Kooperation mit dem CVUA Karlsruhe und Frau Prof. Dr. Holzgrabe.

Mein besonderer Dank gilt meiner Doktormutter, Frau Prof. Dr. Holzgrabe, für ihr Interesse an meiner Arbeit und den wertvollen Anregungen und Ratschlägen und immer sehr zeitnahen Korrekturen.

Bei Herrn Dr. Bernd Diehl möchte ich mich ganz herzlich bedanken für die Einführung in die Welt der NMR, für die vielen Ideen und Diskussion und für die Möglichkeit der Teilnahme am internationalen AOCS-Kongress 2011 in Cincinnati. Auch bei seiner Frau Dr. Gabriele Randel und den Mitarbeitern von Spektral Service möchte ich mich für ihre Hilfsbereitschaft und die freundliche Aufnahme bedanken.

Dem CVUA Karlsruhe danke ich für die Ermöglichung der Promotion, Herrn Dr. Kuballa für die Betreuung der Arbeit und den Mitarbeitern des CVUA Karlsruhe für das gute Arbeitsklima für die Unterstützung und Hilfe bei praktischen und verwaltungstechnischen Angelegenheiten. Hervorheben möchte ich besonders Margit Boehm, Jürgen Geiser und Bernd Siebler, die mich bei den unterschiedlichsten praktischen Fragestellungen tatkräftig unterstützt haben.

Ganz besonders danke ich meinem Kollegen Dr. Panagiotis Steliopoulos für die zahlreichen fruchtbaren wissenschaftlichen und sonstigen Diskussionen, für das Korrekturlesen meiner Arbeit, für sein stets offenes Ohr und dass ich von ihm so viel lernen durfte!

Meinem Mann und meiner Familie danke ich für ihre seelische und moralische Unterstützung und meinem Mann für sein Verständnis und seine Engelsgedult.

Publications, posters and oral presentations

Skiera C, Steliopoulos P, Kuballa T, Holzgrabe U, Diehl B (2012)
^{1}H NMR spectroscopy as a new tool in the assessment of the oxidative state in edible oils. *J Am Oil Chem Soc* 89(8): 1383–1391

parts of this publication are contained in chapter 3

Skiera C, Steliopoulos P, Kuballa T, Holzgrabe U, Diehl B (2012)
^{1}H NMR approach as an alternative to the classical p-anisidine value method. *Eur Food Res Technol* 235(6): 1101–1105

parts of this publication are contained in chapter 5

Skiera C, Steliopoulos P, Kuballa T, Holzgrabe U, Diehl B (2012)
Determination of free fatty acids in edible oils by ^{1}H NMR spectroscopy. *Lipid Technol* 24(12): 279–281

parts of this publication are contained in chapter 4

Skiera C, Steliopoulos P, Kuballa T, Diehl B, Holzgrabe U (2013)
Determination of free fatty acids in pharmaceutical lipids by ^{1}H NMR and comparison with the classical acid value. *JPBA*
http://dx.doi.org/10.1016/j.jpba.2013.04.010 -

parts of this publication are contained in chapter 4

Skiera C, Steliopoulos P, Holzgrabe U, Diehl B (2011)
Assessment of the performance of an NMR assay for the determination of hydroperoxides in lipids, in: Renou J-P, Belton PS, Webb GA (ed.) Magnetic resonance in food science – An exciting future, RSC Publishing, Cambridge, *proceedings* of the 10th International conference on the application of magnetic resonance in food science in September 13 – 15, 2010, Clermont-Ferrand

Skiera C, Steliopoulos P, Kuballa T, Holzgrabe U, Diehl B (2011)
^{1}H NMR method to determine the hydroperoxide amount of edible oils, *oral presentation* at the 102nd AOCS Annual Meeting & Expo (Session: PHO 3.1: Symposium on NMR in lipids) in May 1 – 4, 2011, Cincinnati

Skiera C, Kuballa T, Holzgrabe U, Diehl B (2011)
Vergleich eines neu entwickelten ^{1}H-NMR Verfahrens zur Bestimmung von Hydroperoxiden mit der klassischen POZ-Methode nach Wheeler, *poster contribution* at the 40. Deutscher Lebensmittelchemikertag in Septermber 12 – 14, 2011, Halle

Skiera C, Steliopoulos P, Kuballa T, Holzgrabe U, Diehl B (2012)
^{1}H NMR approach as an alternative to the classical p-anisidine value method, *poster contribution* at the 11th International conference on the applications of magnetic resonance in food science in June 26 - 29, 2012, Wageningen

Skiera C, Steliopoulos P, Kuballa T, Holzgrabe U, Diehl B (2012)
Bestimmung von freien Fettsäuren in Speiseölen mittels ^{1}H-NMR, *poster contribution* at the 41. Deutscher Lebensmittelchemikertag in September 10 – 12, 2012, Münster

Skiera C, Steliopoulos P, Kuballa T, Holzgrabe U, Diehl B (2013)
Untersuchung der bei der Autoxidation von Trioleat gebildeten Monohydroperoxide mittels ^{1}H-NMR Spektroskopie, *poster contribution* at the 42. Deutscher Lebensmittelchemikertag in September 16 – 18, 2013, Braunschweig

Diehl B, Skiera C (2013)
Nuclear Magnetic Resonance (NMR)-Spektroskopie, in Matthäus B, Fiebig H-J (ed.), Speiseöle und –fette, Recht, Sensorik, Analytik, Erling Verlag

Table of contents

1. Introduction 1

1.1 Fats and oils 1

1.2 Quality assessment of fats and oils 3

1.3 Lipid oxidation 6

1.3.1 Formation of primary oxidation products 7

1.3.2 Formation of secondary oxidation products 10

1.4 NMR spectroscopy 11

1.4.1 Principles of NMR 11

1.4.2 Quantitative ^{1}H NMR 14

1.4.3 NMR methods to determine lipid oxidation products 15

2. Aims of thesis 17

3. ^{1}H NMR determination of hydroperoxides 18

3.1 Method development 18

3.2 Hydroperoxide assignment 23

3.3 Hydroperoxides of TAGs 26

3.3.1 Oxidation kinetics of trioleate 28

3.4 Comparison with the classical *PV* 31

3.4.1 Deming regression and relative sensitivity 32

3.4.2 Examination of 444 oil samples 35

3.4.3 Deviations of black seed oil and olive oil 37

4. ^{1}H NMR determination of free fatty acids 40

4.1 Method development 40

4.2 Comparison with the classical *AV* 41

4.3 Specialities of some pharmaceutical lipids 44

4.4 Saponification value 49

5. ^{1}H NMR determination of aldehydes 50

5.1 Method development 50

5.2 Model to determine ANV_{NMR} 52

5.3 Verification of the model 56

6. Conclusion 57

7. Experimental 59
7.1 Material 59
7.1.1 Apparatus 59
7.1.2 Consumables 59
7.1.3 *Samples, standards and chemicals* 60
7.2 Methods 61
7.2.1 Standard NMR experiment 61
7.2.2 Inversion recovery experiment 61
7.2.3 Sample preparation procedures 63
7.2.4 Classical fat indices 63
7.2.5 Sample oxidation 63
7.2.6 Oxidation kinetics of trioleate 64
7.2.7 Water steam distillation 64
8. Statistical data evaluation 65
8.1 Exponential curve fitting 65
8.2 Confidence intervals for *AV* 65
8.3 Confidence intervals for AV_{NMR} 66
8.4 Confidence intervals for *ANV* 67
8.5 Confidence intervals for α_j and ANV_{NMR} 68
9. Summary 69
10. Zusammenfassung 71
11. Raw data and spectra 73
11.1 Raw data of chapter 3 73
11.2 Raw data of chapter 4 80
11.3 Raw data of chapter 5 86
11.4 ^{1}H NMR spectra of fats and oils 92

List of figures 104
List of tables 106
List of abbreviations 107
List of variables 108
References 109

1. Introduction

1.1 Fats and oils

Fats and oils are obtained from fruits, seeds and germs of plants or from suitable fat tissues of animals. Depending on the extraction and processing of the crude oil, we can differentiate refined, cold-pressed and virgin fats and oils. The refining process, including several steps such as degumming, neutralization, bleaching, winterization and deodorization, removes undesirable impurities that are deleterious to the final product (Belitz et al. 2008). According to the Codex alimentarius standard for edible oils and fats, virgin fats and oils are „obtained, without altering the oil, by mechanical procedures, e.g. expelling or pressing, and the application of heat only. They may be purified by washing with water, settling, filtering and centrifuging only“ (Codex Stan 19-1981). The same definition holds for cold-pressed fats and oils with the difference that no thermal treatment is applied.

Chemically, fats and oils consist almost exclusively of triacylglycerols (TAGs), the esters of glycerol and three fatty acid molecules (see figure 1). Fatty acids are aliphatic, usually straight-chain, monocarboxylic acids. Most natural fatty acids have even chain length between C4 and C22. Commonly, in vegetable oils only five fatty acids occur widely in higher amounts: palmitic, stearic, oleic, linoleic and linolenic acid (Belitz et al. 2008).

TAGs with two different fatty acids esterified with the primary hydroxyl groups of glycerol exhibit a chiral centre. Therefore, we can differentiate three distinct non-equivalent attachment sites for fatty acids, called *sn*-1, *sn*-2 and *sn*-3 (*sn* stands for stereospecific numbering) (Belitz et al. 2008).

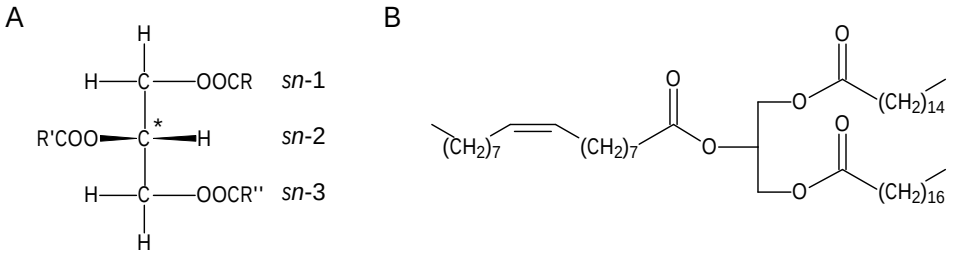

Fig. 1: Structure of A) a TAG in Fischer projection and B) 1-palmitoyl-2-oleyl-3-stearyl-glycerol.

Besides TAGs, about 2 – 5 % minor components are present in vegetable fats and oils. They can be classified into two groups: glycerolipids and non-glycerolipids, also referred to as unsaponifiable matter. Table 1 lists important representatives of both groups (Kamal-Eldin 2005).

Tab. 1 Minor components of fats and oils.

Glycerolipids	Non-Glycerolipids
Diacylglycerols	Sterols
Monoacylglycerols	Tocopherols/tocotrienols
Phospholipids	Triterpene alcohols and their esters
Glycolipids	Hydrocarbons
	Waxes
	Free fatty acids
	Lipid-soluble vitamins
	Pigments
	Phenolic compounds
	Metals and metalloproteins

Fats and oils play a major role in human nutrition. TAGs exhibit a high caloric value (9 kcal/g) that exceeds more than twice the caloric value of carbohydrates and proteins (4 kcal/g). Furthermore, fats and oils are carriers of fat-soluble vitamins and a source of essential fatty acids. In fat-containing food products, lipids strongly affect texture, flavour, mouthfeel and the oxidative stability. The predominant share (about three-quarters) of fats and oils produced by agriculture are used for human food. In addition, fats and oils are important raw materials for the production of animal feed, cosmetics, soap, biodiesel, lubricants, greases and pharmaceuticals (Belitz et al. 2008, Bockisch 2004).

In pharmacy, fats and oils are often used as excipients for lipophilic active ingredients for local, peroral, subcutaneous and intramuscular applications (e.g. ointments, emulsions, plasters, liniments, tablets, suppositories and injection solutions). Specific plant oils like soya oil and olive oil have relevance in dietetic products and for clinical parenteral feeding. In addition, some pharmaceuticals contain plant oils as active ingredience, such as laxatives (castor oil) or bath additives against neurodermatitis (soya oil) (Bracher et al. 2012, Krist et al. 2008). Further lipids being of importance in galenics are waxes, the esters of different fatty acids and long-chain alcohols of similar chain length.

1.2 Quality assessment of fats and oils

The first analytical methods to assess quality and authenticity of fats and oils were so-called empirical methods and were based on volumetric and UV/VIS spectroscopic techniques. An empirical method is a method agreed upon for the purpose of comparative determination where the method itself defines the analytical quantity, i.e. the bias associated with the method is per definition zero (Ellison & Williams 2012). These empirical methods were developed and standardized several decades ago and have only undergone minor changes since then.

Important quality indices for fats and oils are the peroxide value (*PV*), the anisidine value (*ANV*), the acid value (*AV*), the saponification value (*SV*), the iodine value (*IV*), the hydroxyl value (*HV*) and the unsaponificable matter (*USM*). In routine, some of these classical parameters are still widely used. Their disadvantages are the high consumption of solvents and other toxic chemicals and especially the poor specificity (Kamal-Eldin & Pocorny 2005, Shahidi & Zhong 2005).

PV: The *PV* according to Wheeler is a measure of the content of hydroperoxides in fats and oils. The *PV* being expressed in milliequivalents of active oxygen per kilogram (meq/kg) covers all compounds that oxidize potassium iodide under certain defined conditions (ISO 3960:2007).

ANV: The *ANV* is routinely used as an indicator of aldehydes which are secondary oxidation products. The *ANV* determination is based on the chemical reaction between the carbonyl group and p-anisidine. The reaction product is an intensively coloured Schiff base which is measured UV/VIS spectroscopically at λ = 350 nm (ISO 6885:2006).

TOTOX: The *TOTOX* (= Total oxidation products) value is a combination of *PV* and *ANV*. It is defined as the sum of twice the *PV* plus the *ANV*: $TOTOX = 2PV + ANV$. It was introduced to provide a better estimation of the overall quality status of fats and oils (Shahidi & Zhong 2005).

AV: The *AV* represents the free fatty acid (FFA) amount in lipids in mg KOH/g oil. The *AV* is based on the titration with a methanolic potassium hydroxide solution versus phenolphthalein as an endpoint indicator (ISO 660:2009).

SV: The *SV* is determined titrimetrically after saponification and comprises free and bound fatty acids (ISO 3657:2002). The *SV* is a measure for the average chain length of a fat or oil and directly correlates with the average molecular weight of lipids: The smaller the average molecular weight, the greater the *SV* (Ph. Eur. 2011).

IV: The iodine value is defined as the quantity of halogen (expressed as grams iodine) that can be fixed under defined conditions by 100 g of the fat or oil. The method is based on the reaction of the double bonds in the sample with an excess of an iodine-containing reagent, e.g. iodine monobromide with subsequent iodometric titration of the remaining iodine monobromide. The *IV* is a measure of the degree of unsaturation of fats and oils. The higher the *IV*, the more olefinic double bonds are present in the fat or oil. (Ph. Eur. 2011)

HV: The hydroxyl value is a measure of the content of free hydroxyl groups in the sample. It is expressed as the mass of potassium hydroxide (in milligrams) equivalent to the hydroxyl content of one gram of the fat or oil, corrected for carboxyl hydroxyl groups. The method detects hydroxy fatty acids, fatty alcohols, mono- and diglycerides as well as free glycerol. It involves acetylation of the free hydroxyl groups in the sample with acetic anhydride in pyridine solvent and the volumetric determination of the remaining acetic anhydride converted to acetic acid by aqueous hydrolysis (Ph. Eur. 2011).

USM: The term “unsaponifiable matter” defines the substances non-volatile at 100 – 105 °C obtained by extraction with an organic solvent from the fat or oil after it has been saponified. It is expressed in per cent (m/m) (Ph. Eur. 2011). The *USM* gives a general indication of identity and purity of the fat or oil sample. Generally, the *USM* of fats and oils lies in the range from 0.2 % to 3 %. Waxes have considerable higher *USM* values since the method covers fatty alcohols that arise from saponification of waxes (Bracher et al. 2012).

The quality indices *PV*, *AV* and *ANV* play an important role in the assessment of lipid deterioration in official food control of edible fats and oils. At international level, the Codex Alimentarius Standard for edible fats and oils lays down maximum values of *PV* and *AV.* For refined oils *PV* and *AV* may not exceed 10 meq/kg and 0.6 mg/g and for virgin or cold-pressed oils 15

meq/kg and 4 mg/g, respectively (Codex Stan 19-1981). In Europe, except for olive oils, no uniform legislation for quality requirements of edible fats and oils exists. In Germany, legal assessment of edible fats and oils is based on a guideline jointly defined by representatives of industry, science, official food control and consumer protection (LS Speisefette 2001). It is not legally binding, but deviations from it require explanation of the producer. The requirements given by these guidelines are listed in table 2.

Tab. 2 Quality requirements of the German guidelines for edible fats and oils.

	Refined fats and oils	Virgin fats and oils
PV / meq active oxygen/kg oil	5	10
AV / mg KOH/g oil	0.6	4
TOTOX (only vegetable oils)	10	20

Legally binding demands on quality and authenticity of lipids used in pharmaceutical products are given in the European Pharmacopoeia (Ph. Eur.). The Ph. Eur. contains specific and general monographs of active substances and excipients used to prepare pharmaceutical products in Europe. Important quality and authenticity parameters regulated in the monographs of lipids include *AV*, *PV*, *SV, IV, HV* and *USM*. There are no general limits for these classical indices but every monograph gives individual limits. In the case of the quality indices *PV* and *AV,* for most fats and oils, the upper limits are similar to the *PVs* and *AVs* given in table 2 (Ph. Eur. 2011).

As an alternative to the classical indices *PV*, *ANV* and *AV*, different sophisticated instrumental techniques have been applied. These techniques include pH-metry (Tur'yan et al. 1996), chromatography, especially gas chromatography (Gray 1978, Wan et al. 2007, Liu et al. 1997), high performance liquid chromatography (Gladovič et al. 1997, Dobarganes & Velasco 2002), high performance size exclusion chromatography (Kamal-Eldin & Pokorny 2005), Raman spectroscopy (Muik et al. 2005) and FTIR spectroscopy (Shahidi & Zhong 2005, van de Voort et al. 1994, Dubois et al. 1996, Frankel 1991, Guillén & Cabo 2002). Generally, the results are in good accordance with the classical indices. However, up to now, none of them have become widely accepted.

1.3 Lipid oxidation

Fats and oils are susceptible to oxidative processes giving rise to the development of off-flavours and a decrease of the nutritional quality and safety. Autoxidation is the most important process leading to oxidative deterioration. It is based on the spontaneous reaction of atmospheric oxygen with lipids under mild conditions via a radical chain reaction. Within the course of the autoxidation process of lipids, hydroperoxides are formed as primary products that are easily decomposed to secondary products such as aldehydes, ketones, alcohols and acids (Frankel 1998).

The autoxidation process is subdivided into three major phases: initiation, propagation and termination. A simplified scheme of the mechanism is given in figure 2. The initial step of autoxidation is the abstraction of a hydrogen radical ($H^{\cdot}$) from an unsaturated fatty acid (RH) by means of an initiator. The main initiators in fats and oils are radicals formed by the metal-catalysed decomposition of hydroperoxides present as impurities. The propagation phase begins with the addition of molecular oxygen to the alkyl radical ($R^{\cdot}$) (fast reaction). Subsequently, the peroxyl radical ($ROO^{\cdot}$) abstracts a hydrogen atom from another fatty acid (RH) to form a hydroperoxide (ROOH). One single radical can generate about 100 hydroperoxides before chain termination occurs. At atmospheric oxygen pressure the main termination reaction is the combination of two peroxyl radicals leading to an unstable tetroxide intermediate which is rapidly decomposed by the Russell mechanism to produce a ketone, an alcohol and oxygen (Frankel 1998, Russell 1957). At low oxygen pressure termination reactions of alkoxy and alkyl radicals can occur (see figure 2).

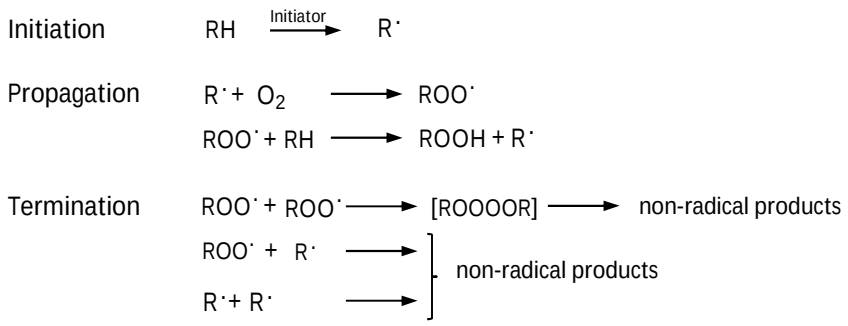

Fig. 2: Scheme of the mechanism of autoxidation.

The second propagation reaction is the rate-limiting step for the hydroperoxide formation. Since the peroxyl radical is relatively stable and thus not very reactive, it selectively abstracts the most weakly bound hydrogen. Therefore, the susceptibility of fatty acids to autoxidation strongly depends

Tab. 3 Dissociation energies of hydrogen atoms (Belitz et al. 2008).

	D_{R-H} (kJ/mol)
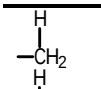	422
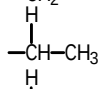	410
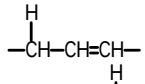	322
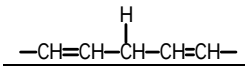	272

on the strength of the CH-bonds. The dissociation energies of different hydrogen atom species, present in fatty acids, are listed in table 3. The dissociation energy of allylic hydrogens is approximately 50 kJ/mol greater than the dissociation energy of bis-allylic hydrogens and 90 kJ/mol smaller than the dissociation energy of hydrogens of saturated fatty acids. These differences explain the divergent oxidation rates of saturated, monounsaturated and polyunsaturated fatty acids at room temperature (Belitz et al. 2008).

1.3.1 Formation of primary oxidation products

The general mechanism depicted in figure 2 holds for autoxidation of all unsaturated fatty acids. In case of oleic acid, the abstraction of the hydrogens at C8 and C11, which are the most weakly bound hydrogens, produces two different three-carbon allylic radicals. Oxygen attack at the end-carbon position of these intermediates leads to the formation of a mixture of 8-, 9-, 10- and 11-hydroperoxides (see figure 3). The stereochemical configuration of the double bond and the proportion of the hydroperoxide species are influenced by kinetic and thermodynamic factors. At room temperature, of the possible eight (*Z*) and (*E*) isomers of methyl oleate hydroperoxides, only six isomers occur in significant amounts (see table 4).

In comparison to oleate, linoleate is 40 times more reactive (Holman & Elmer 1947) being attributed to greater resonance stabilization of the pentadienyl radical intermediate and a high stability of the resulting (*Z*,*E*) and (*E*,*E*) conjugated dienic 9- and 13-hydroperoxides (see figure 3 and table 4). The bis-allylic 11-hydroperoxide is not found, since the relatively unstable bis-allylic peroxyl radical rapidly fragments and re-adds molecular oxygen to form the thermodynamically more stable conjugated diene hydroperoxides. However, it was shown that the 11-hydroperoxide was formed as minor component in the presence of 5 % α-tocopherol (Brash 2000).

Methyl linolenate has two bis-allylic methylene groups and reacts twice as fast as methyl linoleate. Hydrogen abstraction on the two bis-allylic pro-

tons at C11 and C14 (same mechanism as of linoleate) leads to two different pentadienyl radicals. These intermediates react with oxygen to 9-, 12-, 13- and 16-hydroperoxides (see figure 3). For every positional isomer two geometrical isomers are formed, one with the conjugated double bonds in (*E*,*E*) and one in (*Z*,*E*) configuration. Under mild oxidation conditions (25 °C, darkness) the (*Z*,*E*) isomers are formed in significantly higher proportions than the (*E*,*E*) isomers (Chan & Levett 1977b, Fishwick & Swoboda 1977). The amount of 12- and 13-hydroperoxides is about four times smaller than that of 9- and 16-hydroperoxides (see table 4). This can be explained by the tendency of the 12- and 13-peroxyl radicals to undergo either rapid 1,3-cyclization into prostaglandin-like endoperoxides or 1,5-cyclization into two 9- and 16-bicycloendoperoxides (Frankel 1998).

Tab. 4 Proportions of hydroperoxide species of a) methyl oleate, b) methyl linoleate and c) methyl linolenate from autoxidation at 25 °C.

Hydroperoxide species	Shortcut	Prop. / % of total
8-Hydroperoxy-(*Z*)-9-octadecenoate	(*Z*)-8-OOH	14
8-Hydroperoxy-(*E*)-9-octadecenoate	(*E*)-8-OOH	12
9-Hydroperoxy-(*Z*)-10-octadecenoate	(*Z*)-9-OOH	1
9-Hydroperoxy-(*E*)-10-octadecenoate	(*E*)-9-OOH	23
10-Hydroperoxy-(*Z*)-8-octadecenoate	(*Z*)-10-OOH	1
10-Hydroperoxy-(*E*)-8-octadecenoate	(*E*)-10-OOH	22
11-Hydroperoxy-(*Z*)-9-octadecenoate	(*Z*)-11-OOH	14
11-Hydroperoxy-(*E*)-9-octadecenoate	(*E*)-11-OOH	13
9-Hydroperoxy-(*E*)-10-(*Z*)-12-octadecadienoate	(*Z*,*E*)-9-OOH	30
9-Hydroperoxy-(*E*)-10-(*E*)-12-octadecadienoate	(*E*,*E*)-9-OOH	19
13-Hydroperoxy-(*Z*)-9-(*E*)-11-octadecadienoate	(*Z*,*E*)-13-OOH	31
13-Hydroperoxy-(*E*)-9-(*E*)-11-octadecadienoate	(*E*,*E*)-13-OOH	20
9-Hydroperoxy-(*E*)-10-(*Z*)-12-(*Z*)-15-octadecatrienoate	(*E*,*Z*,*Z*)-9-OOH	31
9-Hydroperoxy-(*E*)-10-(*E*)-12-(*Z*)-15-octadecatrienoate	(*E*,*E*,*Z*)-9-OOH	
12-Hydroperoxy-(*Z*)-9-(*E*)-13-(*Z*)-15-octadecatrienoate	(*Z*,*E*,*Z*)-12-OOH	10
12-Hydroperoxy-(*Z*)-9-(*E*)-13-(*E*)-15-octadecatrienoate	(*Z*,*E*,*E*)-12-OOH	
13-Hydroperoxy-(*Z*)-9-(*E*)-11-(*Z*)-15-octadecatrienoate	(*Z*,*E*,*Z*)-13-OOH	11
13-Hydroperoxy-(*E*)-9-(*E*)-11-(*Z*)-15-octadecatrienoate	(*E*,*E*,*Z*)-13-OOH	
16-Hydroperoxy-(*Z*)-9-(Z)-12-(*E*)-14-octadecatrienoate	(*Z*,*Z*,*E*)-16-OOH	49
16-Hydroperoxy-(*Z*)-9-(*E*)-12-(*E*)-14-octadecatrienoate	(*Z*,*E*,*E*)-16-OOH	

[a)] Methyl oleate hydroperoxides by GC-MS and ^{13}C NMR (Frankel et al. 1984)
[b)] Methyl linoleate hydroperoxides by HPLC and ^{13}C NMR (Frankel et al. 1990b)
[c)] Methyl linolenate hydroperoxides by GC-MS (Frankel et al. 1977)

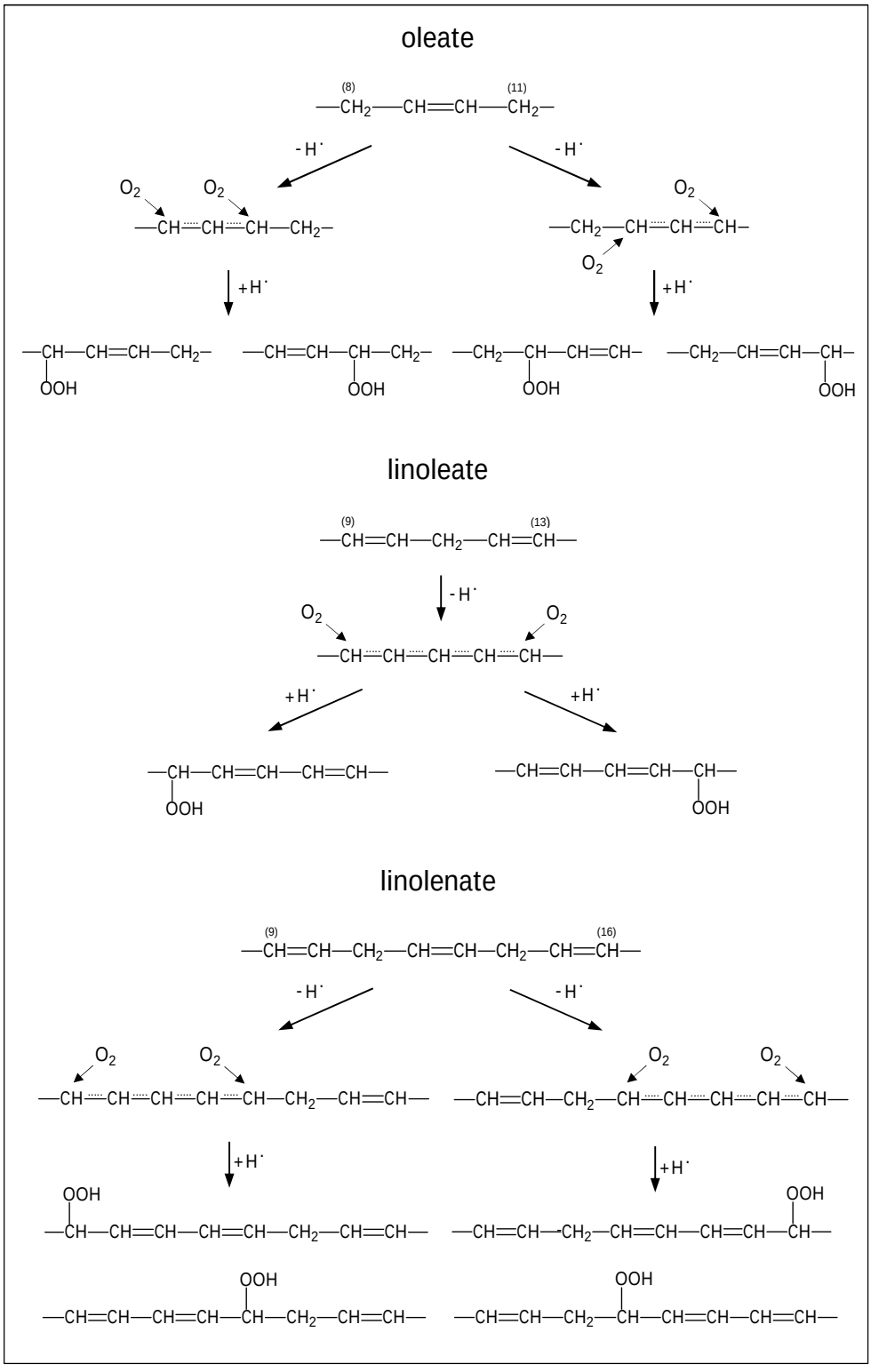

Fig. 3: Autoxidation mechanism of oleic, linoleic and linolenic acid (Frankel 1998).

1.3.2 Formation of secondary oxidation products

The radical chain mechanism depicted in figure 2 is valid only for the early stage of autoxidation. With increasing reaction time, the process becomes more and more complicated since hydroperoxides undergo further reactions forming volatile and non-volatile secondary products.

Volatile oxidation products affecting flavour deterioration include aldehydes, ketones, alcohols and hydrocarbons. The classical mechanism explaining the main volatile decomposition products of the model compounds oleate, linoleate and linolenate is depicted in figure 4. The homolytic cleavage of unsaturated hydroperoxides to alkoxy radicals is followed by homolytic β-scission to form aldehydes, alkyl and olefinic radicals. Alkyl radicals and olefinic radicals undergo further reactions to hydrocarbons, alcohols or primary hydroperoxides and olefins or saturated aldehydes (via 1-enols), respectively (Frankel 1998).

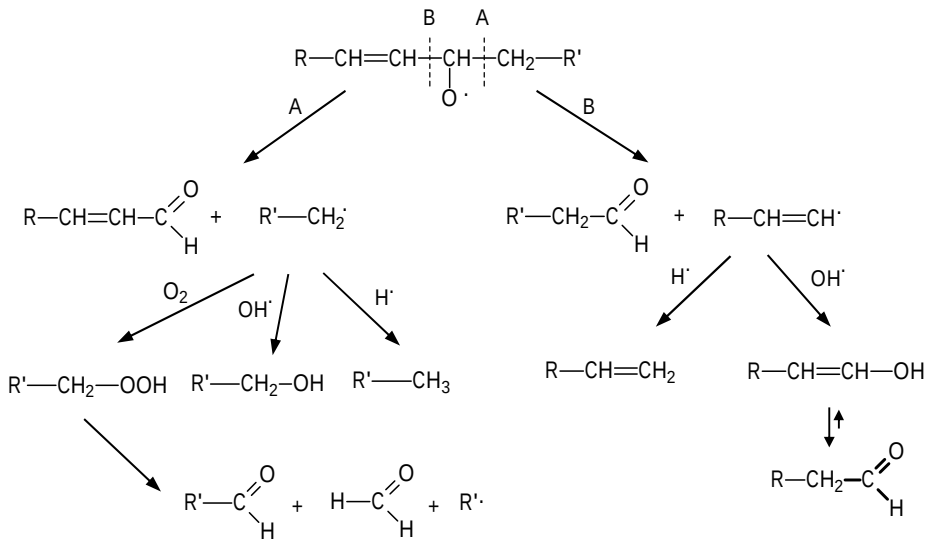

Fig. 4: Thermal or metal-catalysed decomposition of fatty acid monohydroperoxides.

Additionally, in oxidized fats and oils a wide range of non-volatile oxidation products are experimentally found which are due to competing secondary reactions such as epoxidation, cyclization, dimerization and oligomerization. Under mild conditions bis- and trishydroperoxides preferentially emerge in highly oxidized polyunsaturated TAGs. Dimerization and oligomerization reactions are only important in fats and oils exposed to frying or deodorization processes (Frankel 1998).

1.4 NMR spectroscopy

High-resolution NMR spectroscopy (NMR: nuclear magnetic resonance) is a common analytical technique in chemistry for elucidation of structure and dynamics of organic molecules. With the development of new techniques and a continuous improvement of performance, high-resolution NMR spectroscopy has gained importance in new scientific fields including medicine, food science, cosmetics and pharmacy (Holzgrabe et al. 2008). In the last thirty years many NMR applications in the field of authenticity control and the qualitative and quantitative analysis of food ingredients have been published. For references see Hidalgo & Zamora 2003 (fats and oils), Kidric 2008 (beverages), Belloque & Ramos 1999 (milk and dairy products) and Bertram & Andersen 2004 (meat). However, up to now, NMR is not widely used in food control and in food industry. The same holds for the implementation of NMR in the pharmaceutical sector. Although numerous NMR methods dealing with identification of active substances and purity control can be found in literature (Holzgrabe et al. 2008), the number of NMR applications in international pharmacopoeias, e.g. the Ph. Eur. and United States Pharmacopoeia (USP) is still limited.

1.4.1 Principles of NMR

Like all forms of spectroscopy, NMR is based on the interaction of matter with light, more precisely, with the low-energy radiofrequency part of the electromagnetic spectrum with wavelength typically from 30 m down to 40 cm (Keeler 2010). The applicability of NMR requires the presence of so-called “NMR active” nuclei in the sample, i.e. nuclei possessing *spin* (spin quantum number $I_s \neq 0$). Spin is an intrinsic property of a nucleus just like mass or charge, resulting in an angular momentum usually called nuclear spin angular momentum $\hat{S}$. Since spin and magnetism of nuclei are closely linked, the spin angular momentum is closely related to the magnetic momentum $\hat{\varphi}$ that is proportional to $\hat{S}$, where the proportionality constant γ is called gyromagnetic ratio:

$$\hat{\varphi} = \gamma \hat{S}$$

(The hat indicates that $\hat{\varphi}$ and $\hat{S}$ are quantum mechanical operators.) Particles with a positive value of γ (e.g. ^{1}H, ^{13}C) possess a magnetic momentum parallel to the spin angular momentum (Levitt 2009).

Only quantum mechanics can give a complete understanding of how NMR experiments really work – but for the sake of clarity the much simpler vector model will be used below to describe the behaviour of nuclei with spin ½ (e.g. ^{1}H, ^{13}C). Generally, spin angular momenta of nuclei in a sample point in all possible directions in space and are isotropically distributed (see figure 5 A).

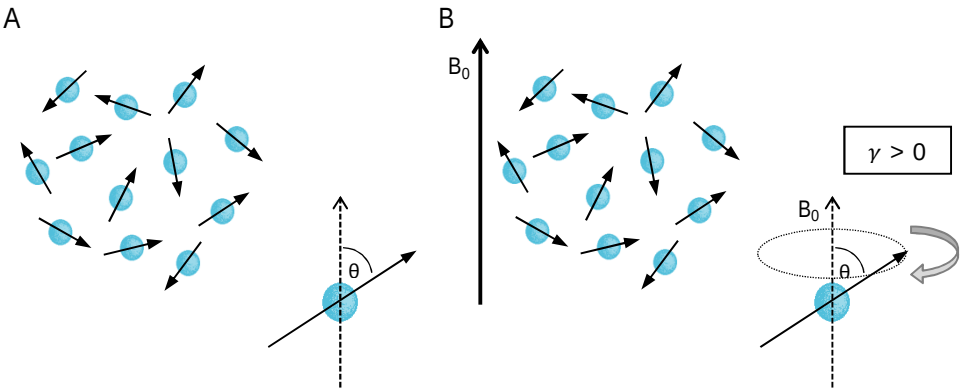

Fig. 5: Spin angular momenta A) randomly directed, B) in a magnetic field with precession.

When a magnetic field B_0 is applied to the sample, interaction of the magnetic momentum φ with the magnetic field, causes the magnetic momentum to *precess*, i.e. to move on a cone around the magnetic field, keeping a constant angle θ between the spin magnetic momentum and the field (see figure 5 B). The frequency of rotation, the so-called Larmor frequency ω_0 in rad/s, is equal to:

$$\omega_0 = -\gamma B^0$$

The angle θ depends almost entirely on the initial direction of the spin angular momentum. However, fast thermal motion of molecules in the sample can cause minor fluctuations of the effective magnetic field experienced by the nucleus. This effect results in very small variations of the angle θ over time. Since there is a slight energetic advantage for the spin angular momentum to be aligned parallel to the external magnetic field, isotropy is broken and the sample becomes magnetized. Summed over the sample a net magnetization arises along the field direction called longitudinal magnetization. It is represented by the bulk magnetization vector. At thermal equilibrium this vector reaches a maximum (Levitt 2009).

In a simple NMR experiment (here: flip angle 90°) the bulk magnetization vector is rotated by $\pi/2$ around the x-axis on the –y-axis by a radiofre-

quency (R.F.) pulse – a small magnetic field oscillation near or at the Larmor frequency ("resonance"). The resulting net magnetization perpendicular to the magnetic field B_0 is called transverse magnetization. When the R.F. pulse is turned off the bulk magnetization vector starts to precess with the Larmor frequency ω_0 about the field (see figure 6). The transverse magnetization gradually decays, since the bulk magnetization vector has the tendency to return to the equilibrium state. This process is called "relaxation". Relaxation takes place both in the xy-plain and in z-direction (Levitt 2009).

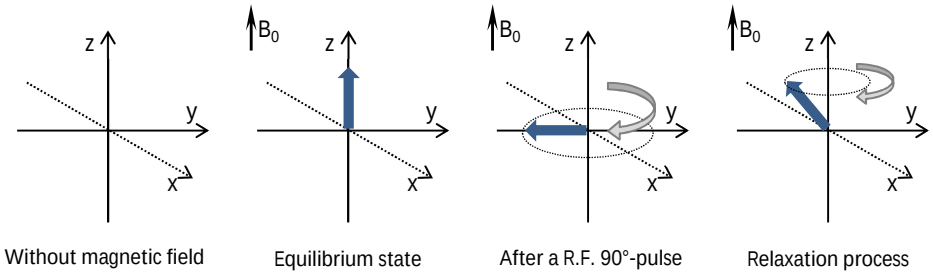

Fig. 6: Bulk magnetization vector in different NMR-relevant states.

The precession of the bulk magnetization vector is detected by a small coil of wire round the sample in x-direction (see figure 7). The precession induces an oscillating current in the coil that is amplified and detected. Relaxation processes cause the signal to decay over time resulting in the free induction decay (FID). The time-dependent FID is transformed to the frequency-domain spectrum by Fourier transformation (Keeler 2010).

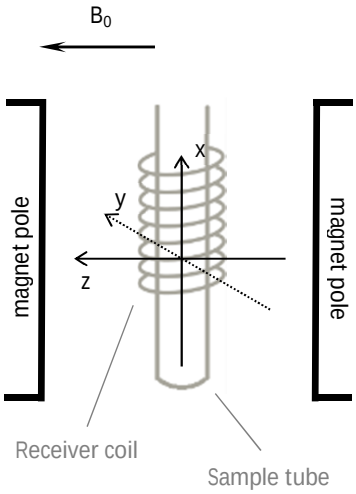

Fig. 7: Detection of the NMR signal.

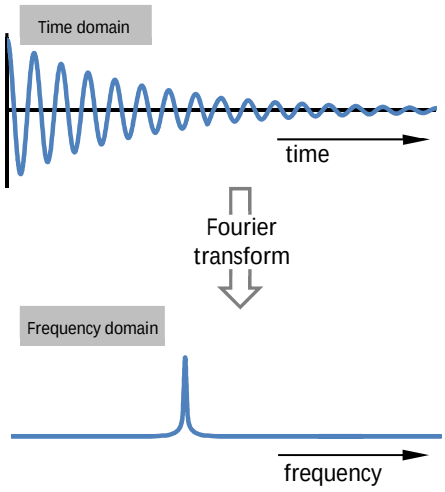

Fig. 8: Fourier transformation.

1.4.2 Quantitative ^{1}H NMR

The fundamental relation of quantitative ^{1}H NMR is the direct proportionality of signal intensity (integrated signal area) I_X to the number of protons N_X giving rise to this signal:

$$I_X = k_S N_X$$

k_S denotes the spectrometer constant (Holzgrabe 2010) being the same for all resonances in the spectrum provided the experimental conditions meet certain requirements:

- Short excitation pulses must be used, typically 10 µs, to make sure that the pulse excitation is uniform for the spectral width of interest.
- The repetition time τ ($\tau \approx$ acquisition time + relaxation delay) must be long enough to allow the bulk magnetization vector to entirely return to its equilibrium state before applying a new pulse. In practice a repetition time of $\tau = 3T_1$ for a 30° pulse often is used, allowing the z-magnetization to recover by 99.3 % (Holzgrabe 2010).

There are several further experimental parameters affecting quantitative accuracy and precision. Prior to quantitative analysis shimming, tuning and matching as well as receiver gain settings must be carefully optimized for the appropriate sample. In addition, the choice of suitable acquisition and processing parameters, including acquisition time, phase and baseline correction, windowing, zerofilling and especially the integration procedure, are of great importance. A comprehensive and more detailed discussion of the optimization of experimental settings for quantitative NMR (qNMR) is given by (Holzgrabe 2010) and (Bharti & Roy 2012).

The two most common qNMR methods are the “relative method” and the “absolute method with internal standard”:

Relative method: The molar ratios n_X/n_Y of two compounds X and Y are obtained directly from the NMR spectrum by comparison of signal intensities considering the number of contributing nuclei *N*.

$$\frac{n_X}{n_Y} = \frac{I_X}{N_X}\frac{N_Y}{I_Y}$$

Extended to *m* compounds the molar ratio of compound X is given by:

$$\frac{n_X}{\sum_{i=1}^{m} n_i} = \frac{I_X/N_X}{\sum_{i=1}^{m} I_i/N_i}$$

Absolute method with internal standard: In order to determine absolute analyte concentrations, an internal standard of known purity P_{IS} is added to the sample in a defined amount *m*. The concentration *c* of the analyte *X* in g/g is obtained by comparison of the signal intensities I_X and I_{IS} considering the molecular weight *M* and the number of nuclei *N* giving rise to the NMR signals (Holzgrabe 2010).

$$c\ \left[\frac{g}{g}\right] = \frac{I_X}{I_{IS}}\frac{N_{IS}}{N_X}\frac{M_X}{M_{IS}}\frac{m_{IS}}{m_X}P_{IS}$$

1.4.3 NMR methods to determine lipid oxidation products

In the last years, the relevance of NMR as an analytical tool for the examination of lipid oxidation has strongly increased. Generally, high-resolution NMR offers several advantages over conventional wet-chemical and chromatographic methods requiring only minor sample preparation, small solvent volumes and short analysis times. Furthermore, NMR is a non-destructive technique providing a straightforward approach to quantitative analysis of oils and fats and enabling a simultaneous detection of different oxidation products in one single analysis. However, NMR is still a relatively new approach to study lipid oxidation. It was not before the nineties that ^{1}H and ^{13}C NMR spectroscopy were applied to provide a general overview over different classes of lipid oxidation products (Claxson et al. 1994, Haywood et al. 1994, Medina et al. 1998, Silwood & Grootveld 1999). Structure elucidation of pure oxidation products has already been exhibited earlier. Recently, several new NMR studies on oxidative deterioration of edible oils under different oxidation conditions have been published by the group of Maria Guillén (Guillén & Ruiz 2006, Guillén & Goicoechea 2009, Guillén & Uriate 2009). However, NMR data on primary and secondary oxidation products are rather scarce. There are some NMR studies dealing with the classification and characterization of hydroperoxides of fatty acid esters (Porter at al. 1990, Porter et al. 1994, Hämäläinen et al. 2001, Pajunen et al. 2008) or TAGs (Frankel et al. 1990a, Neff et al. 1990) and secondary oxidation products (Guillén & Ruiz 2004, Silwood & Grootveld 1999, Claxson et al. 1994). But no systematic studies have been published yet.

The first NMR approach to estimate the deterioration status of lipids was presented by Saito (Saito 1987). The ^{1}H NMR spectra of fats and oils show characteristic signals of the different proton species in a TAG molecule (see figure 9). The ratios of relative intensities between olefinic protons (δ_H 5.1 – 5.6 ppm) to aliphatic protons (δ_H 0.5 – 2.5 ppm) and between

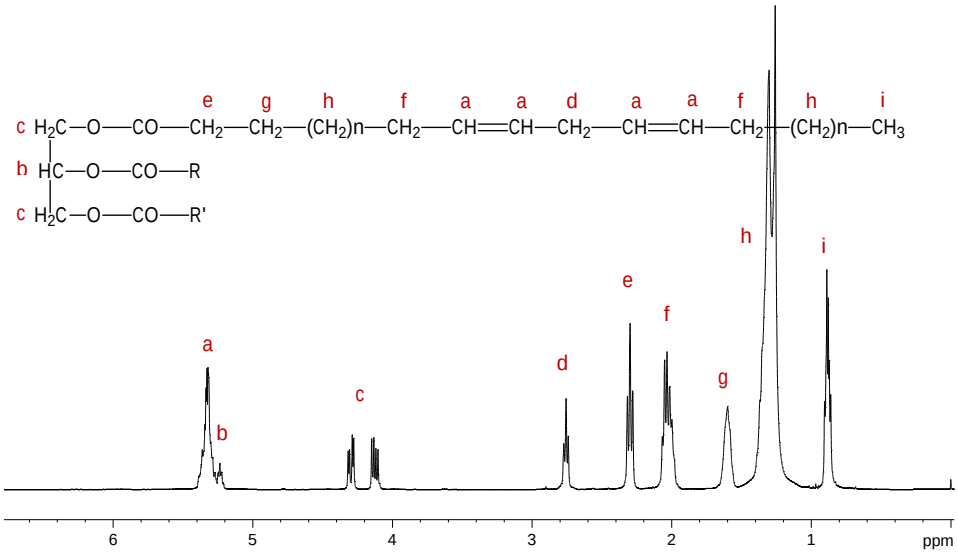

Fig. 9: ^{1}H NMR spectrum of a maize oil in $CDCl_3$.

the aliphatic protons and diallylmethylene protons (δ_H 2.6 – 3.0 ppm) decrease as the oxidative deterioration proceeds. A good compliance between these ratios and the classical *TOTOX* value has been found (Shahidi & Wanasundra 1997). However, this method is not sufficiently sensitive to detect small oxidative changes of fats and oils stored at room temperature.

Another strategy to follow oxidative changes in lipids by ^{1}H NMR is the quantitative determination of primary or secondary oxidation products as analytical markers. Recently, Guillén and Goicoechea reported the use of ^{1}H NMR for a rough quantification of hydroperoxides and aldehydes in oxidized maize oil. This method is based on the integration of the hydroperoxide group (OO*H*) signal and the carbonyl group proton (C*H*O), respectively, considering the proton signal of non-deuterated chloroform (impurity of the solvent $CDCl_3$) as internal standard (Guillén & Goicoechea 2009).

In addition, ^{13}C NMR and ^{31}P NMR have been proposed to determine FFAs in fats and oils (Ng 2000, Dayrit et al. 2008). Generally, the results of the NMR methods were in good agreement with the conventional *AV*. Drawbacks of the ^{31}P and ^{13}C NMR methods are the requirement of a FFA derivatization step prior to ^{31}P NMR analysis and of long measurement times for ^{13}C NMR experiments. Recently, Satyarthi et al. reported the application of ^{1}H NMR spectroscopy to quantify FFAs in nonedible lipids and biodiesel with significant FFA amounts (Satyarthi et al. 2009). This method is based on the integration of the α-carbonyl-CH_2 signal of FFAs and the α-carbonyl-CH_2 signal of esterified fatty acids. Since these signals partially overlap, this method is not sufficiently sensitive to detect small amounts of FFAs in lipids as occurring in commercially available edible oils.

2. Aims of thesis

The general aims of the present thesis were to develop ^{1}H NMR methods to determine hydroperoxides, FFAs and aldehydes in fats and oils. This work deals in detail with:

Hydroperoxides

Effect of solvent and of impurities on peak width and chemical shift of the hydroperoxide proton (OO*H*) signals
Rough assignment of the OO*H* signals to oleic, linoleic and linolenic acid
Kinetic study on trioleate monohydroperoxides to gain information on how many different hydroperoxide species are formed during trioleate autoxidation
Comparison of the analytical performance of the new ^{1}H NMR method and the classical *PV* approach and examination of several oil types with both methods
Causes for the discrepancies between the two methods for olive oils and black seed oils

Free fatty acids

Effect of solvent on peak width of the carboxyl group proton signal of FFAs
Comparison of the analytical performance of the new ^{1}H NMR method and the classical *AV* approach and examination of several oil types with both methods
Adoption of the ^{1}H NMR assay to further lipids with relevance in pharmacy

Aldehydes

Establishing an equation to model the classical *ANV* as a linear combination of the NMR-determined molar aldehyde amount
Comparison of the NMR-determined ANV_{NMR}s with the conventionally measured *ANVs* of several commercially available edible oils of different oil types in order to test the suitability of the model

3. ^{1}H NMR determination of hydroperoxides*

3.1 Method development

In order to determine the hydroperoxide amount in fats and oils, the signal intensity of the hydroperoxide group proton (OO*H*) signals representing the amount of hydroperoxides and the signal intensities of the proton signal of the methylene group directly adjacent to the carbonyl group of fatty acids (α-carbonyl-CH_2) representing the overall TAG amount were compared (relative quantification method). OO*H* protons resonate as singlets in the downfield region of the ^{1}H NMR spectrum. To find the optimal measurement conditions, the influence of solvent, water, FFAs and of sample concentration on the OO*H* signals was investigated.

Effect of solvent

The most common solvent in the NMR analysis of lipids is $CDCl_3$. Using this solvent for oxidized edible fats and oils, the OO*H* protons provide very broad signals with varying chemical shifts in the region of 7.5 to 8.7 ppm. It is well-known that protic groups like those of hydroperoxides and alcohols can form hydrogen bonds and show proton exchange (Beyer et al 2010, Kamal-Eldin & Pokorny 2005, Fribolin 2011). This indicates that protic compounds of the oil matrix or solvent impurities like water or acids interact with the hydroperoxide group and thus induce proton transfer processes which cause broadening of the OO*H* signals. Since narrow signals are a fundamental requirement for a sensitive integration, the effect of different solvents ($CDCl_3$, acetone-d_6, benzene-d_6, DMSO-d_6 and their mixtures with $CDCl_3$) was investigated (note: the solvents were taken from newly opened bottles to minimize the amount of impurities like water). For this purpose an oxidized rapeseed oil with a very low FFA content was dissolved in different solvent mixtures and analysed directly by ^{1}H NMR (see figure 10).

As can be seen in figure 10 A, the usage of pure benzene-d_6 and its mixtures with $CDCl_3$ as solvent does not lead to an appreciable improvement of signal resolution and signal width. Instead the inverse is true. With increasing benzene-d_6 proportion a slight broadening of the OO*H* signals can be observed.

* Parts of this chapter are published in Skiera et al. (2012a)

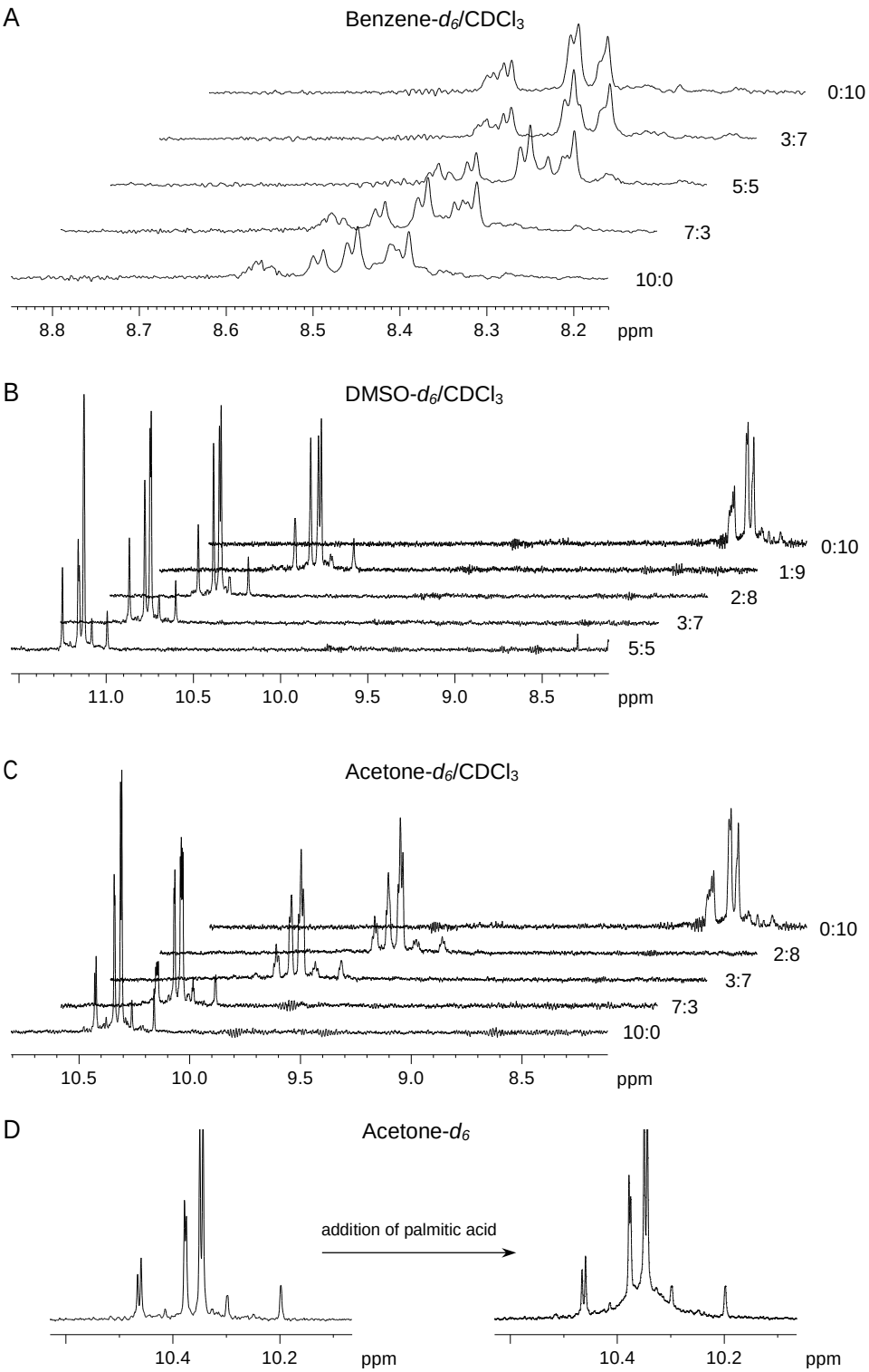

Fig. 10: Downfield region of a rapeseed oil dissolved in A) mixtures of benzene-d_6 with $CDCl_3$, B) mixtures of DMSO-d_6 with $CDCl_3$, C) mixtures of acetone-d_6 with $CDCl_3$ and D) acetone-d_6 with addition of palmitic acid (oil concentration: 500 mg/1.2 ml).

In contrast, the addition of even small DMSO-d_6 amounts to the solvent $CDCl_3$ (10 % DMSO-d_6) causes a strong downfield shift of the OO*H* signals and much sharper signals (see figure 10 B). This can be explained by the property of DMSO-d_6 to slow down proton exchange due to the formation of hydrogen bonds between the hydroperoxide group and the S=O group of DMSO-d_6. The usage of solvent mixtures with more than 20 % DMSO-d_6 only leads to smaller shift differences and minor improvements of resolution and signal height. This effect can be explained by the saturation of the hydroperoxide group with hydrogen bonds. Spectra of oils dissolved in solvent mixtures containing more than 50 % DMSO-d_6 are not shown here since common fats and oils are not entirely soluble in $CDCl_3$/DMSO-d_6 mixtures with 80 % DMSO-d_6 and more.

Similar to DMSO-d_6, acetone-d_6 has a strong effect on the OO*H* signals due to the formation of hydrogen bonds between acetone-d_6 molecules and the hydroperoxide group. The addition of 20 % acetone-d_6 to $CDCl_3$ leads to a strong downfield shift and to an increase of resolution. The usage of acetone-d_6/$CDCl_3$ mixtures with even higher acetone-d_6 proportions causes smaller changes since the OO*H* protons are already saturated with hydrogen bonds (see figure 10 C). The best resolution was observed in pure acetone-d_6. The big disadvantage of acetone-d_6 (and its mixtures with $CDCl_3$) is that in this solvent OO*H* signals and the broad proton signal of the carboxylic group of free acids resonate in the same area of the spectrum (see figure 10 D). Therefore, acetone-d_6 and its mixtures with $CDCl_3$ are not suitable solvents to determine the hydroperoxide amount of edible oils containing FFAs. Based on these results the solvent mixture $CDCl_3$/DMSO-d_6 (5:1, v/v) was found to be the optimal solvent to detect the OO*H* signals in fats and oils. This solvent mixture was used for all further investigations if not otherwise pointed out.

Effect of water and FFAs

The effect of protic goups in the sample solution (oil matrix components or solvent impurities) on the broadening of the OO*H* signals was investigated by taking the example of water and of the carboxylic group of FFAs.

The water content of an oxidized sunflower oil (*PV* = 34 meq/kg, *AV* = 1.2 mg/g) was varied by drying the sample solution for 0, 10, 20, 40, 60 and 120 min over a molecular sieve. The obtained ^{1}H NMR spectra are shown in figure 11.

Furthermore, a rapeseed oil with very low FFA content was spiked at 2, 4, 8, 20 and 40 mg palmitic acid/g oil. The results of these spiked oil samples dissolved in $CDCl_3$/DMSO-d_6 (5:1, v/v) are depicted in figure 12.

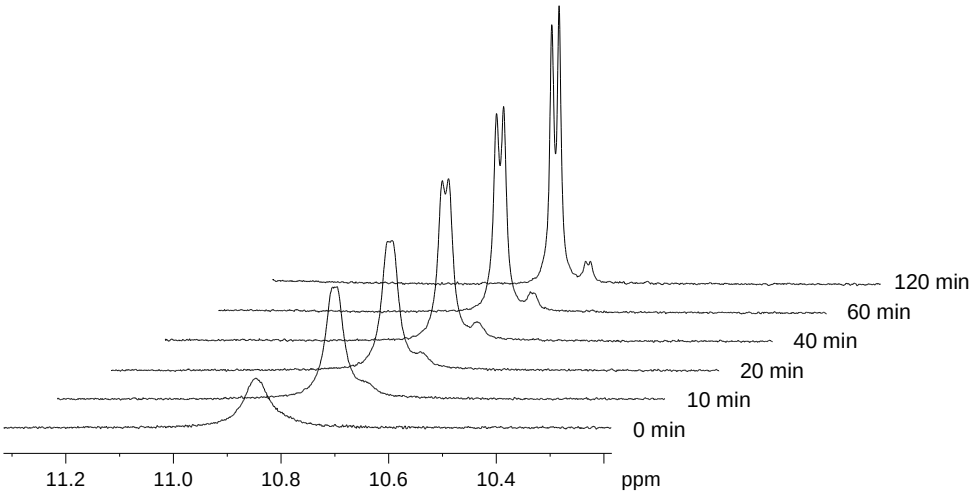

Fig. 11: Downfield region of an oxidized sunflower oil dried for 0, 10, 20, 40, 60 and 120 min over a molecular sieve (oil concentration: 500 mg/1.2 ml).

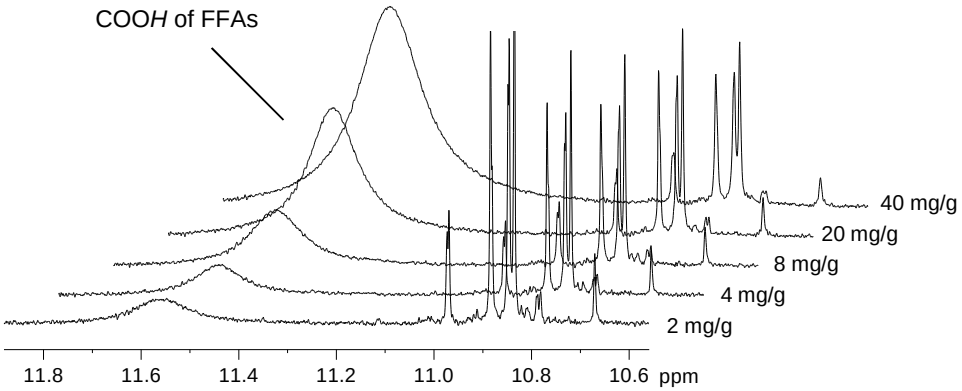

Fig. 12: Downfield region of a rapeseed oil spiked at 2, 4, 8, 20 and 40 mg palmitic acid/g oil (oil concentration: 500 mg/1.2 ml).

These experiments clearly show that both the FFA content and the water content influence the resolution and signal width of the OO*H* signals. It was found that the lower the water and FFA content, the sharper are the OO*H* signals.

Effect of sample concentration

In order to find the optimal sample weight, the influence of sample concentration on the OO*H* signal was investigated. For this purpose, 400 mg, 500 mg, 600 mg, 800 mg and 1000 mg of an oxidized sunflower oil (*PV* = 34 meq/kg, *AV* = 1.2 mg/g) were dissolved in 1.2 ml $CDCl_3$/DMSO-d_6 (5:1, v/v)

and dried over a molecular sieve prior to NMR analysis. Figure 13 depicts the downfield region of the obtained ^{1}H NMR spectra. Resolution of the OO*H* signals decreases steadily with increasing sample weight. Signal heights slightly increase from 400 mg to 600 mg sample weight. Further increase of sample weight does not lead to an increase of signal height but to a broadening of the signals. Since an appreciable enhancement of sensitivity could not be obtained with sample weights above 500 mg/1.2 ml, for all further investigations a sample weight of 500 mg/1.2 ml (250 mg/0.6 ml) solvent was used.

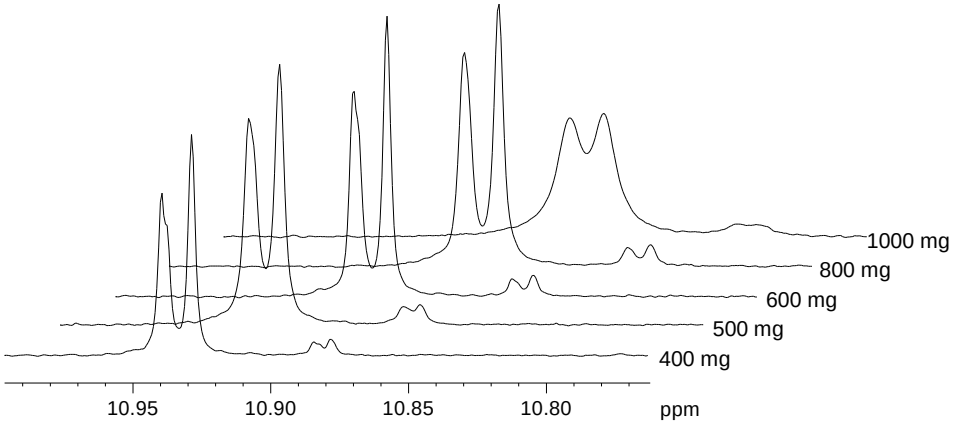

Fig. 13: Downfield region of an oxidized sunflower oil with a sample weight of 400 mg, 500 mg, 600 mg, 800 mg, 1000 mg dissolved in 1.2 ml $CDCl_3$/DMSO-d_6 (5:1, v/v) and dried over a molecular sieve.

On the basis of these findings, the final sample preparation procedure was defined as follows: The sample (250 mg) is dissolved in 0.6 ml of a mixture of $CDCl_3$ and DMSO-d_6 (5:1, v/v) and a small proportion of tetramethylsilane (TMS) as internal shift reference. Then the sample solution is dried over a molecular sieve for 20 to 30 min and analysed by ^{1}H NMR. The obtained NMR spectrum is processed manually and all OO*H* signals resonating as singlets at 10 – 11 ppm are integrated as well as the α-carbonyl-CH_2 signals resonating at δ_H 2.2 – 2.4 ppm. To achieve the hydroperoxide amount in mol/mol TAG the α-carbonyl-CH_2 signal area is normalized to six (one TAG possesses six α-carbonyl-CH_2 protons). In order to recalculate the total hydroperoxide amount in "mmol/kg", the average molecular weight of the different oil types has to be considered. The average molecular weight is directly derived from the ^{1}H NMR spectrum according to the procedure described by Miyake et al. (Miyake et al. 1998).

3.2 Hydroperoxide assignment

A rough assignment of the OO*H* signals that are present in the ^{1}H NMR spectrum of common edible oils was conducted. The three main unsaturated fatty acids of edible oils are oleic, linoleic and linolenic acid. The hydroperoxides of these fatty acids being formed during the autoxidation process are well characterized (see section 1.3). The OO*H* signal pattern is typical for each oil variety and reflects the fatty acid composition of this oil. Figure 14 A shows the OO*H* signals of a high oleic, high linoleic and a high linolenic oil in the range of 10.6 to 11.1 ppm. The assignment is based on a comparison between oils and oxidized oleic, linoleic and linolenic acid methyl ester standards (see figure 14 B).

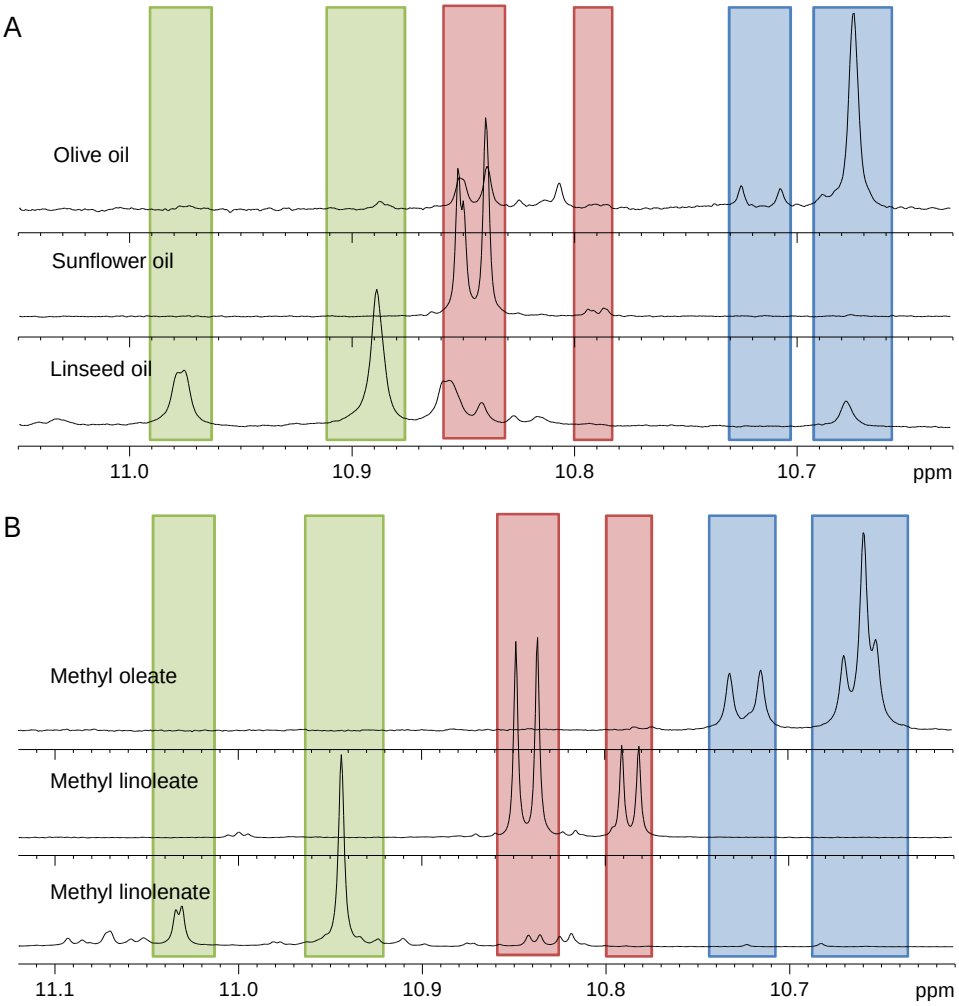

Fig. 14: OO*H* region A) of a high oleic, high linoleic and a high linolenic oil and B) of oxidized fatty acid methyl esters.

A particular characteristic of the OO*H* signal pattern of olive oil is that there are three further signals at δ_H 10.2 - 10.4 ppm (see figure 15) which are not attributed to fatty acid hydroperoxides. These signals could be identified as the OO*H* signals of squalene by comparison with the oxidized squalene standard. Squalene is a hydrocarbon with six non-conjugated double bonds and thus can also be peroxidized.

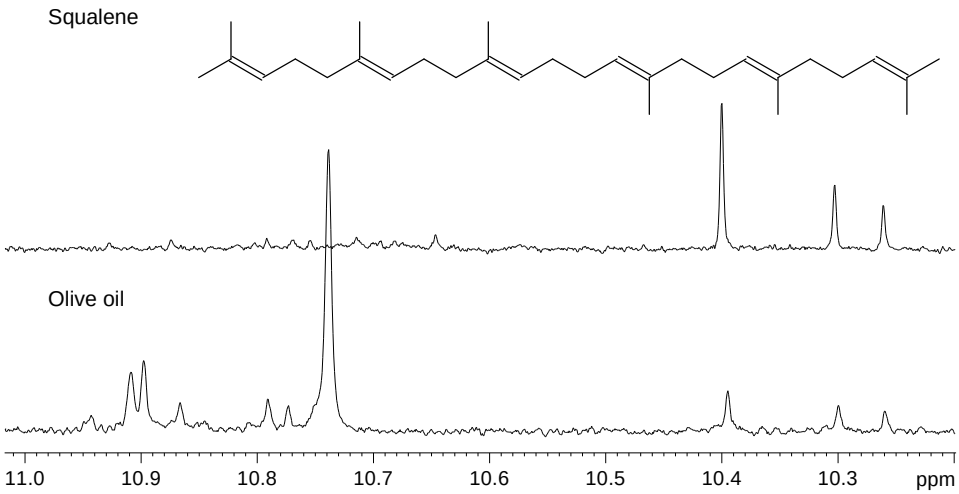

Fig. 15: OO*H* region of olive oil compared to that of oxidized squalene.

In addition, the oxidized standards methyl oleate, methyl linoleate and methyl linolenate were dissolved in pure $CDCl_3$. The downfield region of the obtained spectra is shown in figure 16. Utilizing the solvent $CDCl_3$ instead of $CDCl_3$/DMSO-d_6 (5:1, v/v) leads to a markedly better separation of the OO*H* signals of methyl oleate and methyl linolenate. The spectrum of methyl oleate shows six main OO*H* signals and the spectra of methyl linoleate and methyl linolenate show four main signals. This finding is in accordance with literature data obtained for oxidized fatty acid methyl ester standards (oxidation at 25 °C) by chromatographic methods. Frankel et al. reported the formation of six main methyl oleate hydroperoxides (*Z*)-8-OOH, (*E*)-8-OOH, (*E*)-9-OOH, (*E*)-10-OOH, (*Z*)-11-OOH, (*E*)-11-OOH (14 %, 12 %, 23 %, 22 %, 14 %, 13 %) (Frankel et al. 1984) and four main methyl linoleate hydroperoxides (*Z*,*E*)-9-OOH, (*E*,*E*)-9-OOH, (*Z*,*E*)-13-OOH, (*E*,*E*)-13-OOH, (30 %, 19 %, 31 %, 20 %) (Frankel et al. 1990b). For methyl linolenate eight different hydroperoxide species, four in (*Z*,*E*) and four in (*E*,*E*) configuration were detected (Frankel et al. 1977) but only the (*Z*,*E*) isomers were found in higher amounts at low temperatures, e.g. room temperature. The following ratios of the four positional isomers were reported: 9-OOH: 31 %, 12-OOH: 10 %, 13-OOH: 11 %, 16-OOH: 49 % (see chapter 1.3).

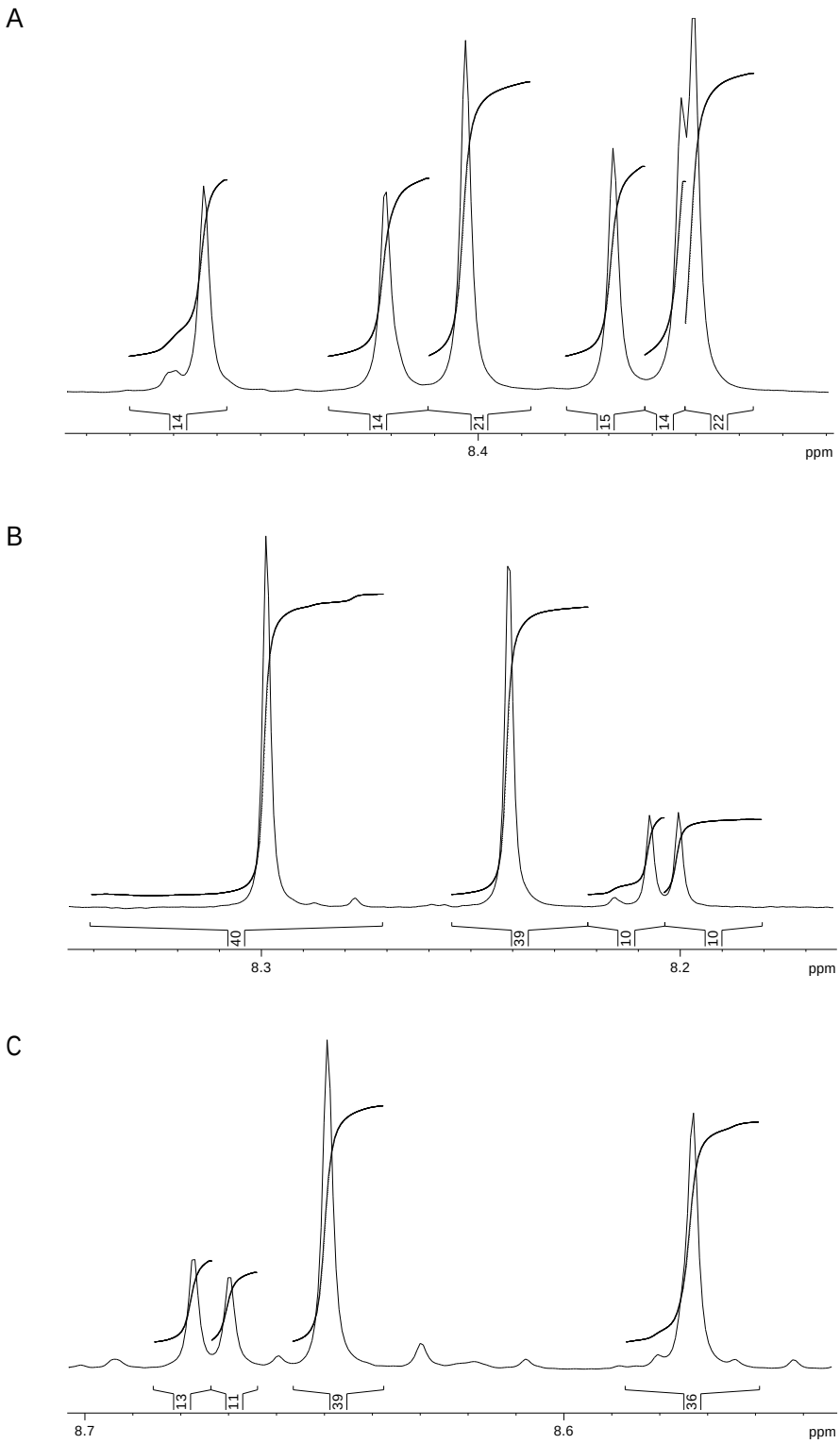

Fig. 16: OO*H* region of oxidized A) methyl oleate, B) methyl linoleate and C) methyl linolenate standards dissolved in $CDCl_3$.

3.3 Hydroperoxides of TAGs

During the autoxidation process of trioleate molecular oxygen can either attack the outer fatty acids (sn-1/3 position) or the inner fatty acid (sn-2 position). When the hydroperoxide group is introduced at one of the outer fatty acids, two chiral centres result – one at the glyceryl methine carbon and one at the carbon directly adjacent to the hydroperoxide group (see figure 17). As a consequence, two diastereomeric structures are obtained. When the hydroperoxide group is introduced at the inner acyl fatty acid, one further diastereomer is conceivable. Since autoxidation of methyl oleate leads to six main hydroperoxides, 18 different monohydroperoxide species of trioleate are possible. Analogously, 12 different hydroperoxide species are conceivable in the case of oxidized trilinoleate.

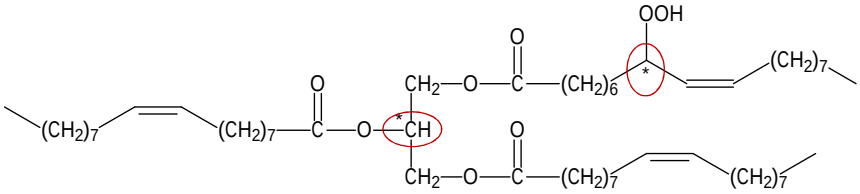

Fig. 17: Chiral centres of a trioleate monohydroperoxide.

To test whether all diastereomers actually are generated, trioleate and trilinoleate were oxidized in the dark in open glass vessels at room temperature for three days (trilinoleate) and at 40 °C for 18 days (trioleate). The oxidized standards were dissolved in $CDCl_3$ containing a small proportion of TMS and analysed directly by ^1H NMR. The obtained spectra are shown in figure 18 and 19.

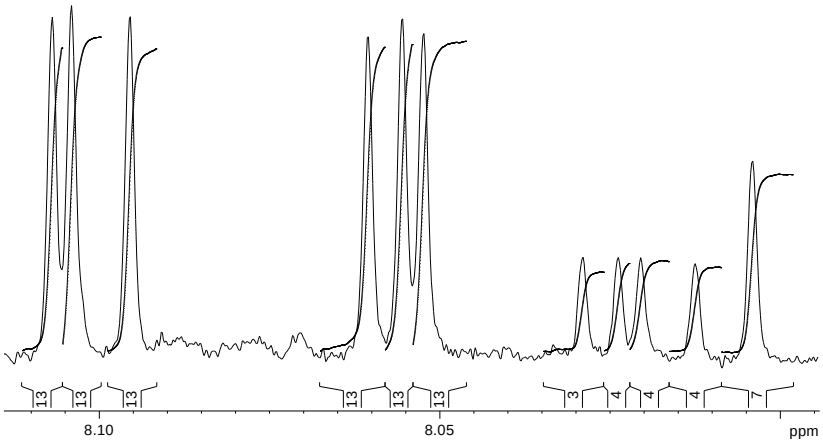

Fig. 18: Downfield region of the ^1H NMR spectrum of oxidized trilinoleate dissolved in $CDCl_3$.

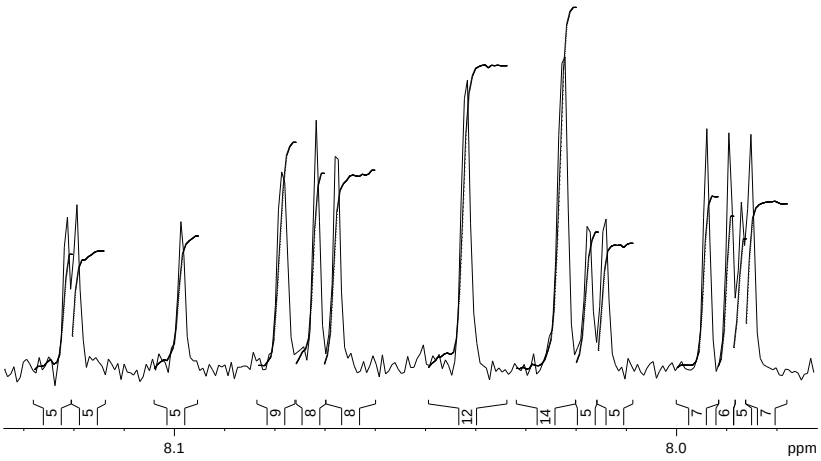

Fig. 19: Downfield region of the ^{1}H NMR spectrum of oxidized trioleate dissolved in $CDCl_3$.

The spectrum of oxidized trilinoleate shows eleven separated OO*H* signals, the expected number minus one. It is well-known from studies on methyl linoleate autoxidation (Chan & Levett 1977a, Porter et al. 1995) that (*E*,*E*)-9-OOH and (*E*,*E*)-13-OOH as well as (*Z*,*E*)-9-OOH and (*Z*,*E*)-13-OOH are formed in equal concentrations, respectively, at different levels of autoxidation. At low temperatures, e.g. room temperature, the (*Z*,*E*) isomers are predominant whereas the proportion of (*E*,*E*) isomers rises with increasing temperature (Frankel 1998). The ^{1}H NMR spectrum of methyl linoleate autoxidized at room temperature in the dark (see figure 16 B) is in accordance with literature. It depicts two big signals (probably (*Z*,*E*) isomers) and two small signals (probably the (*E*,*E*) isomers) in the molar ratio of about 4:1. Provided that there is no preference for one sn-position to be attacked by oxygen during autoxidation of trilinoleate, one would expect two types of hydroperoxides to be formed - the (*Z*,*E*) isomers and the (*E*,*E*) isomers with equal molar concentration levels within one class. This is exactly the result that can be observed for trilinoleate when the signal at 8.005 ppm in figure 18 is assumed to be the sum of two different OO*H* signals with equal molar amounts. The spectrum of oxidized trilinoleate contains six big OO*H* signals (integral area: ~13 % of total), four small signals (integral area: ~3 – 4 % of total) and one further signal (integral area: ~7 % of total). In conclusion, the spectrum of oxidized trilinoleate provides a clear indication for the formation of all twelve expected hydroperoxide stereoisomers and on the absence of a preference for oxidation of fatty acids in position sn-1, -2 and -3. All (*Z*,*E*) and all (*Z*,*Z*) isomers seem to be formed in equimolar concentrations.

In the spectrum of oxidized trioleate we can distinguish at least fourteen separated or partially separated signals. The best resolution of the OO*H*

signals was obtained at low OO*H* concentrations (see figure 19). Resolution of the OO*H* signals decreased at higher oxidation levels of trioleate. This can be explained by the protic nature of hydroperoxides themselves which can fortify proton exchange processes of the OOH group of hydroperoxides in the sample solution. The autoxidation of methyl oleate at room temperature in the dark leads to the formation of two classes of hydroperoxides – four hydroperoxides with an integral area of about 14 % and two hydroperoxides with an integral area of about 22 % of total hydroperoxides (see figure 16 A). These differences in size of the OOH signals are rather small, thus it is not possible to draw conclusions from the OO*H* ratios of separated trioleate hydroperoxides about the number of trioleate hydroperoxides in the sample. To gain information on how many different hydroperoxide species are formed during trioleate autoxidation, a kinetic study on trioleate monohydroperoxides was performed.

3.3.1 Oxidation kinetics of trioleate

1.3 g trioleate were stored at 40 °C in an open glass vessel in the dark. Aliquots were taken for ^{1}H NMR analysis after defined time intervals (0, 7, 11, 14, 16, 18, 25 days). The OO*H* region of the ^{1}H NMR spectrum was divided into six sections in such a way that overlapping signals were grouped in one section (see figure 20). Every section contains an unknown number of different OO*H* resonances. The molar hydroperoxide amount in mmol/mol TAG was determined for every section and these hydroperoxide amounts were plotted versus the time. The results are given in figure 21.

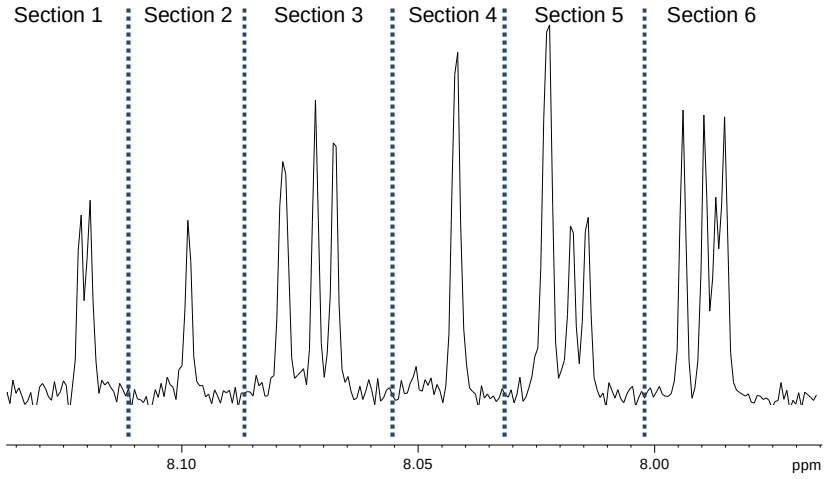

Fig. 20: Downfield region of the ^{1}H NMR spectrum of oxidized trioleate dissolved in $CDCl_3$. The spectrum is divided into six sections.

It is well-known that hydroperoxide formation during the autoxidation process follows an exponential first-order rate law (Kamal-Eldin & Pocorny 2005). The reaction rate is given by:

$$\frac{dc}{dt} = k \cdot c(t) \tag{1}$$

c denotes the hydroperoxide concentration, k denotes the rate constant and t denotes the time). Solving for $c(t)$ and setting $t_0 = 0$ we obtain:

$$c(t) = c_0 \cdot e^{kt} \tag{2}$$

For every section an exponential curve was fitted to the data. The calculated k and c_0 values are given in table 5.

Tab. 5 Parameters of the exponential curves.

section	k 1/days	c_0 mmol/mol
1	0.21	0.012
2	0.21	0.007
3	0.21	0.030
4	0.22	0.014
5	0.21	0.032
6	0.21	0.035

To estimate the number of trioleate hydroperoxides formed during the autoxidation process of trioleate the following assumptions were made:

1. All trioleate hydroperoxide species are formed with the same rate.
2. All trioleate hydroperoxide species exhibit the same initial concentration at the beginning of the exponential process.

The first assumption is plausible since the rate constants for all sections are in good compliance (see table 5). Assumption two is probably not true. Since the autoxidation of methyl oleate under the same oxidation conditions (40 °C, darkness, open vessel) leads to the formation of six hydroperoxide species in the ratio of 14:14:21:15:14:22 (see figure 16 A), we cannot expect an equimolar ratio of trioleate hydroperoxides.

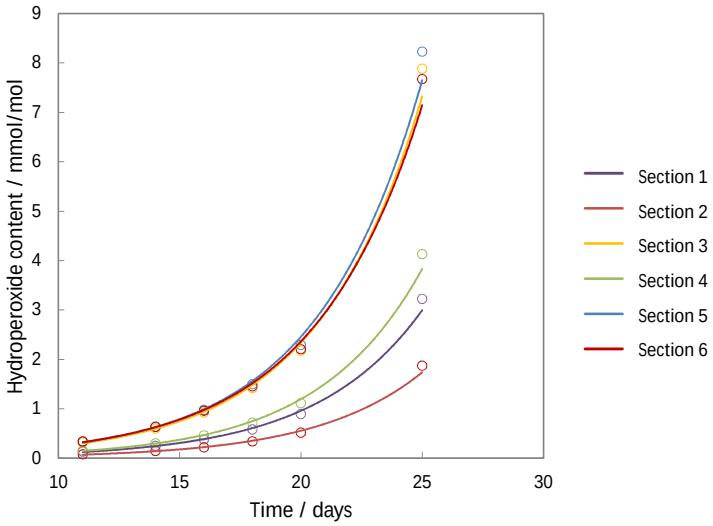

Fig. 21: Kinetics of the hydroperoxide formation of trioleate.

If we proceed on these assumptions, the concentration differences of the individual sections at any time t are exclusively due to the number of different hydroperoxide species present in one section. To estimate the number of trioleate hydroperoxides the experimental data set of $c(t = 16$ days) was chosen. The number of hydroperoxides of section 2 was set to one, since at any sampling time ($t > 7$ days) only a single symmetric signal with the smallest integral area was present in this section. The calculated ratios are listed in table 6. The sum of the ratios is 18, the sum of the rounded ratios is 17. This result strongly indicates that all of the conceivable 18 trioleate monohydroperoxides were formed during trioleate autoxidation.

Tab. 6 Ratios of the hydroperoxide amounts in section 1 to 6.

Section	Calculated c mmol/mol	Number of hydroperoxides	Rounded number of hydroperoxides
1	0.38	1.73	2
2	0.22	1	1
3	0.92	4.21	4
4	0.46	2.11	2
5	0.98	4.45	4
6	0.96	4.38	4
sum		18	17

3.4 Comparison with the classical *PV*

A comparison between the analytical performance of the Wheeler method and the NMR approach is not straightforward. The results obtained by the Wheeler method are affected by an inherent systematic error which is ignored per definition. Additionally, it is difficult to compare the precision of the *PV* expressed in meq/kg with the precision of the hydroperoxide amount expressed in mmol/kg.

To cope with this problem, the following procedure was chosen: Different mixtures of a peroxide-containing and a peroxide-free oil were prepared and analysed by both methods. To make sure that no natural oil components cause a bias in the results, two "artificial" lipids were chosen: an oxidized methyl linoleate standard and a TAG solely consisting of saturated middle-chain fatty acids. Then, the measured *PV*s were plotted versus the NMR-determined peroxide amounts and a straight line was fitted to the data (see figure 22). Taking into account that both quantities are subject to error, Deming regression was applied ([Skiera et al. 2012], details see 3.4.1). The functional relationship between the *PV* and the NMR-determined peroxide amount can be given by the equation:

$$y = 2.42x + 1.10 \qquad (3)$$

To compare the methods, the relative sensitivity of the NMR assay with respect to the Wheeler method, $RS_{NMR/PV}$, was calculated. The obtained result 0.9 clearly indicates that both methods exhibit a similar analytical performance.

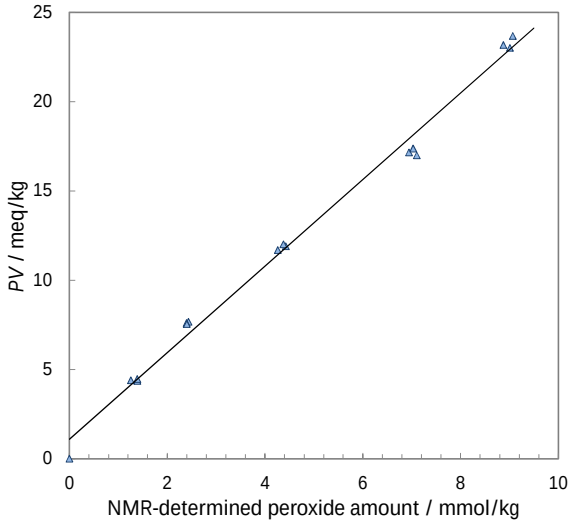

Fig. 22: *PV* in meq/kg versus the NMR-determined peroxide amount in mmol/kg (curve fitting by Deming regression).

3.4.1 Deming regression and relative sensitivity

Assume that the relationship between the *PV*, y, and the true but unknown hydroperoxide amount z is given by a linear model of the form

$$y = Y(z) + \eta = d + gz + \eta \tag{4}$$

$Y(z) = d + gz$ denotes the conditional expectation of y and η represents the random error. η is supposed to follow a normal distribution with mean zero and constant variance σ_η^2. g and d are the model parameters. Analogously, we assume that the NMR-determined peroxide amount x is related to z by the equation

$$x = X(z) + \varepsilon = k + lz + \varepsilon \tag{5}$$

where $X(z) = k + lz$ is the conditional expectation of x and the term ε designates the error. ε is supposed to be normally distributed with mean zero and constant variance σ_ε^2. For the time being, let us assume that all parameters and variances are known. Then, applying the Gaussian law of uncertainty propagation, it follows that for a given y_0 the standard deviation of the estimate $\hat{z}(y_0) = (y_0 - d)/g$ is

$$\sigma_{\hat{z}(y_0)} = \frac{\sigma_\eta}{g} \tag{6}$$

In the same way, we obtain for the standard deviation of the estimate $\hat{z}(x_0) = (x_0 - k)/l$:

$$\sigma_{\hat{z}(x_0)} = \frac{\sigma_\varepsilon}{l} \tag{7}$$

The relative sensitivity (Mandel 1964) of the NMR assay with respect to the Wheeler method, $RS_{NMR/Wheeler}$, is defined as

$$RS_{NMR/Wheeler} = \frac{\sigma_{\hat{z}(y_0)}}{\sigma_{\hat{z}(x_0)}} = \frac{l}{g} / \frac{\sigma_\varepsilon}{\sigma_\eta} \tag{8}$$

If $RS_{NMR/Wheeler}$ appreciably exceeds unity, the NMR approach would have the greater ability to detect a difference in the actual hydroperoxide amount. The opposite conclusion holds when $RS_{NMR/Wheeler}$ is clearly smaller than unity. How can we estimate $RS_{NMR/Wheeler}$? To answer this question, the equations (4) and (5) have to be considered. Solving the equation (5) for z and inserting the result into (4) gives us

$$y = -\frac{g}{l}k + d + \frac{g}{l}x - \frac{g}{l}\varepsilon + \eta \tag{9}$$

By substituting a for $-\frac{g}{l}k + d$ and b for $\frac{g}{l}$, we obtain

$$y - \eta = a + b(x - \varepsilon) \tag{10}$$

or

$$Y = a + bX \tag{11}$$

with $x = X + \varepsilon$ and $y = Y + \eta$. Equation (11) connects the *PV* y to the NMR-determined peroxide amount x and represents a so-called Deming regression model. Minimizing the sum

$$\sum_{i=1}^{n}\left((x_i - X_i)^2 + (y_i - a - bX_i)^2\left(\frac{\sigma_\varepsilon}{\sigma_\eta}\right)^2\right) \tag{12}$$

for a given data set $(x_i, y_i)_{i=1,\dots,n}$ with respect to a , b and X yields the maximum likelihood estimators for $\hat{a}$, $\hat{b}$ and $\hat{X}$:

$$\hat{b} = \frac{\left(\frac{\sigma_\varepsilon}{\sigma_\eta}\right)^2 SS_{yy} - SS_{xx} + \sqrt{\left(\left(\frac{\sigma_\varepsilon}{\sigma_\eta}\right)^2 SS_{yy} - SS_{xx}\right)^2 + 4\left(\frac{\sigma_\varepsilon}{\sigma_\eta}\right)^2 SS_{xy}{}^2}}{2\left(\frac{\sigma_\varepsilon}{\sigma_\eta}\right)^2 SS_{xy}} \tag{13}$$

$$\hat{a} = \bar{y} + \hat{b}\bar{x} \tag{14}$$

$$\hat{X}_i = x_i + \frac{\left(\frac{\sigma_\varepsilon}{\sigma_\eta}\right)^2 \hat{b}}{1 + \left(\frac{\sigma_\varepsilon}{\sigma_\eta}\right)^2 \hat{b}^2}\left(y_i - \hat{a} - \hat{b}x_i\right) \tag{15}$$

where $SS_{yy} = \sum(y_i - \bar{y}_i)^2$, $SS_{xx} = \sum(x_i - \bar{x}_i)^2$ and $SS_{xy} = \sum(x_i - \bar{x}_i)(y_i - \bar{y}_i)$. With $\frac{g}{l} = b$, we can rewrite equation (8) as

$$RS_{NMR/Wheeler} = \left(b\frac{\sigma_\varepsilon}{\sigma_\eta}\right)^{-1} \tag{16}$$

To compute $\hat{b}$ and to estimate the relative sensitivity, an estimate for $\sigma_\varepsilon / \sigma_\eta$ is needed. The latter can be obtained as follows: Firstly, n different mixtures of a peroxide-free and a peroxide-containing oil are prepared with mixing ratios $v_{i=1,\dots n}$. Analysing these samples by both methods provides the x_i and y_i. Then, we regress x_i on v_i and y_i on v_i by simple linear least-squares fitting (see figure 23 A and B) and calculate the corresponding residual stand-

ard deviations rsd_{vx} and rsd_{vy}. Since v is proportional to z, σ_ε and σ_η can be estimated as follows:

$$\hat{\sigma}_\varepsilon = rsd_{vx} = \sqrt{\frac{1}{n-2}\sum(x_i - \hat{x}(v_i))^2} \tag{17}$$

$$\hat{\sigma}_\eta = rsd_{vy} = \sqrt{\frac{1}{n-2}\sum(y_i - \hat{y}(v_i))^2} \tag{18}$$

A

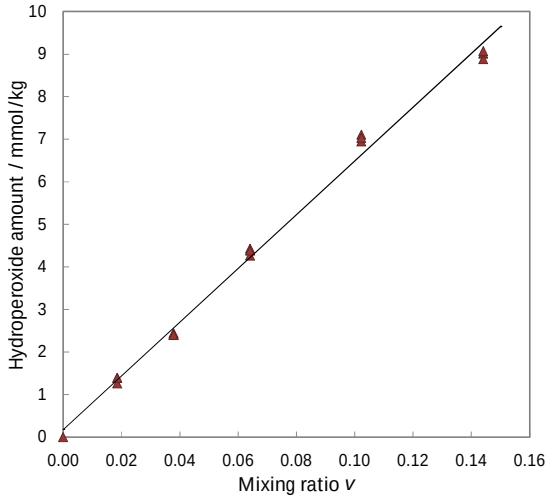

B

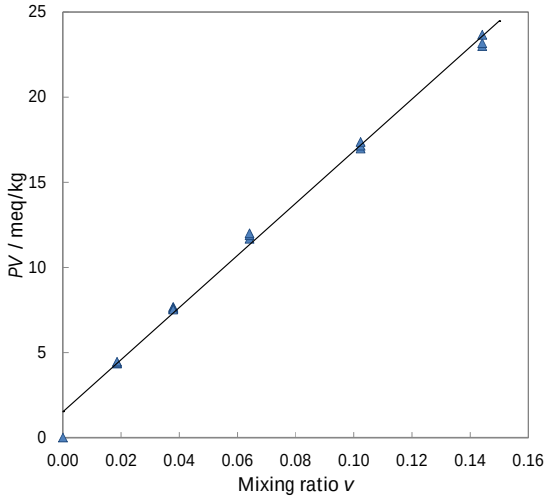

Fig. 23: Plot of A) the NMR-determined hydroperoxide amount in mmol/kg versus the mixing ratio v and B) the classical *PV* versus the mixing ratio v.

3.4.2 Examination of 444 oil samples

444 oil samples were analysed using both methods. The following oil types were chosen: olive oil (23 %), sunflower oil (19 %), rapeseed oil (13 %), nut oils (walnut oil, hazelnut oil, peanut oil, almond oil, macadamia nut oil, pistachio oil) (12 %), thistle oil (9 %), pumpkin seed oil (7 %), maize oil (5 %), linseed oil (3 %), black seed oil (2 %), grape seed oil (2 %), plant oil (composed of different vegetable oils), argan oil, soya oil, coconut fat, rice oil, sesame oil and palm oil (with rapeseed oil).

Figure 24 displays the observed results and, additionally, the line given by equation (3). As can be seen, the latter fits the data well, on the whole. The results of single oil varieties are extracted from the overall picture (see figure 25). The data of most oils, e.g. sunflower oils, rapeseed oils, nut oils, maize oils, grape seed oils and thistle oils are in good agreement with equation 3.

However, some oil types exhibit considerable deviations, especially black seed oils, pumpkin seed oils and olive oils. While the *PVs* of black seed oils are far too high, as expected from the NMR values, the *PVs* of the olive oils and pumpkin seed oils are too low. In order to find the reason for these discrepancies, further investigations for black seed oil and olive oil were performed.

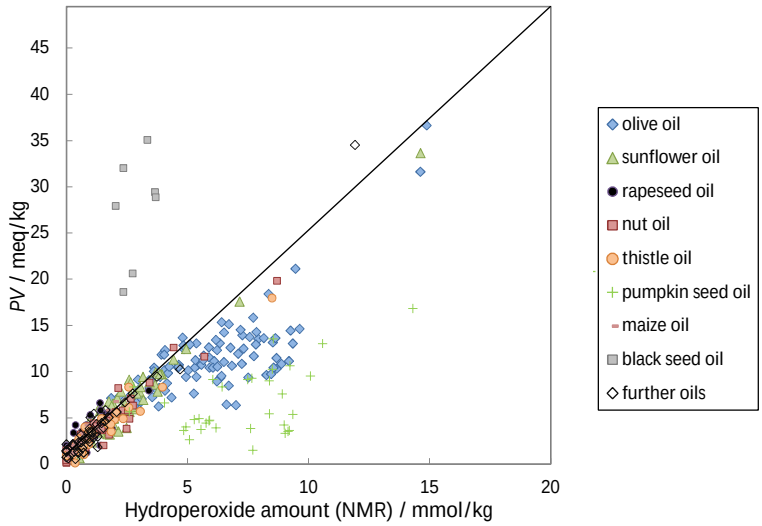

Fig. 24: Plot of the *PV* versus the NMR-determined hydroperoxide amount for 444 oil samples.

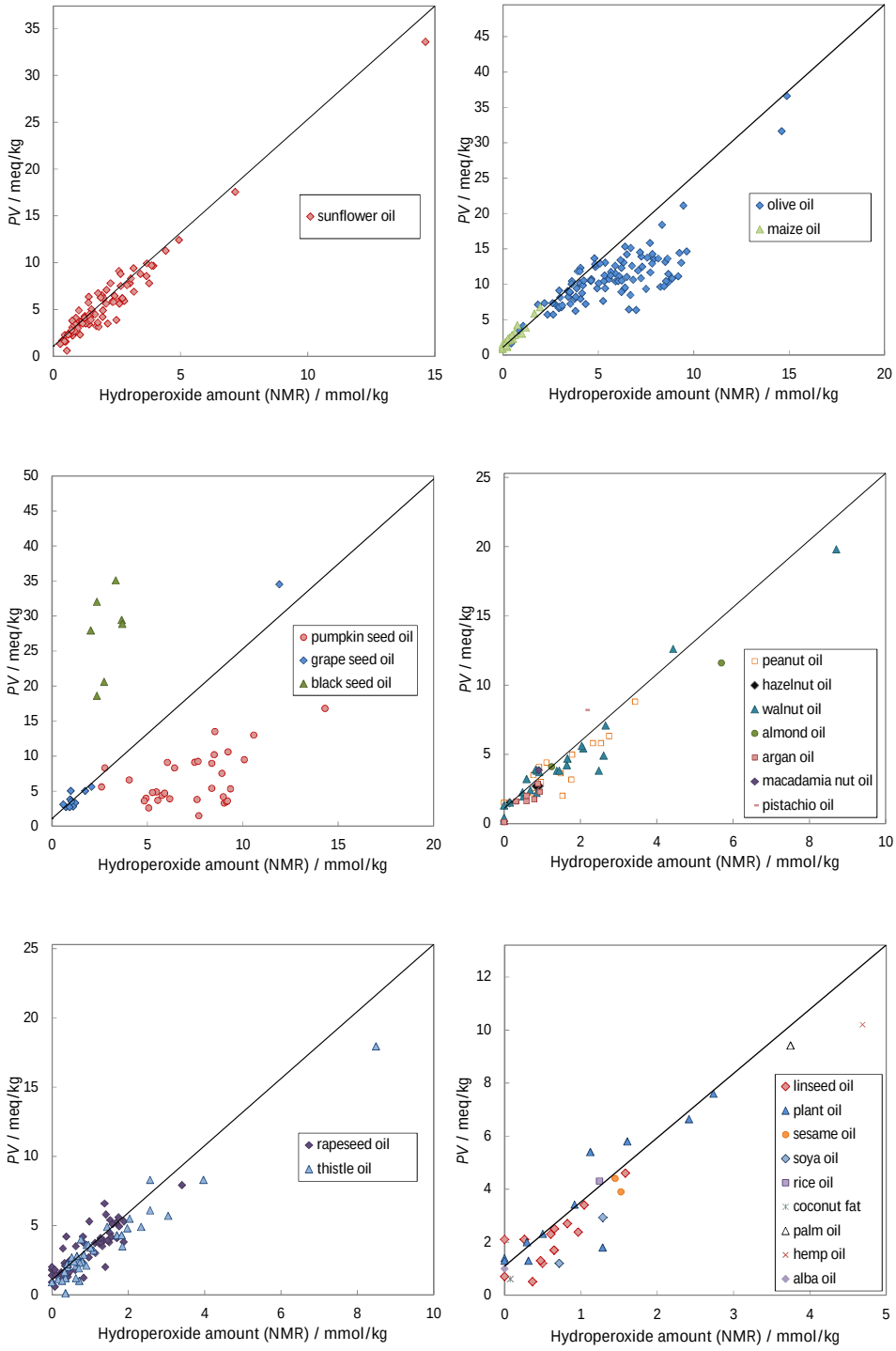

Fig. 25: *PV* in meq/kg plotted versus the NMR-determined hydroperoxide amount in mmol/kg.

3.4.3 Deviations of black seed oil and olive oil

Black seed oil, also called black cumin oil, is obtained from the seeds of the herbal plant "*Nigella sativa* Linn." Traditionally, the seeds and their oil are not only used in foods but also have a long history of folklore usage in various systems of medicines (Sharma et al. 2009). In the last years black seed oil has gained relevance as food supplement on the European and US market.

Six different black seed oils were analysed with both methods. All oils showed far too high *PVs* as one would expect in view of the NMR results. According to literature black seed oil contains on average 0.5 up to a maximum of 1.5 % of essential oil (Sharma et al. 2009) suggesting that natural oxidizing compounds of the essential oil of black seed oils may influence the iodometric titration. Therefore, volatile compounds of one of the oils were removed using water steam distillation and the dried oil residue and the original oil were both examined with the *PV* method and the NMR method. The comparison of the two oils showed that the *PV* according to Wheeler was reduced to one third of the original value whereas no significant difference in the hydroperoxide content determined by the NMR method could be observed. This result proves that in case of black seed oil, the official *PV* method covers not only hydroperoxides (or other similar products of fat oxidation) but also natural oxidizing compounds of the oil matrix.

The main component of black seed essential oil is thymoquinone, a pharmacologically active terpene with significant antioxidative properties (Burits & Bucar 2000, Butt & Sultan 2010). The structure of thymoquinone and characteristic NMR resonances of thymoquinone in a black seed oil are shown in figure 26.

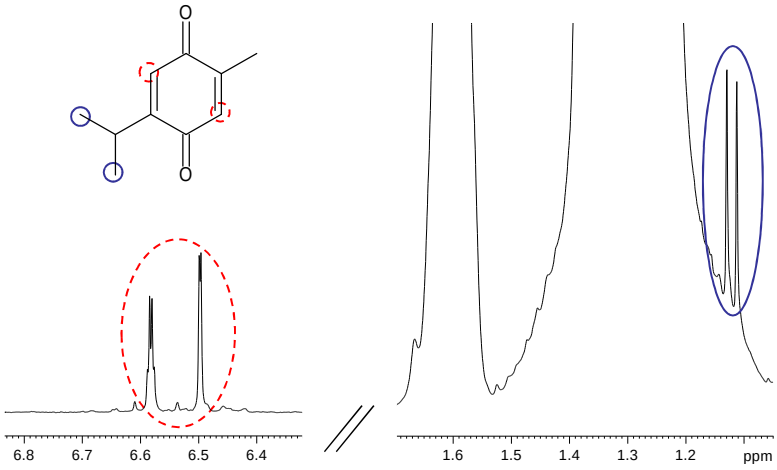

Fig. 26: ^{1}H NMR spectrum of a black seed oil containing thymoquinone as minor component.

Since quinones are commonly known for their strong redox activity, thymoquinone was a highly suspicious compound. Thus, a pure analytical thymoquinone standard was used for further investigations. Adding 2.4 mg/g thymoquinone to a black seed oil sample with an original thymoquinone content of 2.5 mg/g raised the classical *PV* from 32 to 61 meq/kg oil. This result indicates that thymoquinone has a strong effect on the *PV* according to Wheeler. Thymoquinone was identified as at least one compound of black seed oil that is responsible for the far too high *PVs*.

In the case of olive oil the *PVs* were too low compared with the values obtained by the NMR method. A total of 104 olive oils – mainly extra virgin olive oils - were investigated by both methods. As can be seen in figure 25, the individual olive oils vary considerably and exhibit a negative bias. Further investigations revealed that one possible reason might be the high content of specific phenolic compounds.

The total phenol content in extra virgin olive oil reaches from 50 to 800 mg/kg. It strongly depends on several factors including cultivar, degree of maturation, climate and to a high extent on the manufacturing process. The types of phenols in extra virgin olive oil are different from those of the olive fruit. Olives mainly contain the polar glycosides oleuropein and ligstroside, the esters of elenolic acid and hydroxytyrosol and tyrosol. During ripening, the aglycons are formed by beta-glucosidase activity. Due to hydrolytical processes hydroxytyrosol and tyrosol are formed in the olive oil (see figure 27). Their concentration is generally low in fresh oils but increases during oil storage (Soler-Rivas et al. 2000, Vissers et al. 2004).

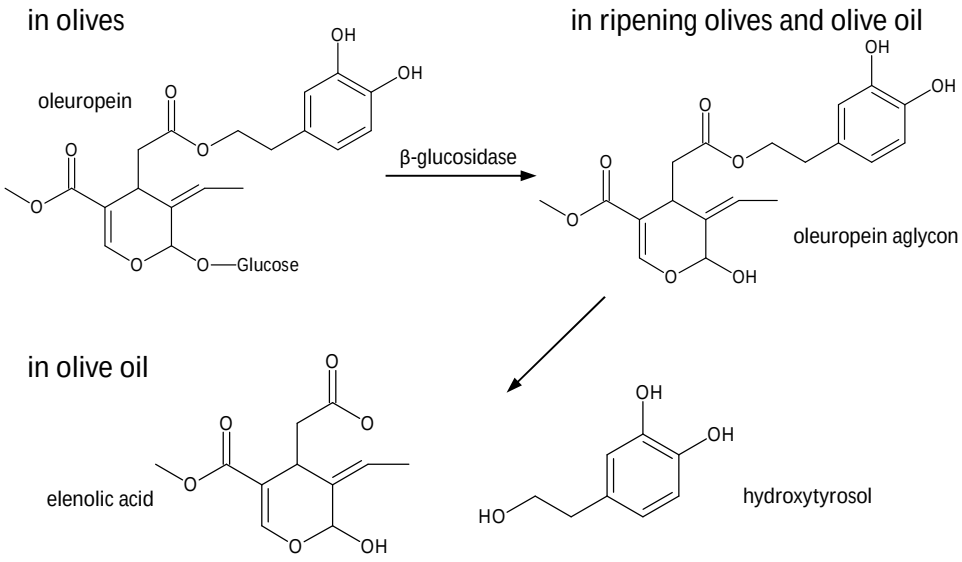

Fig. 27: Formation of hydroxytyrosol in olive oils (Vissers et al. 2004).

Servili and Montedoro reported an average value (for 116 olive oil samples) of 1.9 mg/kg for hydroxytyrosol and 349 mg/kg for secoiridoids that contain hydroxytyrosol in their structure (Servili & Montedoro 2002).

In order to investigate the influence of the hydroquinone hydroxytyrosol on the *PV* results, the pure hydroxytyrosol (10 mg/kg) standard was added to an olive oil. This led to a decrease of the *PV* of 4.8 meq/kg oil. This simple experiment clearly shows that hydroxytyrosol is one of the compounds occurring in the olive oil matrix that influences the *PV* determination and leads to erroneous *PV* results. This obviously means that for olive oils with high hydroxytyrosol content the *PV* is smaller in comparison to an olive oil with the same hydroperoxide content that has lower hydroxytyrosol amounts. This finding is of particular importance because virgin olive oil is a product of high commercial value that underlies a strict quality control. In the European Union the assessment of the quality of olive oils is regulated by the Commission Regulation (EEC) No 2568/91 on the characteristics of olive oil and olive-residue oil and on the relevant methods of analysis. It sets the limit of the *PV* according to Wheeler to 20 meq/kg for extra virgin olive oils and virgin olive oils, respectively, and to 5 meq/kg for refined olive oils.

The results clearly show that natural compounds of the oil matrix can have an influence on the *PV* according to Wheeler. Since the *PV* is a deterioration index that may be strongly affected by factors which have nothing to do with deterioration, a reevaluation of this parameter is suggested.

4. ^{1}H NMR determination of free fatty acids*

4.1 Method development

The ^{1}H NMR approach for the determination of FFAs in fats and oils is based on the integration of the carboxyl group proton (COO*H*) signal of FFAs. The carboxyl group is a protic group just like the hydroperoxide group. Thus it is strongly influenced by other protic groups being present in the sample solution (oil matrix components or solvent impurities). In pure $CDCl_3$ fast proton exchange processes cause line broadening or even make the COO*H* signal disappear (Günther 1996). However, for a sensitive integration narrow signals are an important requirement.

The influence of different proportions of DMSO-d_6 in the solvent mixture with $CDCl_3$ on the COO*H* signal was investigated. For this purpose a linseed oil was dissolved in mixtures of $CDCl_3$ with 0 %, 0.8 %, 1.7 %, 4.2 %, 8.3 %, 17 %, 25 % DMSO-d_6 and the sample solution was dried over a molecular sieve. The results are shown in figure 28. As it can be seen, even very small DMSO-d_6 amounts succeed to slow down proton exchange, so that the COO*H* signal can be detected. Increasing the DMSO-d_6 proportion in the solvent leads to a considerable downfield shift and to much narrower signals. The drying procedure with a molecular sieve prior to NMR analysis fortifies this effect, reducing the content of the protic compound H_2O in the sample solution.

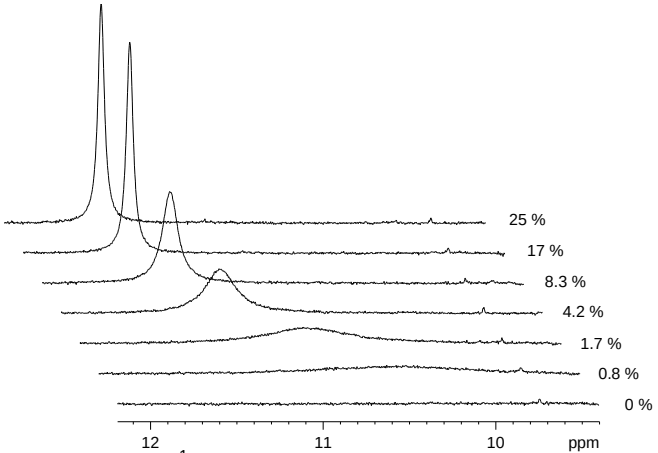

Fig. 28: Downfield region of the ^{1}H NMR spectrum of a linseed oil dissolved in different mixtures of $CDCl_3$/DMSO-d_6 with 0 % to 25 % DMSO-d_6 (v/v).

* Parts of this chapter are published in Skiera et al. (2012c) and Skiera et al. (2013)

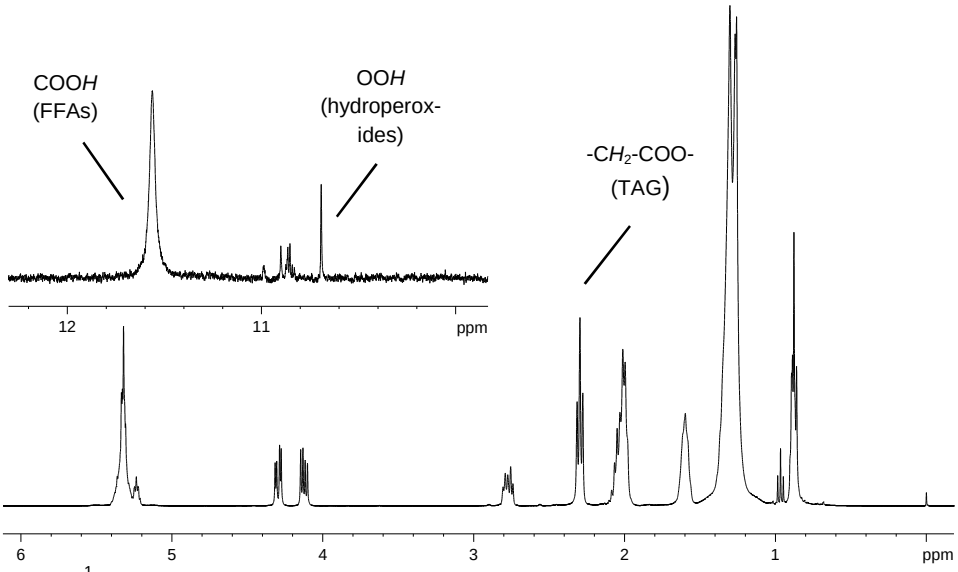

Fig. 29: ^{1}H NMR spectrum of a rapeseed oil dissolved in $CDCl_3$/DMSO-d_6 (5:1, v/v).

Based on these results the same sample preparation procedure as described in section 3.1 (with 17 % DMSO-d_6) was found to be optimal. It was applied for all further investigations. A typical ^{1}H NMR spectrum of a rapeseed oil is depicted in figure 29. The COO*H* protons of all FFAs resonate as singlet in the downfield region at about δ_H 11.6 ppm. For the quantification of FFAs, the COO*H* signal as well as the α-carbonyl-CH_2 signal resonating at δ_H 2.2 – 2.4 ppm (see figure 29) were integrated. To obtain the FFA amount in mmol/mol TAG the α-carbonyl-CH_2 signal area was normalized to 6000, since one TAG possesses six α-carbonyl-CH_2 protons.

4.2 Comparison with the classical *AV*

In order to find the mathematical equation that relates the NMR-determined molar FFA amount to the classical *AV*, the analytical standard palmitic acid was added to a refined rapeseed oil in different proportions and these mixtures were analysed by both methods. (The classical *AVs* of all samples were analysed according to the international standard ISO 660:2009). Then, the measured *AVs* were plotted versus the NMR-determined FFA amounts and a straight line was fitted to the data (see figure 30). Taking into account that both quantities are subject to error, Deming regression was applied (for details see section 3.4.1). The functional relationship between the *AV* and the NMR-determined FFA amount was found to be given by the equation:

$$y = 0.068x + 0.046 \qquad (19)$$

To compare the methods, the relative sensitivity of the NMR assay with respect to the *AV* method, $RS_{NMR/AV}$, was calculated (definition see section 3.4.1). The calculation of the relative sensitivity was done according to the mathematical procedure described in section 3.4.1. If $RS_{NMR/AV}$ appreciably exceeds unity, this would mean that of the two methods, the NMR approach has the greater ability to detect a difference in the actual FFA amount. The opposite conclusion holds when $RS_{NMR/AV}$ is clearly smaller than unity. The obtained result $RS_{NMR/AV}$ = 0.9 clearly indicates that both methods exhibit a similar analytical performance.

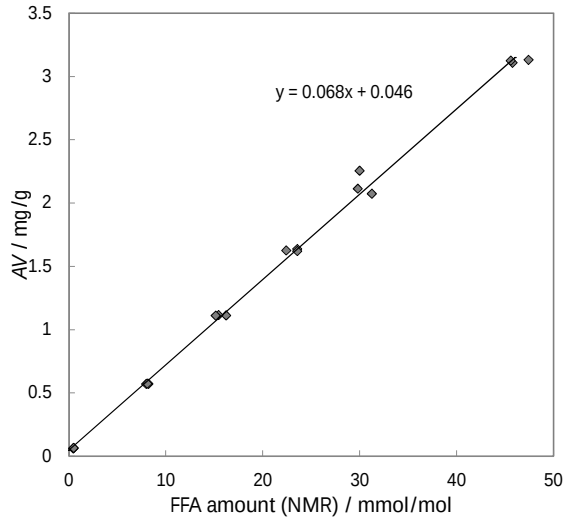

Fig. 30: *AV* in mg KOH/g oil versus the NMR-determined FFA amount in mmol/mol TAG (curve fitted by Deming regression).

420 oil samples of different oil varieties were analysed using both methods. The following oil types were chosen: olive oil (24 %), sunflower oil (21 %), rapeseed oil (14 %), nut oils (walnut oil, hazelnut oil, peanut oil, almond oil, grape seed oil, sesame oil, macadamia nut oil, pistachio oil) (11 %), thistle oil (9 %), pumpkin seed oil (7 %), maize oil (5 %), linseed oil (3 %), plant oil (composed of different vegetable oils), argan oil, soya oil, coconut oil and black seed oil. The classical *AVs* were plotted versus the NMR-determined molar FFA amounts. Figure 31 depicts the results and, additionally, the straight line given by equation 19. As can be seen, the data of the oils are in good agreement with equation 19. However, the results for the pumpkin seed oils exhibit systematic deviations. The classical *AVs* are slightly higher as one would expect in view of the NMR results. This may be explained by the dark colouring of pumpkin seed oil. For strongly coloured oils the titration method is not suitable since an exact determination of the phenolphthalein endpoint is not possible.

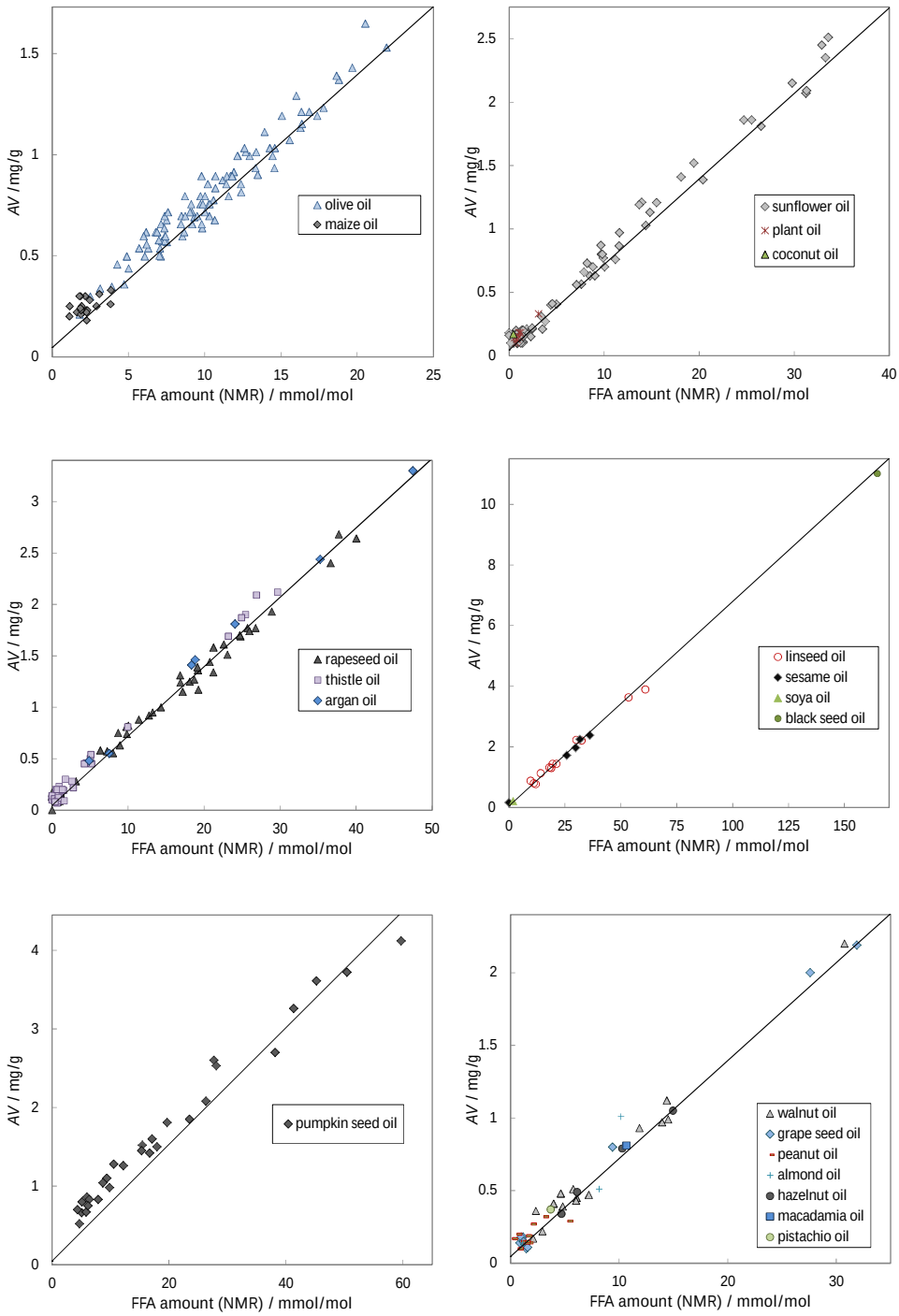

Fig. 31: Plot of the *AVs* versus the NMR-determined FFA amounts of 420 oil samples, overlaid by the straight line from equation 19.

4.3 Specialities of some pharmaceutical lipids

Most oil varieties examined in the last section (4.2) are commonly used both, in pharmaceuticals and as edible oils. These oil types include olive oil, sunflower oil, rapeseed oil, maize oil, peanut oil, linseed oil, sesame oil and soya oil. In the present section the applicability of the new ^{1}H NMR method to further lipids with relevance in pharmacy was tested.

Fatty oils

The molar FFA content of codliver oil, hard fat, cacao butter and castor oil was determined according to the ^{1}H NMR method described in section 4.1 with the only difference that the sample weight was reduced to 100 mg/1 ml solvent. The molar FFA amount in mmol/mol was converted into the AV_{NMR} using the model equation 19. Additionally the classical *AVs* of the same lipid samples were determined. The results for cod liver oil, cacao butter and hard fat are listed in table 7. The 95 % confidence intervals of the classical *AVs* were calculated on the basis of replicate measurements. For AV_{NMR}*s* the 95 % confidence intervals were determined via a bootstrapping procedure (see chapter 8.3).

Tab. 7 Comparison of AV_{NMR} and the classical AV.

Lipid	*AV* / mg KOH/g oil	AV_{NMR} / mg KOH/g oil
Cod liver oil	0.17 ± 0.07	0.15 ± 0.10
Cod liver oil*	2.9 ± 0.1	2.8 ± 0.1
Cacao butter 1	2.8 ± 0.1	2.9 ± 0.2
Cacao butter 2	3.3 ± 0.1	3.1 ± 0.1
Hard fat 1	0.18 ± 0.07	0.12 ± 0.01
Hard fat 1*	2.8 ± 0.1	2.2 ± 0.1
Hard fat 2*	3.3 ± 0.1	2.7 ± 0.1
Castor oil	0.85 ± 0.07	0.72 ± 0.10
Castor oil*	6.0 ± 0.1	6.1 ± 0.2

*spiked with palmitic acid

The results from both methods are in good agreement. Only in the case of hard fat, small deviations were observed. The results of two different hard fat samples spiked with pure palmitic acid are separately shown in table 7. The AV_{NMR}*s* are significantly smaller than the corresponding *AVs*. This result may be explained by the smaller average molecular weight of hard fat compared to that of rapeseed oil, the oil used to develop the model equation 19.

Hard fat is a mixture of mono-, di- and triacylglycerides of saturated C11 – C17 fatty acids with a lauric acid proportion of 37 % to 51 % (Blaschek et al. 2012), i.e. hard fat has a considerable smaller average molecular weight than rapeseed oil. To remedy this, it was proceeded as follows: The molar FFA content (mol FFA/g) was determined adding a defined amount of the internal reference standard TCNB to the weighted sample. The COO*H* signal at 11.4 ppm and the TCNB signal at 7.7 ppm were integrated and the AV_{NMR} in mg KOH/g was calculated according to equation 20:

$$AV_{NMR} = \frac{M_{KOH}}{m_{sample}} * \frac{m_{TCNB} * P_{TCNB}}{M_{TCNB}} * \frac{I_{COOH}}{I_{TCNB}} * 1000 \qquad (20)$$

(*m* denotes the mass in mg, *P* the purity, *M* the molecular weight in g/mol, and *I* the NMR integral area). The obtained result for the sample "hard fat 2 plus palmitic acid" of 3.2 ± 0.2 mg KOH/g shows a good compliance with the classical *AV* (3.3 ± 0.2 mg KOH/g).

The ^{1}H NMR spectrum of a castor oil did not exhibit any COO*H* signal, even when palmitic acid was added to the sample (25 mg per g sample). Further investigations were made in order to find the reason for this phenomenon. Castor oil differs from other plant oils concerning its fatty acid distribution. Ricinoleic acid, a mono-unsaturated C18-carbon fatty acid with a hydroxyl functional group on the twelfth carbon, accounts for 85 – 92 % of the fatty acid amount of castor oil (Ph. Eur. 2011). First of all, it was tested whether the alcohol group of ricinoleic acid was responsible for the absence of the COO*H* signal in the ^{1}H NMR spectrum. For this purpose 3-pentanol and ricinoleic acid methyl ester were added in different concentrations to a thistle oil (see figure 32 A and B). The spectra depicted in figure 32 A and B show that the presence of alcohol groups in the oil sample leads to a broadening of the COO*H* signal. Higher concentrations of 3-pentanol and ricinoleic acid methyl ester even cause the signal to disappear entirely. In the next step sample weight of castor oil was continuously reduced for a constant solvent volume (see figure 32 C). A similar effect was observed. At castor oil concentrations of 63 mg/0.6 ml or below, a COO*H* signal appeared in the NMR spectrum. Finally, the DMSO-d_6 amount in the solvent mixture was varied. The DMSO-d_6 proportion was increased from 17 % (usual solvent mixture) up to 83 % (v/v). This change of the solvent mixture also had a big effect on the COO*H* signal. From a DMSO-d_6 proportion of 33 % the signal became visible in the ^{1}H NMR spectrum (see figure 32 D).

Experiments with castor oil showed that the presence of alcohol groups in the sample solution leads to a strong broadening of the COO*H* signal and for high concentrations of alcohol groups even to a loss of the signal using

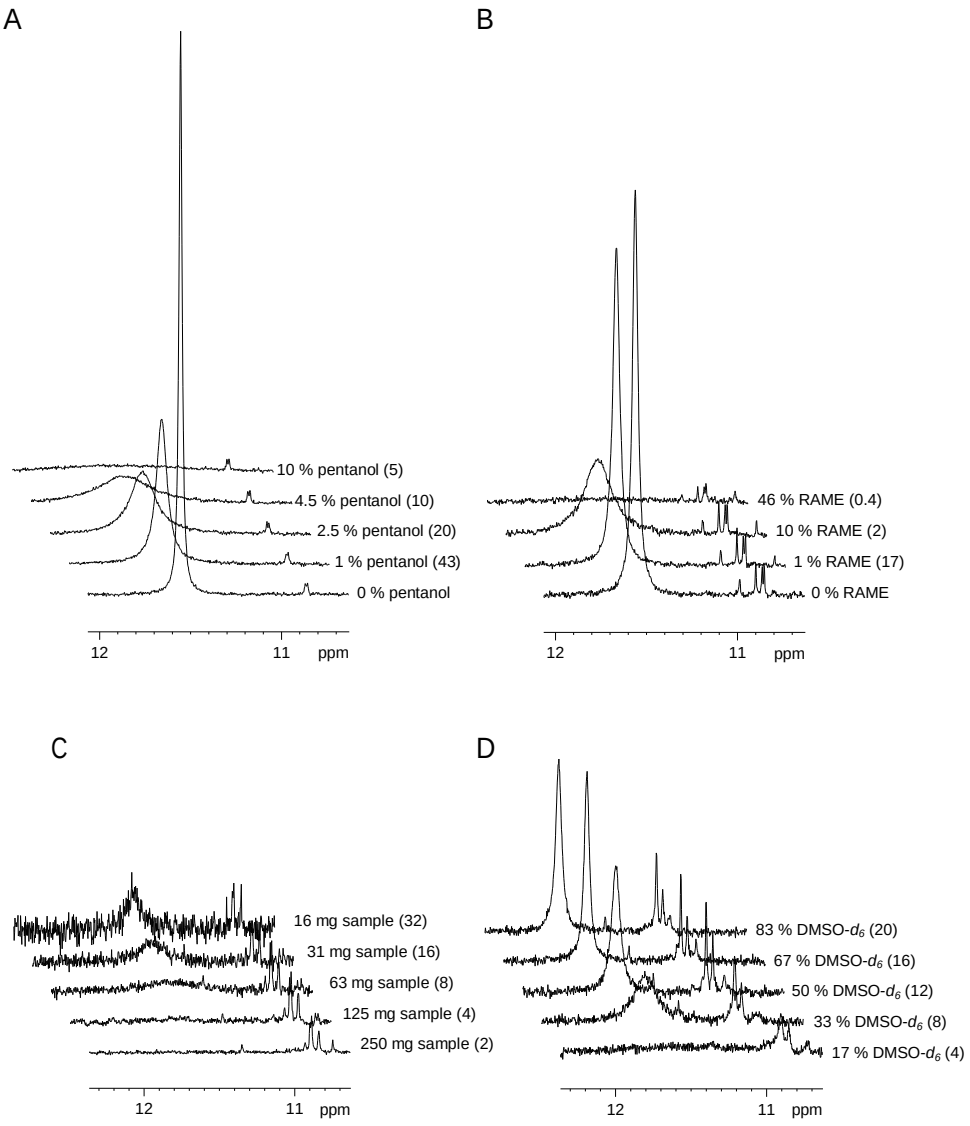

Fig. 32: Downfield region of the ^{1}H NMR spectra of A) a thistle oil spiked with 0 %, 1 %, 2.5 %, 4.5 %, 10 % 3-pentanol in a mixture of $CDCl_3$/DMSO-d_6 (5:1, v/v); B) a rapeseed oil spiked with 0 %, 1 %, 10 %, 46 % ricinoleic acid methyl ester (RAME) in a mixture of $CDCl_3$/DMSO-d_6 (5:1, v/v); C) a castor oil with a sample weight of 250 mg, 125 mg, 63 mg, 31 mg, 16 mg dissolved in 0.6 ml of a mixture of $CDCl_3$/DMSO-d_6 (5:1, v/v); D) a castor oil dissolved in a mixture of $CDCl_3$/DMSO-d_6 with 17 % DMSO-d_6, 33 % DMSO-d_6, 50 % DMSO-d_6, 67 % DMSO-d_6, 83 % DMSO-d_6. The factors in brackets give the calculated excess of DMSO-d_6 molecules in comparison to hydroxyl groups in the sample solution.

the solvent $CDCl_3$/DMSO-d_6 (5:1, v/v). There seems to be no difference between alcohol groups of a short-chain alcohol or the hydroxyl group that is present in ricinoleic acid. Alcohol groups are protic groups, this means that they contain easily exchangeable protons. The simultaneous presence of carboxyl and hydroxyl groups in the sample solution may affect fast proton exchange between both functional groups. DMSO-d_6 has the ability to slow down proton exchange processes forming strong hydrogen bonds with protic groups. Both effects compete against each other. Depending on the molar concentration of hydroxyl groups and DMSO-d_6 in the sample solution, the one or the other effect predominates. In contrast to other plant oils, castor oil contains up to 92 % of ricinoleic acid, thus the sample solution possesses a strong excess of protic groups. Applying the original sample preparation procedure (see section 4.1) to castor oil, the amount of DMSO-d_6 molecules in the sample solution is not sufficient to slow down proton exchange in a way that COO*H* signals can be observed. Reducing the castor oil concentration, while keeping the DMSO-d_6 concentration constant (see figure 32 C), leads to a reduction of the amount of hydroxyl groups. The concentration ratio changes in favour of DMSO-d_6 and the COO*H* signals become visible in the spectrum. The same applies for the increase of the proportion of DMSO-d_6 in the solvent mixture (see figure 32 D). The legend of figure 32 A-D contains for every ^{1}H NMR spectrum a factor that gives the molar excess of DMSO-d_6 molecules in comparison to hydroxyl groups in the sample solution. Generally, a fivefold to tenfold DMSO-d_6 excess was necessary for the COO*H* signal to become visible in the spectrum. In consequence of these results the sample preparation procedure for castor oil was modified as follows: 20 mg of sample were dissolved in 0.8 ml $CDCl_3$/DMSO-d_6 (2:1, v/v) and directly measured by NMR after drying over a molecular sieve. The obtained NMR results were in good agreement with the results of the classical *AV* method (see table 7).

Oleyl oleate

The model equation to convert the molar FFA amount to the AV_{NMR} cannot be applied for oleyl oleate, since it is not a TAG. Oleyl oleate consists of the esters of oleic acid and a mixture of unsaturated fatty alcohols, mainly (*Z*)-9-octadecenyl alcohol (Blaschek et al. 2012). Therefore, a different approach was required. The molar FFA amount in "mol FFA/mol oleyl oleate" is given by the relative integral of the COO*H* signal of FFAs, when the α-carbonyl-CH_2 integral is normalized to two. Considering the molecular weight of oleyl oleate and of potassium hydroxide, the molar FFA amount can be converted into the AV_{NMR} in mg KOH/g according to the following equation:

$$AV_{NMR} = c * \frac{M_{KOH}}{M_{Oleyl\ oleat}} * 1000 \quad (21)$$

(*c* denotes the molar FFA amount in mol/mol and *M* the molecular weight in g/mol). The average molecular weight of oleyl oleate was assumed to be the molecular weight of oleic acid oleyl ester. The obtained AV_{NMR}*s* are in good agreement with the classical *AVs* (see table 8) (note: The 95 % confidence intervals of *AV* and AV_{NMR} were determined on the basis of replicate measurements.).

Tab. 8 Comparison of AV_{NMR} and the classical AV of oleyl oleate.

Lipid	*AV* / mg KOH/g oil	AV_{NMR} / mg KOH/g oil
Oleyl oleate	0.12 ± 0.07	0.08 ± 0.07
Oleyl oleate*	2.8 ± 0.1	2.7 ± 0.1

*spiked with palmitic acid

Waxes

Similar to oleyl oleate, the original ^{1}H NMR method cannot be directly applied to waxes. Instead, the procedure described for hard fat was used. Since the solubility of white beeswax (Cera alba) and yellow beeswax (Cera flava) in the solvent mixture of $CDCl_3$ and DMSO-d_6 (5:1, v/v) is very low, the sample weight was reduced to 5 mg/1 ml. For wool wax and artificial spermaceti 100 mg of sample were dissolved in 1 ml. The spectra were processed and integrated three times. The mean values are depicted in table 9 (note: The uncertainty of measurement was not estimated since no replicate measurements were performed). The mean AV_{NMR}*s* are in good agreement with the classical *AVs* of the waxes.

Tab. 9 Comparison of AV_{NMR} and the classical AV of waxes.

Lipid	*AV* / mg KOH/ g oil	AV_{NMR} / mg KOH/ g oil
Cera flava 1	18.3	18.2
Cera flava 2	21.6	20.8
Cera alba	21.4	19.7
Wool wax	0.93	0.82
Wool wax*	3.0	2.8
Artificial spermaceti	0.22	0.17
Artificial spermaceti*	2.8	2.6

*spiked with palmitic acid

4.4 Saponification value

An additional index providing information on the acid content of lipids is the so-called saponification value (*SV*). This parameter is determined titrimetrically after saponification and comprises free and bound fatty acids (ISO 3657:2002). The *SV* directly correlates with the average molecular weight of lipids. The smaller the average molecular weight, the greater the *SV*. Up to now, the *SV* is still of some importance in pharmacy. For several lipids this index is part of the quality requirements given by the monographs of the Ph. Eur. ^{1}H NMR spectroscopy provides a fast and simple alternative to the classical *SV* determination. A defined amount of sample and of the internal standard TCNB are dissolved in a deuterated solvent (here: $CDCl_3$) and analysed by ^{1}H NMR. The obtained spectrum is processed manually and the TCNB signal at δ_H 7.7 ppm and the α-carbonyl-CH_2 signal at δ_H 2.2 – 2.4 ppm are integrated. The SV_{NMR} is calculated according to the following equation:

$$SV_{NMR} = \frac{M_{KOH}}{m_{sample}} * \frac{m_{TCNB} * P_{TCNB}}{M_{TCNB}} * \frac{\frac{1}{2} * I_{\alpha-Carbonyl-CH_2}}{I_{TCNB}} * 1000 \qquad (22)$$

(*m* denotes the mass in mg, *P* the purity, *M* the molecular weight in g/mol, and *I* the NMR integral area). In a small study the *SVs* of five lipid samples were determined by both the classical and the NMR method. The following lipids were chosen: linseed oil, hard fat, cacao butter, peanut oil and rapeseed oil. The results are listed in table 10. For both methods only single measurements were performed. The ^{1}H NMR spectra were processed and integrated three times and the mean value was calculated. The results given in table 10 indicate that both methods lead to comparable results. However, further data are required to confirm this.

Tab. 10 SV and SV_{NMR} of different lipid samples.

Lipid	*SV* / mg KOH/g oil	SV_{NMR} / mg KOH/g oil
Linseed oil	188	189
Hard fat	234	236
Cacao butter	189	191
Peanut oil	186	186
Rapeseed oil	193	191

Note: No uncertainty given, since only single measurements were performed.

5. ^{1}H NMR determination of aldehydes*

5.1 Method development

The sample preparation procedure optimized for the determination of hydroperoxides and FFAs (see section 3.1 and 4.1) was tested for different edible oils. The resulting spectra were compared to the spectra that were obtained when the same edible oils were simply dissolved in $CDCl_3$. Since signal heights and signal shapes of the carbonyl group proton (C*H*O) resonances of aldehydes were slightly better in $CDCl_3$, this solvent was chosen for the quantification of aldehydes. According to literature (Guillén & Goicoechea 2009, Guillén & Ruiz 2008), different aldehyde species are formed by the oxidation of edible oils depending on the oxidizing conditions and the oil type, like n-alkanals, (*E*)-2-alkenals, (*E*,*E*)-2,4-alkadienals, (*Z*,*E*)-2,4-alkadienals, 4,5-epoxy-(*E*)-2-alkenals, 4-hydroxy-(*E*)-alkenals and 4-hydroperoxy-(*E*)-alkenals. For chemical structures see figure 33. Examination of the ^{1}H NMR spectra of 400 oil samples within the course of this thesis revealed that the aldehyde concentrations in commercial edible oils generally are low and that mainly the three aldehyde species n-alkanals, (*E*)-2-alkenals and (*E*,*E*)-2,4-alkadienals are detected. The aldehyde proton region of a mixture of n-hexanal, (*E*)-2-hexenal and (*E*,*E*)-2,4-hexadienal (as well as (*Z*,*E*)-2,4-hexadienal as an impurity of the (*E*,*E*)-2,4-hexadienal standard) is shown in figure 34.

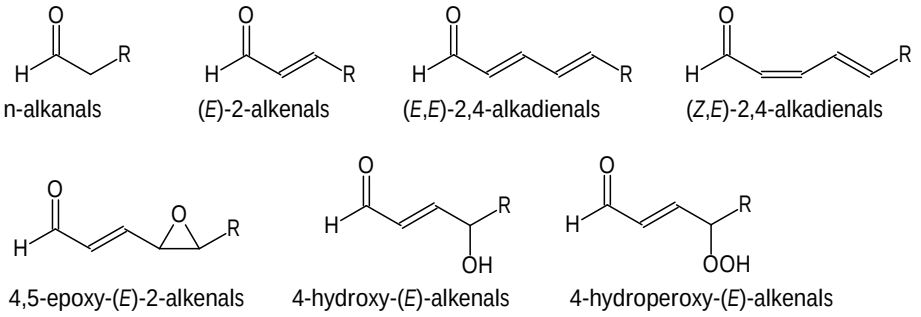

Fig. 33: Aldehyde species in fats and oils (Guillén & Goicoechea 2009).

* Parts of this chapter are published in Skiera et al. (2012b)

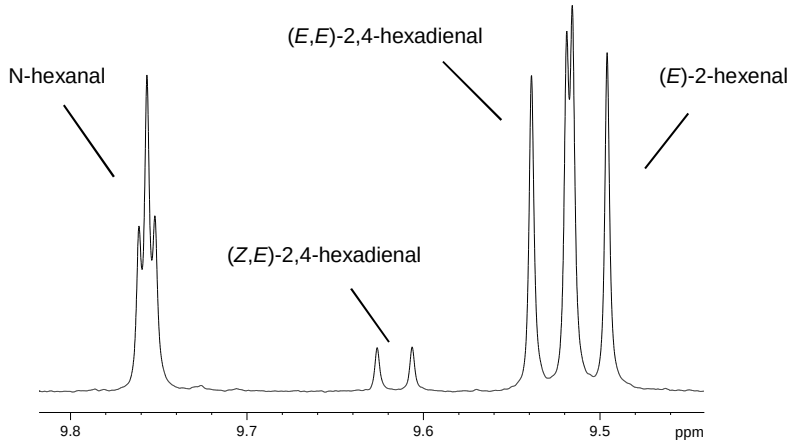

Fig. 34: Carbonyl region of the ^{1}H NMR spectrum of a mixture of n-hexanal, (*Z*,*E*)-2,4-hexadienal, (*E*,*E*)-2,4-hexadienal and (*E*)-2-hexenal.

The C*H*O protons of n-alkanals resonate as triplet at δ_H 9.76 ppm, C*H*O protons of (*E*)-2-alkenals as doublet at δ_H 9.51 ppm and C*H*O protons of (*E*,*E*)-2,4-alkadienals as doublet at δ_H 9.53 ppm. The lower chemical shifts (about 0.25 ppm) of the unsaturated aldehydes in comparison to saturated aldehydes may be explained by the magnetic anisotropic effect of the C=C double bond (see figure 35).

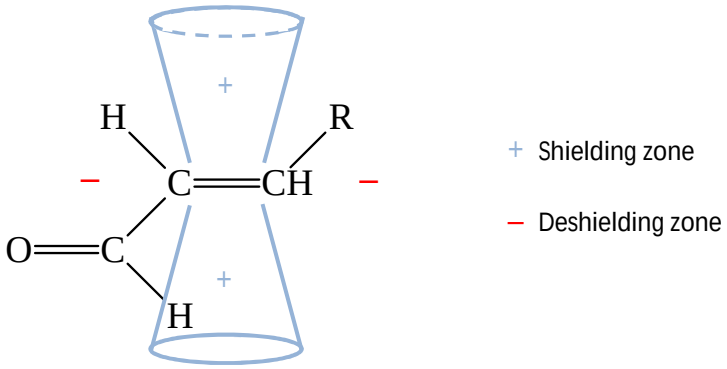

Fig. 35: Possible explanation of the observed shift differences of saturated and unsaturated aldehydes.

In order to quantify the individual aldehyde species the C*H*O signals were integrated as well as the proton signal of the glyceryl methylene group (glyceryl-CH_2) appearing at δ_H 3.8 – 4.6 ppm. To determine the aldehyde amount in mmol/mol TAG the integral of the glyceryl-CH_2 signal was normalized to a value of 4000 (one TAG possesses four glyceryl-CH_2 protons) (see figure 36). The processing and integration for every spectrum was performed three times. For further calculations the mean values were used.

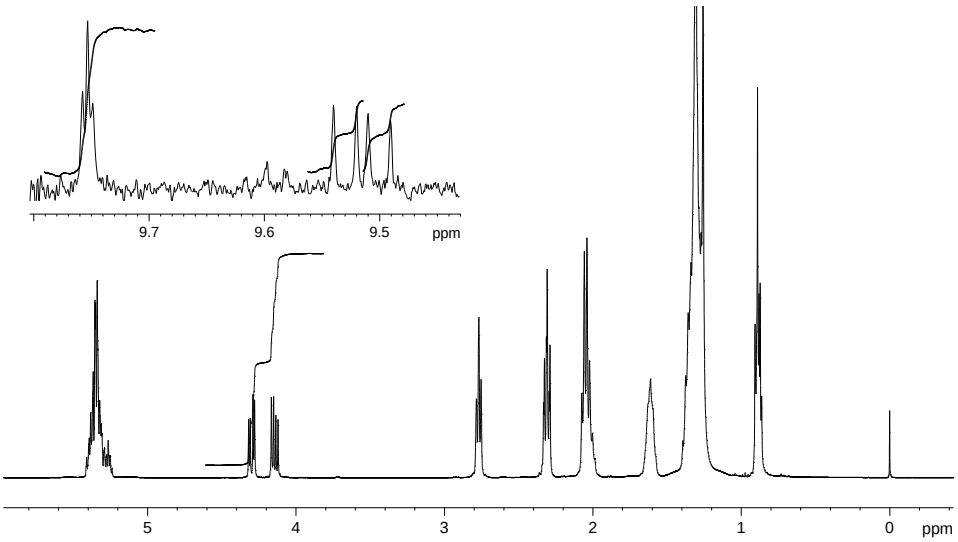

Fig. 36: ^{1}H NMR spectrum of a grape seed oil with zoomed downfield region.

5.2 Model to determine *ANV*$_{NMR}$

The *ANV* method is based on the UV/VIS spectroscopic measurement of the reaction product between p-anisidine and the aldehydes in the test solution (ISO 6885:2006). The classical *ANV* is a sum parameter depending not only on the aldehyde concentration in the sample, but also to a large extent on the molecular structure of the aldehydes. According to Pardun (Pardun 1974) the reaction products of p-anisidine with alkanals, 2-alkenals and 2,4-alkadienals (see figure 37) possess different absorption maxima and absorption coefficients at the measurement wavelength (350 nm). For example, the reaction product of an unsaturated aldehyde exhibits a higher absorption coefficient at $\lambda = 350\ \mathrm{nm}$ than derivatives of saturated aldehydes. As a consequence, unsaturated aldehydes give higher *ANV* results than saturated aldehydes, e.g. *ANVs* obtained from n-hexanal and (*E*)-2-heptenal (Pardun 1974, Kamal-Eldin & Pocorny 2005).

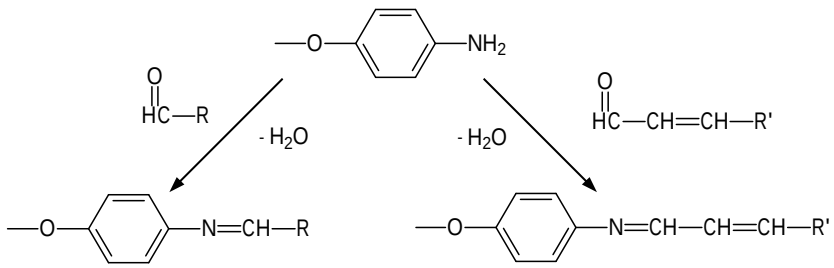

Fig. 37: Reaction of saturated and unsaturated aldehydes with p-anisidine.

To establish an equation that relates the *ANV* to the normalized NMR integrals of aldehydes, the following assumptions were made:

1. The *ANV* of a specific aldehyde species (i.e. n-alkanals, (*E*)-2-alkenals and (*E*,*E*)-2,4-alkadienals) is directly proportional to the corresponding normalized NMR integral.
2. The *ANV* of a mixture represents a linear combination of the normalized NMR integrals of the aldehydes.
3. Aldehydes of the same species with different chain length exhibit the same coefficients (e.g. $a_{hexanal} = a_{nonanal}$).

N-hexanal, (*E*)-2-hexenal and (*E*,*E*)-2,4-hexadienal were chosen as model aldehydes. For each compound six different mixtures of the aldehyde standard and Delios V (an artificial TAG solely consisting of saturated middle chain fatty acyl residues) were prepared. These mixtures were analysed by both the novel ^{1}H NMR method and the classical *ANV* method. The data are given in figure 38.

For n-hexanal and (*E*)-2-hexenal a model of the form

$$ANV = ax + \varepsilon \tag{23}$$

(*a* denotes the compound specific coefficient, *x* the normalized NMR integral and ε the random error) was fitted to the respective data set by least squares regression (Draper & Smith 1998) to obtain the estimates $\hat{a}_{alkanal}$ und $\hat{a}_{alkenal}$. Since the (*E*,*E*)-2,4-hexadienal standard contains 12 % of its isomer (*Z*,*E*)-2,4-hexadienal as a contaminant, the following model was applied to the corresponding data set:

$$ANV = a_{alkadienal}x_{alkadienal} + a_{(Z,E)}x_{(Z,E)} + \varepsilon \tag{24}$$

Table 11 shows the calculated coefficients and the associated 95 % confidence intervals. The coefficient $\hat{a}_{(Z,E)}$ does not deviate significantly from zero. This can be explained by the relatively small proportion of (*Z*,*E*)-2,4-hexadienal combined with the low precision of the *ANV* and the low precision of the integrals of the small NMR signals. Since (*Z*,*E*)-2,4-hexadienal is in general not present in commercial oil samples, $\hat{a}_{(Z,E)}$ is not relevant for our model.

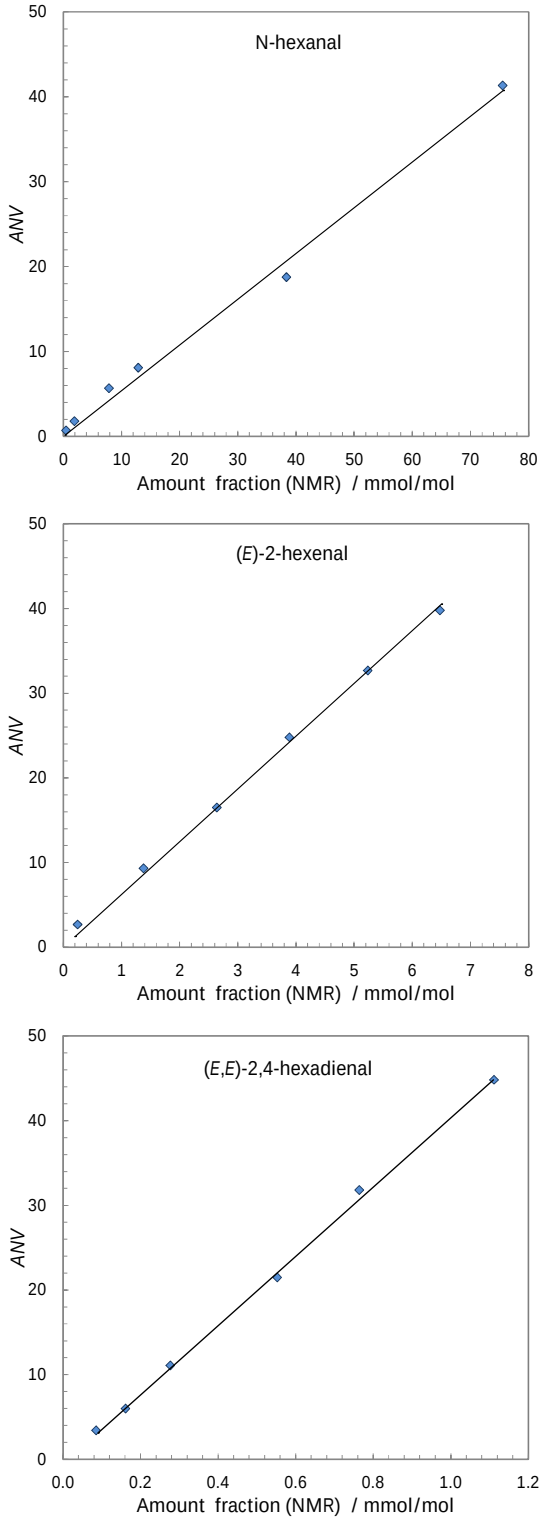

Fig. 38: Plots of the *ANV* versus the NMR-determined amount fraction for the aldehyde standards.

Tab. 11. Compound specific coefficients to model the ANV.

Aldehyde standards	Coefficients	95 % Confidence intervals
n-hexanal	$\hat{a}_{alkanal}$ = 0.54	[0.50 - 0.58]
(*E*)-2-hexenal	$\hat{a}_{alkenal}$ = 6.2	[6.0 - 6.4]
(*E*,*E*)-2,4-hexadienal	$\hat{a}_{alkadienal}$ = 34	[21 - 48]
(*Z*,*E*)-2,4-hexadienal	$\hat{a}_{(Z,E)}$ = 44	[–54 - 143]

The coefficients of n-hexanal, (*E*)-2-hexenal and (*E*,*E*)-2,4-hexadienal are considerably different. $\hat{a}_{alkenal}$ exceeds $\hat{a}_{alkanal}$ 12 times and $\hat{a}_{alkadienal}$ is even 63 times higher than $\hat{a}_{alkanal}$! This means that (*E*)-2-hexenal contributes 12 times more to the *ANV* than n-hexanal and (*E*,*E*)-2,4-hexadienal contributes 63 times more to the *ANV* than n-hexanal. These findings are in agreement with the results of Pardun (Pardun 1974). He found that the absorption of the (*E*)-2-heptenal product is 12 times higher and the absorption of the (*E*,*E*)-2,4-decadienal product is 40 times higher than the absorption of the n-hexanal product. Combining our results, we can express the *ANV* as

$$ANV = 0.54x_{alkanal} + 6.2x_{alkenal} + 34x_{alkadienal} \quad (25)$$

where $x_{alkanal}$, $x_{alkenal}$ and $x_{alkadienal}$ designate the ^{1}H NMR determined molar concentration of n-alkanals, (*E*)-2-alkenals and (*E*,*E*)-2,4-alkadienals.

5.3 Verification of the model

In order to verify the model, 79 commercial oil samples were measured by both methods (data see table 20). The modelled *ANVs* were plotted versus the classical *ANVs* and a straight line was fitted to the data (see figure 39). Taking into account that both quantities are subject to error, Deming regression was applied (Mandel 1964). 95 % confidence intervals were calculated for both the empirical and the modelled *ANV*. If the confidence intervals overlap, then both *ANVs* are considered to be not significantly different. (Note: This way of proceeding is in fact overly conservative but in our case more convenient.) 86 % of the oil samples with *ANVs* above 0.9 showed overlapping confidence intervals. The aldehyde signals in the ^{1}H NMR spectrum of oils with *ANVs* below 0.9 were often too small for a precise integration.

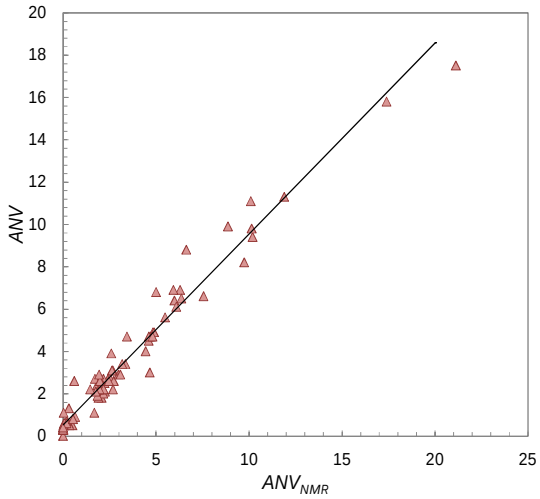

Fig. 39: Plot of the *ANVs* versus the NMR-determined *ANVs* of 79 oil samples.

In conclusion it appears that the NMR method is suitable to reproduce the results of the classical *ANV* method. Yet, in contrast to the latter, the NMR method has the crucial advantage of providing quantitative information on the content of individual aldehyde species.

6. Conclusion

The principal idea of this thesis was to check weather the simple measurement of an ^{1}H NMR spectrum can replace the conventional methods used in pharmaceutical analysis and food chemistry. It appears that the newly developed ^{1}H NMR methods are suitable to reproduce the classical fat indices *PV*, *AV* and *ANV* of fats and oils by providing the molar amounts of hydroperoxides, FFAs and aldehydes, respectively. They are an excellent alternative to the conventional determination of fat indices and offer several advantages over the classical methods:

Generally, NMR spectroscopy is a fast and non-destructive technique for which only simple and minor sample preparation is needed. In contrast to the classical wet-chemical methods, the ^{1}H NMR measurements require only small solvent volumes and no toxic chemicals like p-anisidine. A big advantage of the NMR methods is the notable saving in time. One NMR experiment takes about 25 minutes. On the first view this seems to be quite long compared to a titration procedure, but it must be taken into account that NMR experiments can be run automatized (autosampler) and that from one ^{1}H NMR spectrum of a fat or oil different analytical parameters can be obtained simultaneously, including

- the deterioration markers hydroperoxides, free fatty acids and aldehydes,
- a rough fatty acid distribution,
- minor compounds in fats and oils like squalene (olive oil) or thymoquinone (black seed oil).

Furthermore, adulteration or contamination of fats and oils may be assessed using statistical data evaluation methods, e.g. PCA (Mannina et al. 2009, Fauhl et al. 2000).

Unlike the classical quality indices that are merely sum parameters, the novel ^{1}H NMR methods have the crucial advantage of being highly selective and of providing quantitative information about individual hydroperoxide and aldehyde species. The comparison of the classical *PV* method with the ^{1}H NMR method clearly showed that the classical method leads to erroneous results in the case of black seed oil and olive oil since the oil matrix of these oils has an influence on the *PV* results. It was shown that the *PV* is a deterioration index that may be strongly affected by factors which have nothing to do with deterioration.

However, despite these benefits, NMR spectroscopy has not been widely established yet in routine analysis of fats and oils. One reason might be that, up to now, NMR spectroscopy is not part of the classical equipment of laboratories that conduct lipid analysis and that this technique requires high investment and maintainance costs as well as skilled operators.

In addition, the classical fat indices are still firmly established in Ph. Eur. and legislation on edible fats and oils, i.e. legally binding limits for these indices exist. Since the classical deterioration indices can be misleading, it appears reasonable to replace statutory provisions on quality indices by the concentrations of deterioration markers, which can be directly determined using techniques like the NMR methods described in this thesis.

7. Experimental

7.1 Material

7.1.1 Apparatus

NMR spectrometer	Bruker Advance 400 MHz, Bruker Biospin (Rheinstetten, Germany)
NMR probe head	PA SEI 40081HCD05 Z BOT, Bruker Biospin (Rheinstetten, Germany)
Analytical balance	Satorius Micro MC 210 P, Satorius GmbH (Göttingen, Germany)
Precision balance	MC1 LC 6200 S, Satorius GmbH (Göttingen, Germany)
Centrifuge	Varifuge 30R Sepatech, Heraeus (Kleinostheim, Germany)
Vortex mixer	VWR International GmbH (Darmstadt, Germany)
Shaker	Compact shaker KS 15B control, Edmund Bühler GmbH (Hechingen, Germany)
Universal oven	Model UFB 500, Memmert (Schwabach, Germany)
Ultrasonic bath	Sonorex digitec, Bandelin (Berlin, Germany)
UV/VIS spectrometer	Specord 200, Analytikjena (Jena, Germany)
Pipettes	Reference, Eppendorf (Hamburg, Germany), Multipette@ plus, Eppendorf (Hamburg, Germany)

7.1.2 Consumables

NMR sample tube	(thin walled) 5 mm*178 mm, VWR International GmbH (Darmstadt, Germany)
Plastic tube (15 ml)	Sarstedt (Numbrecht, Germany)
Screw top vial G4 (4 ml)	Ziemer (Langerwehe, Germany)
Screw top vial G8 (8 ml)	Ziemer (Langerwehe, Germany)
Pipette tips	Eppendorf (Hamburg, Germany)

7.1.3 Samples, standards and chemicals

Fat, oil and wax samples and oleyl oleate were provided by the Chemisches und Veterinäruntersuchungsamt Karlsruhe and the University of Würzburg. Delios® V, an artificial TAG consisting mainly of capryl and capric acid, was donated from Cognis (Mannheim, Germany).

Methyl oleate (>99 %)	Sigma-Aldrich (Taufkirchen, Germany)
Methyl linoleate (99.0 %)	Sigma-Aldrich (Taufkirchen, Germany)
Methyl linolenate (99.3 %)	Sigma-Aldrich (Taufkirchen, Germany)
Methyl ricinoleate (>99 %)	Sigma-Aldrich (Taufkirchen, Germany)
Trioleate (>97 %)	Sigma-Aldrich (Steinheim, Germany)
Trilinoleate (≥98 %)	Sigma-Aldrich (Taufkirchen, Germany)
Thymoquinone (99 %)	Sigma-Aldrich (Taufkirchen, Germany)
Hydroxytyrosol (>98 %)	Applichem (Darmstadt, Germany)
Palmitic acid (99.7 %)	Cognis (Mannheim, Germany)
Squalene (≥98 %)	Sigma-Aldrich (Taufkirchen, Germany)
Hexanal (for synthesis)	Merck (Ulm, Germany)
(*E*)-2-hexen-1-al (98 %)	Sigma-Aldrich (Taufkirchen, Germany)
(*E*,*E*)-2,4-hexadienal (98.1 %)	Sigma-Aldrich (Taufkirchen, Germany)
Na_2SO_4 (water-free) (≥99 %)	Sigma-Aldrich (Taufkirchen, Germany)
Molecular sieve (5 Å)	Merck (Darmstadt, Germany)
$CDCl_3$ (99.8 atom% D)	Roth (Karlsruhe, Germany)
DMSO-d_6 (99.9 atom% D)	Merck (Ulm, Germany)
Benzene-d_6 (99.5 atom% D)	Roth (Karlsruhe, Germany)
Acetone-d_6 (99.8 atom% D)	Euriso-top (Saarbrücken, Germany)
TMS (>99.9 %)	Roth (Karlsruhe, Germany)
TCNB, standard for quantitative NMR (99.66 %)	Sigma-Aldrich (Taufkirchen, Germany)

Chemicals for the determination of the classical fat indices *PV*, *AV*, *ANV* and *SV* were of analytical grade and complied with the requirements of the ISO standards: ISO 3960:2007, ISO 660:2009, ISO 6885:2006, ISO 3657:2002, respectively.

7.2 Methods

7.2.1 Standard NMR experiment

The data acquisition on the Bruker 400 MHz spectrometer was performed with TOPSPIN version 2.1 (Bruker, Rheinstetten, Germany). The ^{1}H NMR experiments were carried out at 300 K without spinning the sample using a flip angle of 30°. The standard acquisition and processing parameters were:

Spectral width	20.5396 ppm
Acquisition time	7.97 s
Relaxation delay	1 s
Number of scans	128
Number of dummy scans	2
Data points	128 K
Processed data points	128 K
Window function	EM
Lb value	0.3 Hz

For quantifications with the internal standard TCNB the relaxation delay was adjusted to 10 s.

To enhance the resolution of the spectra of oxidized trioleate and oxidized trilinoleate (depicted in figure 18, 19 and 20), the FIDs were multiplied with a Lorentz-Gauss function. The following settings were chosen: $gb = 0.33, lb = -0.3$.

7.2.2 Inversion recovery experiment

T_1 measurements were performed applying the inversion recovery impulse sequence (t1ir) for all quantified compounds. For the T_1 determination the following samples were used:

OO*H* signals: oxidized standards of methyl oleate, methyl linoleate, trioleate and trilinoleate
COO*H* signals of FFAs, α-carbonyl-CH_2 signals of TAGs, TCNB signal: different lipid samples (Cera alba, Cera flava, hard fat, olive oil, walrat) spiked with palmitc acid and TCNB

C*H*O signals of aldehydes, glyceryl-CH_2 signals of TAGs: sunflower oil spiked with n-hexanal, (*E*)-2-hexenal and (*E*,*E*)-2,4-hexadienal

The lipid samples were prepared using the preparation procedures described in section 7.2.3. The number of experiments and delay times τ between the 180° and 90° pulses were individually set according to the results of preliminary tests. The main acquisition and processing parameters of the inversion recovery experiment are listed below:

Spectral width	20.8 ppm
Acquisition time	0.99 s
Relaxation delay	25 s
Number of scans	2
Number of dummy scans	2
Data points F1	16
Data points F2	8 K
Window function F2	EM
Window function F1	SINE
Lb value	1 Hz

To determine the T_1 relaxation times, τ_0 (τ when the signal intensity is zero) was estimated from the obtained spectra and T_1 was calculated according to the equation $\tau_0 = T_1 ln2$. The following T_1 values were obtained:

α-Carbonyl CH_2	0.7 - 0.8 s
Glyceryl-CH_2	0.4 s
OO*H*	1.5 – 3.0 s
COO*H*	1.6 – 2.2 s
TCNB	5.0 – 5.6 s
C*H*O (hexanal)	3.3 s
C*H*O ((*E*)-2-hexenal)	3.6 s
C*H*O ((*E*,*E*)-2,4-hexadienal)	4.6 s

7.2.3 Sample preparation procedures

For the determination of the molar concentration of hydroperoxides and FFAs, the sample (250 mg) was dissolved in 0.6 ml of a mixture of $CDCl_3$ and DMSO-d_6 (5:1, v/v) and a small proportion of tetramethylsilane (TMS) as an internal reference. Then the sample was dried over molecular sieve by shaking. After about 20 to 30 min of shaking, this mixture was placed in a 5-mm diameter NMR tube. (Note: The first 60 oil samples were dried over sodium sulfate (Na_2SO_4) instead of molecular sieve.)

For the determination of the molar concentration of aldehydes the sample (200 mg) was dissolved in 0.8 ml $CDCl_3$ and analysed by ^1H NMR.

7.2.4 Classical fat indices

PV: The *PV* of all samples was analysed according to the international standard ISO 3960:2007. The sample was dissolved in a mixture of isooctane and glacial acetic acid. Then a saturated potassium iodide solution was added to the sample and the liberated iodine was titrated with a thiosulfate solution and starch as an endpoint indicator. In the case of *PV*s above 30 meq/kg the procedure was modified as follows: In spite of 5 g, 1 to 2 g sample were weighted.

AV: The *AV* of all samples was determined according to the international standard ISO 660:2009. The sample was dissolved in a mixture of ethanol and diethylether and titrated with a potassium hydroxide solution to the phenolphthalein endpoint.

ANV: The *ANV* was analysed according to the international standard ISO 6885:2006. The sample was dissolved in isooctane and brought to reaction with p-anisidine (in acetic acid). The increase in absorbance at 350 nm was measured and the *ANV* was calculated.

SV: The *SV* was determined according to the international standard ISO 3657:2002. A known quantity of sample was refluxed with an excess amount of ethanolic potassium hydroxide. After saponification, the remaining excessive potassium hydroxide was titrated against hydrochloric acid to the phenolphthalein endpoint.

7.2.5 Sample oxidation

Methyl oleate, methyl linoleate, triloleate and trilinoleate were oxidized in an open plastic vessel at 40 °C in the dark. Methyl linolenate was oxidized at -25 °C in a closed glass vessels in the dark.

7.2.6 Oxidation kinetics of trioleate

1.3 g trioleate standard were stored in a compartment dryer at 40 °C in an open glass vessel in the dark. Aliquots of 208 mg were taken after 0, 7, 11, 14 and 16 days and aliquots of 100 mg after 18, 20 and 25 days. The trioleate aliquots were dissolved in $CDCl_3$ (208 mg/0.5 ml or 100/0.6 ml) and directly analysed by ^1H NMR. Six spectral regions were defined (see figure 20). In every region, the molar hydroperoxide amount in mmol/mol TAG was determined. For that purpose, all resonances in one region were integrated as well as the glyceryl-CH_2 signal at δ_H 3.9 – 4.6 ppm and the glyceryl-CH_2 signal was normalized to 4000 (one TAG possesses four glyceryl-CH_2 protons). The molar hydroperoxide amounts are listed in table 12.

7.2.7 Water steam distillation

The oil sample (~15 g) was filled into the inner glass flask of the water steam distillation apparatus according to Antonacopoulos (see figure 40) and distilled water was filled into the outer 2 l glass flask. The distilled water was heated until boiling using a heating mantle. When the water was boiling the valve of the outer flask was closed to start the distillation process. The distillation was stopped after approximately 30 min. The oil residue was transferred to centrifuge tubes and centrifuged for 10 min at 3000 U/min. Then the supernatant was transferred into a glass flask for additional experiments.

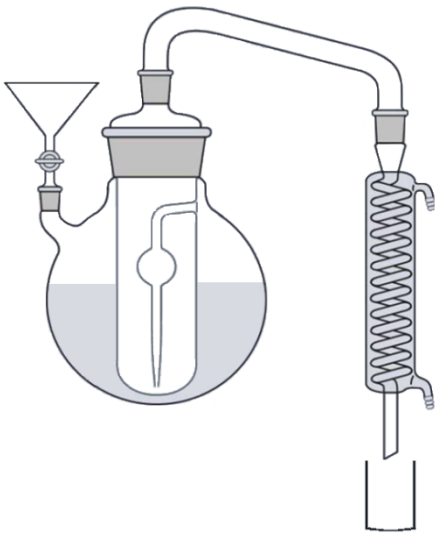

Fig. 40: Water steam distillation apparatus according to Antonacopoulos (Antonacopoulos 1960).

8. Statistical data evaluation

8.1 Exponential curve fitting

Exponential curves were fitted to the data by minimizing the sum of squared deviations (see chapter 3.3.1, for data see table 12). Calculations were implemented in Excel 2010.

The exponential equation (2) is transformed by taking the natural logarithm of both sides of the equation to get the linear equation

$$\ln(c(t)) = \ln(c_0) + k \cdot t$$

$$\varphi(t) = \ln(c_0) + k \cdot t$$

where $\varphi(t) = \ln(c(t))$. A common strategy to estimate the coefficients $\ln(c_0)$ and k is to perform ordinary least-squares fitting. However, when ordinary least-squares fitting is applied to the data pairs (t,φ) the sum of the squares of the residuals in $\varphi(t)$ is minimized rather than those in $c(t)$. Therefore, for regression analysis of (t,φ) global weighting according to de Levie was performed. This means that weighting by the reciprocal squared derivative of $\varphi(t)$ with respect to t was incoporated in regression analysis since the dependent variable $c(t)$ is regarded as homoscedastic (de Levie 2001, Steliopoulos & Stickel 2007).

8.2 Confidence intervals for *AV*

95 % confidence intervals for the *AVs* of cod liver oil, cacao butter, hard fat, castor oil and oleyl oleate (in chapter 4.3) were determined on the basis of the raw data used to calculate the "ideal" straight line (equation 19) (data see table 15, with *x* = spiked palmitic acid amount in mg/g and *y* = classical *AV* in mg/g).

$$CI: \ \hat{\mu} \pm rsd_{xy} \cdot t_{0.95,f}$$

where rsd_{xy} denotes the residual standard deviation and t the $(1-\alpha)$-quantile of the t distribution with f degrees of freedom.

8.3 Confidence intervals for AV_{NMR}

95 % confidence intervals for the AV_{NMR}s (in chapter 4.3) were determined via a non-parametric bootstrapping procedure. The so-called bootstrap is a computer-based resampling technique that provides a way to infer measures of the variability in statistical estimates derived from experimental data. It can be used to determine standard errors and confidence intervals or to conduct hypothesis tests. The bootstrap technique provides a valuable alternative to classical statistical procedures, especially when these procedures turn out to be quite complex or are intractable. A comprehensive introduction to the theory and implementation of the bootstrap methodology is given by Efron and Tibshirani (Efron & Tibshirani 1993). To construct the 95 % confidence intervals the percentile bootstrap approach was used. Computations were implemented using Excel 2010. The Deming model is

$$Y = a + bX$$

with $Y = y - \eta$ and $X = x - \varepsilon$. To construct the 95 % confidence interval for $Y_0 = a + bX_0$ about the estimate $\hat{a} + \hat{b}x_0$ for a given x_0, we need the 0.025- and the 0.975-quantile of the distribution of the differences

$$\lambda = Y_0 - \left(\hat{a} + \hat{b}x_0\right) = a + b(x_0 - \varepsilon) - \left(\hat{a} + \hat{b}x_0\right)$$

These quantiles are estimated by generating a large number, say B, of bootstrap estimates

$$\lambda^{*1,\dots,B} = \hat{a} + \hat{b}(x_0 - \varepsilon^{*1,\dots,B}) - \left(\hat{a}^{*1,\dots,B} + \hat{b}^{*1,\dots,B}x_0\right)$$

The bootstrap estimates are sorted from smallest to largest. The $(0.025 \cdot B)^{th}$ and $(0.975 \cdot B)^{th}$ of the ordered values are chosen to calculate the interval limits as

$$Y_{lower} = \lambda^*_{0.025} + \left(\hat{a} + \hat{b}x_0\right)$$

and

$$Y_{upper} = \lambda^*_{0.975} + \left(\hat{a} + \hat{b}x_0\right)$$

The algorithm proceeds as follows:

1. Fit the Deming model to the data $(x_i, y_i)_{i=1,\dots,n}$ to obtain $\hat{a}$ and $\hat{b}$.
2. Sample n pairs from $(x_i, y_i)_{i=1,\dots,n}$, randomly with replacement, so obtaining $(x_i^{*1}, y_i^{*1})_{i=1,\dots,n}$.
3. Fit a Deming model to the data (x_i^{*1}, y_i^{*1}), yielding $\hat{a}^{*1}$ and $\hat{b}^{*1}$. Generate a realisation of a normally distributed random variable with expectation value 0 and variance $\sigma^2 = \hat{\sigma}_\varepsilon^2$ to obtain $\hat{\varepsilon}_0^{*1}$. Calculate for x_0 the bootstrap estimate
   $\lambda^{*1} = \hat{a} + \hat{b}(x_0 - \hat{\varepsilon}_0^{*1}) - (\hat{a}^{*1} + \hat{b}^{*1} x_0)$.
4. Repeat steps 2 – 3 a large number of times, say B. Sort the bootstrap estimates $\lambda^{*1}, \dots, \lambda^{*B}$ into ascending order of magnitude. Choose the $(0.025 \cdot B)^{th}$ and $(0.975 \cdot B)^{th}$ of the ordered values and calculate
   $Y_{lower} = \lambda_{0.025}^{*} + (\hat{a} + \hat{b} x_0)$ and $Y_{upper} = \lambda_{0.975}^{*} + (\hat{a} + \hat{b} x_0)$.

8.4 Confidence intervals for *ANV*

For the determination of the 95 % confidence intervals for *ANVs*, published results of a round robin test on the *ANV* determination [L13.00-15 2008] were applied (see table 19). The data reveal that the repeatability standard deviation σ_R depends on the *ANV*. The relation between $\hat{\mu}$ and $\hat{\sigma}_R$ was determined by means of least-squares regression:

$$\hat{\sigma}_R = 0.012 \cdot \hat{\mu} + 0.11$$

$$CI: \quad \hat{\mu} \pm \hat{\sigma}_R \cdot t_{0.95,f}$$

8.5 Confidence intervals for $\boldsymbol{a_j}$ and ANV_{NMR}

95 % confidence intervals for the compound specific coefficients a_j (chapter 5.2) were determined as follows (for data see table 18):

$$CI: \ \hat{a}_j \pm \hat{\sigma}_j \cdot t_{0.95,f}$$

$\hat{\sigma}_j{}^2$ is the j-th diagonal element of $\hat{\sigma}^2(X'X)''$ where $\hat{\sigma}^2$ is the residual variance [Draper & Smith 1998].

95 % confidence intervals for the ANV_{NMR}s were calculated using the Gaussian law of uncertainty propagation:

$$CI: \ \hat{\mu} \pm \hat{\sigma} \cdot t_{0.95,f}$$

$$\hat{\sigma}^2(\hat{\mu}) = x_1{}^2\sigma^2(\hat{a}_1) + x_2{}^2\sigma^2(\hat{a}_2) + x_3{}^2\sigma^2(\hat{a}_3)$$

9. Summary

In food and pharmaceutical analysis, the classical indices peroxide value (*PV*), acid value (*AV*) and p-anisidine value (*ANV*) still play an important role as quality and authenticity control parameters of fats and oils. These indices are sum parameters for certain deterioration products (*PV* for hydroperoxides, *AV* for free fatty acids, *ANV* for aldehydes) and are obtained using volumetric or UV/VIS spectroscopic analytical approaches. ^{1}H NMR spectroscopy provides a fast and simple alternative to these classical approaches. In the present work, novel ^{1}H NMR methods to determine hydroperoxides, free fatty acids and aldehydes in fats and oils were developed.

Hydroperoxides

The influence of solvent, water, free fatty acids and sample weight on the hydroperoxide group proton (OO*H*) signal was investigated. On the basis of the obtained results, the sample preparation procedure of the new ^{1}H NMR method was established. A rough assignment of the hydroperoxide group signals in edible fats and oils to methyl oleate, methyl linoleate and methyl linolenate was conducted. Furthermore, to gain information on how many different hydroperoxide species originate from trioleate autoxidation, a kinetic study on trioleate monohydroperoxides was performed. The evaluation of the data strongly indicates that all of the conceivable 18 trioleate monohydroperoxides were formed during trioleate autoxidation. The analytical performance of the NMR method was compared to that of the classical *PV* approach by means of the so-called “relative sensitivity” according to Mandel. It was shown that both methods exhibit a similar analytical performance. A total of 444 edible oil samples were analysed using both methods. For some oil varieties considerable discrepancies were found between the results. In the case of black seed oil and olive oil two substances were identified that influence the classical *PV* determination and thus cause positive (black seed oil) and negative (olive oil) deviations from the theoretical *PV* expected from the NMR values.

Free fatty acids

In order to find the optimal solvent mixture to measure the carboxyl group protons (COO*H*) of free fatty acids in fats and oils, the effect of solvent on the COO*H* signal was investigated for different mixtures of $CDCl_3$ and DMSO-d_6. The comparison of the NMR method with the classical *AV* method by

means of the relative sensitivity revealed that both methods exhibit a similar analytical performance. 420 edible oil samples were analysed by both approaches. Except for pumpkin seed oil, where slight deviations were observed, there was a good compliance between the results obtained from the two methods. Furthermore, the applicability of the ^{1}H NMR assay to further lipids with relevance in pharmacy was tested. For hard fat, castor oil, waxes and oleyl oleate modifications of the original sample preparation procedure of the NMR method were necessary to achieve comparable results for both methods.

AIdehydes

The new ^{1}H NMR method enables the determination of the molar amounts of n-alkanals, (*E*)-2-alkenals and (*E*,*E*)-2,4-alkadienals. It was illustrated that the *ANV* can be modelled as a linear combination of the NMR integrals of these aldehyde species. A functional relationship was derived on the basis of calibration experiments. The suitability of the model was shown by comparing the NMR-determined *ANVs* with the measured classical *ANVs* of 79 commercially available edible oils of different oil types.

In conclusion, the new ^{1}H NMR methods provide an excellent alternative to the determination of the classical indices *PV*, *AV* and *ANV*. They have several advantages over the classical methods including the consumption of small solvent amounts, the ability to automatize measurement and to acquire several different parameters out of the same NMR spectrum. Especially concerning their selectivity, the ^{1}H NMR methods are highly superior to the classical methods.

10. Zusammenfassung

Im Bereich der Lebensmittel- und pharmazeutischen Analytik besitzen die klassischen Fettkennzahlen Peroxidzahl (POZ), Säurezahl (SZ) und p-Anisidinzahl (AnZ) bis heute eine große Bedeutung in der Qualitäts- und Authentizitätskontrolle von Fetten und Ölen. Diese Kennzahlen sind Summenparameter für bestimmte Verderbsprodukte (POZ für Hydroperoxide, SZ für freie Fettsäuren, AnZ für Aldehyde) und werden mittels volumetrischer oder UV/VIS-spektroskopischer Verfahren ermittelt. ^{1}H-NMR Spektroskopie bietet eine einfache und schnelle Alternative zu den klassischen Fettkennzahlen. In der vorliegenden Arbeit wurden neue ^{1}H-NMR Methoden zur Bestimmung von Hydroperoxiden, freien Fettsäuren und Aldehyden in Fetten und Ölen entwickelt.

Hydroperoxide

Der Einfluss des Lösungsmittels, von Wasser, freien Fettsäuren und der Probeneinwaage auf das Hydroperoxidgruppensignal wurde untersucht. Anhand der Ergebnisse wurde die Probenaufarbeitungsprozedur für die neue ^{1}H-NMR Methode erarbeitet. Es wurde eine grobe Zuordnung der Hydroperoxidgruppensignale in Fetten und Ölen zu Methyloleat, Methyllinoleat und Methylinolenat vorgenommen. Weiterhin wurde eine kinetische Studie für Trioleat-Monohydroperoxide durchgeführt, um Informationen darüber zu erhalten, wieviel verschiedene Hydroperoxidspezies bei der Autoxidation von Trioleat gebildet werden. Das Ergebnis weist stark darauf hin, dass alle 18 möglichen Monohydroperoxide entstehen. Die analytische Leistungsfähigkeit der NMR-Methode und der klassischen POZ-Methode wurde mit Hilfe der sog. „relative sensitivity“ nach Mandel verglichen. Es wurde gezeigt, dass beide Methoden eine vergleichbare analytische Leistungsfähigkeit besitzen. Insgesamt wurden 444 Speiseölproben mit beiden Methoden untersucht. Für einige Ölarten wurden beträchtliche Diskrepanzen zwischen der POZ und den NMR-Ergebnissen beobachtet. Im Fall von Schwarzkümmelöl und Olivenöl wurden zwei Substanzen identifiziert, die bei der klassischen POZ-Bestimmung miterfasst werden und dadurch für die positiven (Schwarzkümmelöl) und negativen (Olivenöl) Abweichungen von den aufgrund der NMR-Ergebnisse theoretisch zu erwartenden POZ-Werten verantwortlich sind.

Freie Fettsäuren

Zur Optimierung der Messbedingungen wurde der Einfluss des Lösungsmittels auf das Carboxylgruppensignal von freien Fettsäuren für verschiedene Mischungen von $CDCl_3$ und DMSO-d_6 untersucht. Die NMR-Methode wurde mit der klassischen SZ-Methode mit Hilfe der „relative sensitivity" verglichen. Dabei wurde eine vergleichbare analytische Leistungsfähigkeit für beide Methoden festgestellt. 420 Speiseöle wurden mit beiden Methoden analysiert. Mit Ausnahme der Analysenergebnisse von Kürbiskernölen, die geringe Abweichungen zeigten, wurde eine gute Übereinstimmung der Ergebnisse beider Methoden beobachtet. Weiterhin wurde die Anwendbarkeit der ^{1}H-NMR-Methode für weitere Lipide mit Bedeutung in der Pharmazie getestet. Durch Modifikation der ursprünglichen Analysenvorschrift der NMR-Methode wurden für Hartfett, Rizinusöl, Wachse und Oleyloleat mit beiden Methoden vergleichbare Ergebnisse erhalten.

Aldehyde

Mit der neuen ^{1}H-NMR Methode können die molaren Gehalte von n-Alkanalen, (E)-2-Alkenalen und (E,E)-2,4-Alkadienalen bestimmt werden. Die vorliegende Arbeit zeigt, dass die AnZ als eine Linearkombination der normalisierten NMR-Integrale der Aldehyde modelliert werden kann. Ein funktionaler Zusammenhang wurde auf Grundlage von Kalibrationsexperimenten abgeleitet. Die Eignung des Modells wurde durch den Vergleich der mittels NMR bestimmten AnZ mit der klassischen AnZ von 79 kommerziell erhältlichen Speiseölen verschiedener Ölarten gezeigt.

Abschließend lässt sich sagen, dass die neuen ^{1}H-NMR-Methoden eine sehr gute Alternative zu der Bestimmung der klassischen Fettkennzahlen POZ, SZ and AnZ darstellen. Sie besitzen mehrer Vorteile gegenüber den klassischen Methoden wie beispielsweise der geringe Lösungsmittelverbrauch, die Automatisierbarkeit der Messung und die Möglichkeit mehrere unterschiedliche Parameter aus demselben NMR-Spektrum bestimmen zu können. Es hat sich gezeigt, dass die ^{1}H-NMR-Methoden den klassischen Methoden insbesondere hinsichtlich ihrer Selektivität weit überlegen sind und damit fehlerhafte Befunde, wie sie z. B. bei der POZ-Bestimmung auftreten können, vermieden werden.

11. Raw data and spectra

11.1 Raw data of chapter 3

Tab. 12 Oxidation kinetics of trioleate: hydroperoxide amounts in mmol/mol.

Sampling time point / days	Section 1	Section 2	Section 3	Section 4	Section 5	Section 6
0	0	0	0	0	0	0
7	0	0	0	0	0	0
11	0.07	0.02	0.14	0.06	0.19	0.19
14	0.15	0.08	0.33	0.12	0.37	0.42
16	0.31	0.18	0.62	0.22	0.78	0.73
18	0.56	0.33	1.40	0.75	1.39	1.39
20	1.03	0.61	2.62	1.38	2.72	2.61
25	3.21	1.86	7.83	4.10	8.18	7.62

Tab. 13 Analysis of Delios V spiked with different proportions of oxidized methyl linoleate.

Spike level	*v*	*PV* / meq/kg	NMR results / mmol/kg
*PV*0	0.00	0.00	0.0
*PV*1	0.02	4.36	1.4
*PV*1	0.02	4.40	1.3
*PV*1	0.02	4.46	1.4
*PV*2	0.04	7.68	2.4
*PV*2	0.04	7.60	2.4
*PV*2	0.04	7.54	2.4
*PV*3	0.06	11.68	4.3
*PV*3	0.06	11.89	4.4
*PV*3	0.06	12.00	4.4
*PV*4	0.10	16.98	7.1
*PV*4	0.10	17.15	6.9
*PV*4	0.10	17.38	7.0
*PV*5	0.14	23.00	9.0
*PV*5	0.14	23.17	8.9
*PV*5	0.14	23.67	9.1

Tab. 14 Results obtained from the analysis of 444 fats and oils by the NMR and the PV method.

No.	c_{NMR} / mmol/kg	*PV* / meq/kg	No.	c_{NMR} / mmol/kg	*PV* / meq/kg	No.	c_{NMR} / mmol/kg	*PV* / meq/kg
Rapeseed oil								
1	1.5	4.5	20	1.5	3.8	39	0.3	1.4
2	0.5	2.5	21	0.3	1.5	40	0.5	2.4
3	0.4	1.5	22	0.8	4.2	41	1.4	5.8
4	0.1	0.6	23	0.0	1.8	42	1.4	6.6
5	1.8	5.0	24	0.0	2.0	43	1.7	5.2
6	0.8	3.8	25	0.0	1.4	44	0.5	1.6
7	0.4	1.3	26	0.2	1.5	45	1.6	5.1
8	1.9	3.8	27	1.0	2.7	46	0.1	1.8
9	1.4	3.9	28	1.0	3.3	47	0.4	4.2
10	0.4	2.0	29	0.0	0.9	48	1.4	2.0
11	1.1	3.8	30	1.5	5.4	49	1.3	3.8
12	1.7	4.1	31	1.7	5.6	50	0.6	3.5
13	0.2	1.6	32	0.1	1.4	51	1.9	5.3
14	0.3	1.2	33	0.6	1.8	52	1.3	4.1
15	0.8	1.2	34	1.1	3.0	53	1.0	5.3
16	1.2	3.7	35	1.5	3.9	54	0.3	2.1
17	0.3	3.4	36	0.3	2.3	55	3.4	7.9
18	0.2	1.6	37	0.8	2.4	56	1.7	4.1
19	1.6	4.2	38	1.3	3.5			
Thistle oil								
1	8.5	17.9	14	0.8	2.4	27	0.6	1.2
2	0.4	1.2	15	2.0	4.8	28	2.3	4.9
3	1.5	4.9	16	1.1	3.2	29	4.0	8.3
4	2.6	8.3	17	0.9	2.1	30	1.8	4.3
5	0.0	0.9	18	2.6	6.1	31	0.3	1.7
6	0.9	3.6	19	0.7	2.4	32	0.3	1.0
7	0.8	2.9	20	2.0	5.5	33	0.8	4.0
8	0.4	2.0	21	0.2	1.1	34	0.7	2.8
9	1.0	3.6	22	0.7	2.3	35	0.4	2.2
10	0.4	0.1	23	1.0	3.4	36	0.5	2.4
11	3.0	5.7	24	1.7	4.3	37	0.5	2.7
12	0.7	1.0	25	1.8	3.5	38	0.6	2.4
13	0.6	2.1	26	0.7	1.9			

No.	c_{NMR} / mmol/kg	*PV* / meq/kg	No.	c_{NMR} / mmol/kg	*PV* / meq/kg	No.	c_{NMR} / mmol/kg	*PV* / meq/kg
				Olive oil				
1	8.3	18.4	36	6.5	11.0	71	5.6	10.7
2	2.7	7.2	37	6.2	8.9	72	6.6	6.4
3	6.3	13.0	38	9.2	11.1	73	8.9	10.8
4	6.5	14.2	39	14.9	36.6	74	8.6	10.4
5	3.4	9.0	40	8.6	13.6	75	8.5	9.7
6	4.8	13.7	41	5.4	9.4	76	7.8	12.9
7	4.9	12.4	42	5.3	7.6	77	6.2	12.3
8	7.0	6.3	43	5.3	11.2	78	7.2	14.5
9	8.7	10.3	44	3.8	7.9	79	7.1	11.9
10	8.7	11.4	45	5.9	11.5	80	6.1	10.4
11	5.9	12.6	46	3.8	6.2	81	8.2	13.6
12	6.8	10.6	47	6.1	11.1	82	6.7	15.1
13	7.7	11.6	48	5.7	11.7	83	5.0	10.1
14	9.4	13.0	49	4.1	7.9	84	3.0	6.8
15	7.5	9.3	50	3.4	8.2	85	5.7	11.2
16	7.9	13.5	51	2.9	6.6	86	0.9	3.4
17	7.8	14.3	52	3.8	8.2	87	0.4	1.6
18	7.2	10.8	53	2.6	7.3	88	3.5	8.8
19	7.6	13.7	54	2.3	5.7	89	4.2	10.5
20	6.8	12.6	55	14.6	31.6	90	1.8	7.1
21	4.3	7.2	56	3.6	10.4	91	3.9	9.4
22	6.7	8.4	57	4.0	10.1	92	6.2	13.4
23	7.3	12.5	58	3.1	6.7	93	5.1	12.9
24	9.3	14.4	59	0.9	3.5	94	3.0	8.1
25	5.4	13.0	60	1.1	4.1	95	3.5	8.9
26	8.5	13.1	61	3.9	11.8	96	3.6	10.0
27	5.9	10.4	62	6.4	15.3	97	2.2	7.3
28	5.4	10.7	63	4.9	9.4	98	4.1	12.3
29	6.4	9.3	64	7.3	13.9	99	3.0	9.1
30	8.3	9.6	65	4.8	12.8	100	4.0	11.8
31	9.6	14.6	66	4.6	10.4	101	4.6	10.5
32	5.3	10.4	67	4.6	10.7	102	3.1	7.0
33	7.7	15.8	68	4.2	9.8	103	3.5	7.2
34	9.5	21.1	69	4.2	8.7	104	6.2	10.5
35	6.4	9.5	70	2.6	5.7			

No.	c_{NMR} / mmol/kg	*PV* / meq/kg	No.	c_{NMR} / mmol/kg	*PV* / meq/kg	No.	c_{NMR} / mmol/kg	*PV* / meq/kg
Sunflower oil								
1	3.7	8.6	30	0.5	0.6	59	3.0	7.8
2	4.9	12.4	31	1.1	3.6	60	0.9	4.1
3	7.2	17.6	32	1.2	4.3	61	0.7	3.8
4	3.7	9.9	33	2.1	7.1	62	2.6	9.1
5	4.4	11.3	34	0.8	3.7	63	1.0	4.9
6	2.5	3.9	35	3.8	7.8	64	2.7	8.8
7	1.6	4.5	36	1.3	3.5	65	1.9	4.2
8	1.4	6.3	37	0.9	3.7	66	2.3	7.8
9	0.8	2.8	38	0.9	2.7	67	2.9	7.6
10	1.7	3.2	39	1.4	3.8	68	3.1	8.3
11	1.4	5.7	40	2.3	5.9	69	3.2	6.9
12	3.9	9.7	41	1.8	3.6	70	1.4	4.5
13	1.9	6.5	42	0.8	2.2	71	2.7	6.2
14	2.8	5.9	43	0.9	2.7	72	2.0	6.2
15	1.5	5.0	44	3.4	8.8	73	2.7	6.2
16	0.6	2.3	45	1.2	4.1	74	1.2	3.5
17	0.4	2.3	46	2.3	5.8	75	3.2	9.4
18	1.8	6.7	47	2.0	4.9	76	0.7	3.1
19	0.9	3.4	48	0.9	3.4	77	0.3	1.3
20	0.4	1.7	49	0.9	2.7	78	2.7	7.5
21	1.1	3.8	50	2.1	5.6	79	0.7	2.8
22	0.5	1.6	51	2.5	5.8	80	2.0	4.9
23	1.1	2.3	52	2.6	5.6	81	1.9	6.3
24	1.2	3.9	53	1.0	3.0	82	1.2	4.1
25	2.4	6.5	54	0.7	2.4	83	2.4	5.8
26	14.6	33.6	55	0.4	1.6	84	1.4	4.2
27	2.1	3.5	56	0.8	2.7	85	3.9	9.7
28	1.8	3.2	57	0.6	2.4	86	1.5	3.9
29	1.4	3.4	58	0.6	2.3			
Grape seed oil								
1	0.7	2.7	5	0.9	2.7	9	2.1	5.6
2	1.2	3.3	6	1.0	3.8	10	11.9	34.5
3	1.1	2.8	7	1.0	3.5	11	0.6	3.1
4	1.0	5.0	8	1.7	5.0			

No.	c_{NMR} / mmol/kg	*PV* / meq/kg	No.	c_{NMR} / mmol/kg	*PV* / meq/kg	No.	c_{NMR} / mmol/kg	*PV* / meq/kg
Pumpkin seed oil								
1	8.4	9.0	12	5.8	4.4	23	6.1	9.1
2	5.9	4.7	13	9.2	10.6	24	7.7	1.5
3	8.9	7.5	14	9.2	3.6	25	4.8	3.6
4	9.4	5.3	15	4.9	4.0	26	6.4	8.3
5	7.5	9.1	16	5.5	4.9	27	10.1	9.5
6	7.7	9.2	17	5.1	2.6	28	10.6	13.0
7	6.2	3.9	18	5.9	4.7	29	8.5	13.5
8	5.6	3.7	19	9.0	4.2	30	8.5	10.2
9	9.0	3.3	20	4.1	6.6	31	14.3	16.8
10	7.6	3.8	21	8.4	5.4	32	2.6	5.6
11	9.2	3.5	22	5.3	4.8	33	2.8	8.3
Maize oil								
1	1.2	3.8	9	1.7	5.8	17	0.8	4.2
2	0.0	0.8	10	0.5	2.3	18	0.4	2.1
3	0.5	2.7	11	1.0	3.0	19	0.4	2.5
4	0.0	1.2	12	0.2	1.1	20	0.3	2.3
5	0.6	2.8	13	0.2	2.0	21	0.6	3.2
6	0.0	1.0	14	0.1	1.8	22	0.5	2.8
7	0.0	1.5	15	0.2	1.3			
8	2.0	6.7	16	0.2	1.7			
Walnut oil								
1	8.7	19.8	9	0.0	1.3	17	4.4	12.6
2	0.5	1.9	10	0.1	1.5	18	1.6	4.2
3	1.7	4.7	11	2.5	3.8	19	2.0	5.6
4	2.6	4.9	12	0.6	3.2	20	0.8	3.9
5	0.9	2.2	13	0.0	0.2	21	0.7	2.4
6	2.1	5.4	14	1.4	3.8	22	1.4	3.8
7	0.5	2.3	15	0.0	0.4	23	0.9	3.7
8	2.7	7.1	16	0.9	3.8			
Plant oil								
1	0.9	3.4	5	1.1	5.4	9	0.0	1.3
2	1.6	5.8	6	0.3	1.3	10	2.7	7.6
3	0.5	2.3	7	0.3	1.4	11	1.3	1.8
4	0.3	2.0	8	2.4	6.6			

No.	c_{NMR} / mmol/kg	*PV / meq/kg*	No.	c_{NMR} / mmol/kg	*PV / meq/kg*	No.	c_{NMR} / mmol/kg	*PV / meq/kg*
Linseed oil								
1	1.0	2.4	6	1.6	4.6	11	0.3	2.1
2	0.6	2.3	7	1.0	3.4	12	0.6	1.7
3	0.5	1.2	8	0.7	2.5	13	0.6	1.7
4	0.5	1.3	9	0.0	0.7	14	0.3	2.1
5	0.8	2.7	10	0.0	2.1	15	0.4	0.5
Peanut oil								
1	1.5	3.6	6	1.5	2.0	11	3.4	8.8
2	1.8	3.2	7	0.8	3.5	12	2.3	5.8
3	2.8	6.3	8	0.9	4.1	13	2.5	5.8
4	1.8	5.0	9	0.8	2.2	14	1.0	3.0
5	0.0	1.5	10	0.9	2.7	15	1.1	4.4
Argan oil								
1	0.9	2.9	4	0.8	1.8	7	0.3	1.6
2	0.6	1.6	5	0.0	0.1			
3	0.9	2.3	6	0.6	2.0			
Black seed oil								
1	2.4	18.6	4	3.7	28.9	7	2.0	27.9
2	3.7	29.4	5	3.3	35.1			
3	2.4	32.0	6	2.7	20.6			
Almond oil								
1	1.2	4.1	2	5.7	11.6			
Hazelnut oil								
1	0.1	1.5	2	0.9	2.7	3	0.8	2.7
Sesame oil								
1	1.4	4.4	2	1.5	3.9			
Soja oil								
1	1.3	2.9	2	0.7	1.2			
Pistachio oil								
1	2.1	8.2						
Coconut oil								
1	0.1	0.6						
Macadamia nut oil								
1	0.9	3.8						

No.	c_{NMR} / mmol/kg	*PV* / meq/kg	No.	c_{NMR} / mmol/kg	*PV* / meq/kg	No.	c_{NMR} / mmol/kg	*PV* / meq/kg
Rice oil								
1	0.9	3.8						
Palm oil (+ rapeseed oil)								
1	3.7	9.4						
Hemp oil								
1	4.7	10.2						
Alba oil								
1	0.0	1.4						

11.2 Raw data of chapter 4

Tab. 15 Analysis of a rapeseed oil spiked with different palmitic acid amounts.

Spike level	mg palmitic acid/g oil	*AV* / mg KOH/g oil	NMR result / mmol/mol TAG
*AV*1	0.0	0.060	0.45
*AV*1	0.0	0.064	0.50
*AV*1	0.0	0.064	0.51
*AV*2	2.3	0.57	8.2
*AV*2	2.3	0.57	8.0
*AV*2	2.3	0.57	8.1
*AV*3	4.6	1.11	16.2
*AV*3	4.,6	1.11	15.4
*AV*3	4.6	1.11	15.2
*AV*4	6.9	1.64	23.6
*AV*4	6.9	1.63	22.4
*AV*4	6.9	1.62	23.6
*AV*5	9.2	2.26	30.0
*AV*5	9.2	2.11	29.8
*AV*5	9.2	2.07	31.3
*AV*6	13.6	3.13	47.4
*AV*6	13.6	3.11	45.8
*AV*6	13.6	3.12	45.6

Tab. 16 AV_{NMR}: Replicate measurements of oleyl oleate.

Sample	AV_{NMR} / mg/g	Sample	AV_{NMR} / mg/g
Oleyl oleate	0.13	Oleyl oleate*	2.71
	0.06		2.67
	0.05		2.70
	0.07		2.71
	0.05		2.92

Tab. 17 Results obtained from the analysis of 420 fats and oils by the NMR and AV method.

No.	*AV* / mg/g	c_{NMR} / mol‰	No.	*AV* / mg/g	c_{NMR} / mol‰	No.	*AV* / mg/g	c_{NMR} / mol‰
Rapeseed oil								
1	0.6	8.0	20	0.1	1.4	39	1.8	26.8
2	0.1	0.0	21	0.1	0.6	40	1.4	19.2
3	0.8	8.7	22	0.1	0.0	41	2.6	40.0
4	0.1	0.0	23	0.3	3.2	42	1.8	25.7
5	0.6	7.3	24	1.6	22.6	43	1.3	18.7
6	2.7	37.7	25	1.7	24.8	44	1.2	17.2
7	0.9	11.4	26	0.2	0.7	45	1.3	16.9
8	0.6	6.4	27	1.6	21.2	46	0.2	1.1
9	0.8	9.8	28	0.7	9.9	47	1.7	26.0
10	0.1	0.6	29	0.1	0.3	48	0.2	1.1
11	0.2	0.0	30	1.0	13.2	49	0.1	0.4
12	0.0	0.0	31	1.3	18.1	50	1.3	21.2
13	0.1	0.5	32	0.8	10.0	51	1.7	24.7
14	0.1	0.8	33	1.2	16.9	52	1.2	19.3
15	0.1	0.4	34	0.1	1.0	53	1.4	19.1
16	0.1	0.4	35	0.1	1.0	54	0.2	0.5
17	0.9	12.8	36	1.9	28.9	55	1.5	23.1
18	1.0	14.3	37	0.1	1.3	56	2.4	36.7
19	0.1	0.3	38	1.4	20.8	57	0.6	8.9
Thistle oil								
1	0.2	2.8	14	0.1	0.5	27	0.1	0.3
2	0.2	0.5	15	0.8	10.0	28	0.5	5.1
3	0.5	5.2	16	0.3	2.6	29	0.5	4.3
4	1.9	25.5	17	0.1	0.8	30	2.1	29.7
5	0.2	1.6	18	1.9	24.9	31	0.2	0.7
6	0.3	1.8	19	0.2	1.0	32	0.2	1.4
7	0.1	0.0	20	2.1	26.9	33	0.1	0.8
8	0.2	0.6	21	0.2	1.5	34	0.1	0.7
9	0.2	0.6	22	0.2	0.5	35	0.1	0.7
10	0.1	0.7	23	0.2	0.9	36	0.1	0.8
11	1.7	23.2	24	0.5	4.5	37	0.1	1.6
12	0.1	0.0	25	0.5	5.0	38	0.1	0.4
13	0.1	0.0	26	0.1	0.0			

No.	*AV* / mg/g	c_{NMR} / mol‰	No.	*AV* / mg/g	c_{NMR} / mol‰	No.	*AV* / mg/g	c_{NMR} / mol‰
				Olive oil				
1	0.7	9.3	36	1.0	14.3	71	0.3	2.5
2	0.6	7.5	37	0.9	10.2	72	0.9	14.6
3	0.3	3.9	38	0.9	11.7	73	0.9	13.3
4	0.6	7.2	39	0.3	3.1	74	0.7	7.5
5	0.6	7.2	40	1.0	12.1	75	0.5	4.9
6	0.2	1.8	41	0.9	10.7	76	0.7	9.8
7	0.6	7.4	42	0.6	6.2	77	1.1	15.6
8	0.9	11.2	43	1.0	12.7	78	0.5	6.1
9	1.0	13.4	44	0.5	5.7	79	0.9	11.5
10	0.5	7.1	45	0.6	6.9	80	0.9	12.4
11	0.5	4.9	46	0.7	7.1	81	0.7	10.0
12	1.2	16.3	47	1.1	16.3	82	0.7	8.4
13	0.7	9.5	48	1.0	12.6	83	0.7	7.4
14	0.9	11.8	49	0.6	7.4	84	0.8	10.7
15	0.7	9.2	50	0.7	8.5	85	0.6	6.0
16	1.2	16.9	51	0.7	9.0	86	0.9	11.8
17	0.9	11.9	52	0.9	9.8	87	0.7	7.6
18	1.0	14.5	53	0.5	7.1	88	0.8	10.3
19	0.6	9.8	54	1.0	14.6	89	0.8	9.1
20	1.4	18.8	55	0.5	6.3	90	1.1	13.9
21	1.4	19.7	56	1.6	20.5	91	0.6	6.8
22	0.8	9.7	57	0.9	11.4	92	0.6	6.9
23	0.8	9.7	58	0.6	8.5	93	0.5	4.3
24	0.8	8.7	59	0.6	7.0	94	0.8	9.9
25	0.6	7.4	60	1.2	17.4	95	0.8	10.0
26	1.4	18.7	61	1.2	16.4	96	0.7	8.7
27	0.6	7.4	62	1.5	21.9	97	0.8	12.4
28	0.8	11.6	63	0.8	10.3	98	0.4	5.0
29	1.2	15.1	64	1.3	16.0	99	0.6	8.7
30	1.0	12.2	65	0.5	5.7	100	0.6	6.2
31	0.9	13.5	66	0.7	10.3			
32	0.5	7.0	67	0.8	10.6			
33	0.9	13.5	68	1.2	17.8			
34	1.0	12.9	69	0.7	10.7			
35	0.7	9.2	70	0.4	4.7			

No.	*AV* / mg/g	c_{NMR} / mol‰	No.	*AV* / mg/g	c_{NMR} / mol‰	No.	*AV* / mg/g	c_{NMR} / mol‰
Sunflower oil								
1	0.4	5.0	30	0.2	0.7	59	0.2	1.2
2	0.6	8.5	31	0.1	1.4	60	0.2	1.0
3	0.6	7.6	32	0.1	1.2	61	0.1	0.8
4	0.9	11.6	33	0.8	9.7	62	0.2	1.3
5	0.2	1.9	34	0.8	9.9	63	0.7	10.0
6	0.2	0.8	35	0.2	0.9	64	2.5	32.9
7	1.1	14.8	36	0.2	0.7	65	0.8	9.8
8	0.2	1.4	37	0.1	1.1	66	2.1	31.2
9	0.1	0.8	38	0.2	1.0	67	0.7	8.2
10	0.1	1.3	39	0.6	7.1	68	0.3	3.4
11	1.2	15.5	40	0.1	1.2	69	0.2	1.5
12	1.0	14.4	41	0.2	1.2	70	0.7	7.9
13	1.4	20.4	42	0.1	0.5	71	1.5	19.4
14	0.1	0.9	43	1.2	13.7	72	0.2	2.4
15	0.2	2.3	44	0.2	1.2	73	0.2	2.4
16	0.2	1.7	45	0.1	0.2	74	2.2	29.8
17	0.1	0.8	46	0.9	9.6	75	0.2	2.4
18	0.7	8.8	47	0.2	0.8	76	2.1	31.3
19	0.1	1.3	48	0.4	4.4	77	0.1	1.1
20	0.2	0.9	49	1.9	24.7	78	0.2	3.5
21	0.1	1.2	50	1.8	26.5	79	2.4	33.3
22	0.2	0.0	51	2.5	33.6	80	0.2	1.5
23	0.2	0.8	52	0.1	1.1	81	0.2	1.0
24	0.2	0.0	53	0.1	1.0	82	0.8	11.2
25	1.4	18.1	54	0.1	0.9	83	1.9	25.5
26	1.2	13.9	55	0.1	1.1	84	3.1	38.1
27	0.3	3.8	56	0.2	1.1	85	0.1	1.1
28	0.1	1.5	57	0.4	4.5	86	0.6	9.0
29	0.2	1.0	58	1.0	11.6	87	0.2	1.2
Linseed oil								
1	2.2	30.1	5	3.6	53.5	9	1.3	18.1
2	0.9	9.6	6	1.4	19.5	10	3.9	61.0
3	1.1	14.2	7	1.3	18.9	11	1.4	21.2
4	0.8	11.1	8	0.8	12.0	12	2.2	32.5

No.	*AV* / mg/g	c_{NMR} / mol‰	No.	*AV* / mg/g	c_{NMR} / mol‰	No.	*AV* / mg/g	c_{NMR} / mol‰
Pumpkin seed oil								
1	0.7	5.1	11	1.5	15.4	21	4.1	59.7
2	0.8	5.1	12	0.7	5.8	22	0.8	7.9
3	1.1	9.4	13	1.0	8.7	23	0.8	6.4
4	0.7	4.3	14	3.3	41.3	24	1.5	15.3
5	1.6	17.1	15	1.4	16.7	25	2.1	26.3
6	1.5	18.0	16	2.6	27.7	26	1.9	23.5
7	1.8	19.7	17	3.7	50.4	27	0.5	4.7
8	3.6	45.2	18	1.3	10.5	28	0.8	6.1
9	0.9	6.0	19	2.5	28.1	29	2.7	38.1
10	1.3	12.2	20	1.0	9.8			
Maize oil								
1	0.3	2.5	8	0.3	2.2	15	0.2	2.3
2	0.3	3.9	9	0.3	3.8	16	0.2	1.9
3	0.2	2.3	10	0.3	1.9	17	0.2	2.3
4	0.3	3.1	11	0.3	1.8	18	0.2	2.2
5	0.3	1.1	12	0.2	2.0	19	0.2	1.9
6	0.3	1.9	13	0.2	1.6	20	0.2	1.9
7	0.3	2.9	14	0.2	1.1			
Walnut oil								
1	0.4	4.0	7	2.2	30.8	13	0.5	6.1
2	0.2	2.1	8	1.0	14.0	14	0.4	2.3
3	0.9	11.9	9	1.1	14.4	15	0.4	6.0
4	0.5	4.7	10	0.4	4.0	16	1.0	14.5
5	0.2	3.0	11	0.5	5.8	17	0.5	4.6
6	0.5	7.2	12	0.4	4.8	18	0.4	7.9
Peanut oil								
1	0.2	0.2	6	0.1	1.2	11	0.1	0.7
2	0.1	1.6	7	0.2	1.5	12	0.1	1.4
3	0.3	1.9	8	0.3	3.1	13	0.2	1.0
4	0.1	0.7	9	0.3	5.3	14	0.2	1.2
5	0.2	0.6	10	0.2	1.0	15	0.2	1.4
Sesame oil								
1	2.4	36.2	3	2.3	31.7	5	1.7	25.8
2	0.2	0.0	4	2.0	29.8			

No.	*AV* / mg/g	c_{NMR} / mol‰	No.	*AV* / mg/g	c_{NMR} / mol‰	No.	*AV* / mg/g	c_{NMR} / mol‰
Grape seed oil								
1	2.0	27.6	6	0.1	1.5	11	0.8	9.4
2	0.1	0.9	7	0.1	1.3	12	0.2	1.2
3	0.2	1.0	8	0.2	1.2	13	2.2	31.9
4	0.2	0.9	9	0.1	1.6			
5	0.1	1.4	10	0.2	1.0			
Plant oil								
1	0.2	1.1	4	0.2	1.1	7	0.1	0.6
2	0.3	3.1	5	0.1	0.8			
3	0.1	0.7	6	0.2	1.2			
Argan oil								
1	0.5	4.9	4	1.5	18.8	7	3.3	47.5
2	2.4	35.3	5	1.8	24.1			
3	0.6	7.5	6	1.4	18.4			
Hazelnut oil								
1	0.5	6.1	3	0.3	4.7			
2	0.8	10.3	4	1.1	15.0			
Almond oil								
1	0.1	1.1	2	0.5	8.2	3	1.0	10.2
Soya bean oil								
1	0.2	1.9						
Black seed oil								
1	11.0	164.8						
Macadamia nut oil								
1	0.8	10.7						
Pistachio oil								
1	0.4	3.7						
Coconut oil								
1	0.2	0.5						

11.3 Raw data of Chapter 5

Tab. 18 Analysis of mixtures of aldehyde standards and Delios V by the NMR and ANV method.

	n-Hexanal		(*E*)-2-Hexenal		(*E*,*E*)-2,4-Hexadienal	(*Z*,*E*)-2,4-Hexadienal
ANV	c_{NMR} / mol‰	*ANV*	c_{NMR} / mol‰	*ANV*	c_{NMR} / mol‰	c_{NMR} / mol‰
0.7	0.5	2.7	0.2	3.4	0.09	0.00
1.8	1.9	9.3	1.4	6.0	0.16	0.02
5.7	7.8	16.5	2.6	11.1	0.28	0.03
8.1	12.9	24.8	3.9	21.5	0.55	0.07
18.7	38.4	32.7	5.2	31.8	0.76	0.11
41.3	75.6	39.8	6.5	44.8	1.11	0.15

Tab. 19 Results of a round robin test on the ANV method: ANVs of dublicate measurements (mean values) of 8 different fats and oils with corresponding repeatability standard deviation $\hat{\sigma}_R$ and number of considered laboratories (L13.00-15 2008).

ANV (mean value)	$\hat{\sigma}_R$	No. of labs
3.46	0.09	16
0.95	0.08	17
6.86	0.17	17
25.5	0.31	16
31.5	0.72	17
4.59	0.28	15
0.33	0.07	14
96.8	1.22	16

Tab. 20 Results obtained from the analysis of 79 fats and oils by the NMR and the ANV method.

No.	Oil variety	$c_{alkanal}$ / mmol/mol	$c_{alkenal}$ / mmol/mol	$c_{alkadienal}$ / mmol/mol	ANV_{NMR}	$\sigma(ANV_{NMR})$	*CI* (95 %)	*ANV*	$\sigma(ANV)$	*CI* (95 %)	compliant
1	Maize oil	0.82	0.21	0.61	21.1	2.7	6.5	17.5	0.3	0.7	Yes
2	Maize oil	0.10	0.00	0.10	3.4	0.5	1.1	3.4	0.2	0.3	Yes
3	Maize oil	0.28	0.06	0.005	2.2	0.2	0.6	2.5	0.1	0.3	Yes
4	Maize oil	0.24	0.10	0.05	2.5	0.2	0.6	2.8	0.1	0.3	Yes
5	Thistle oil	0.35	0.18	0.11	4.8	0.5	1.2	4.9	0.2	0.4	Yes
6	Thistle oil	0.13	0.09	0.04	2.1	0.2	0.5	1.8	0.1	0.3	Yes
7	Thistle oil	0.34	0.17	0.10	4.4	0.4	1.1	4.0	0.2	0.3	Yes
8	Thistle oil	0.37	0.19	0.10	4.7	0.5	1.1	4.7	0.2	0.4	Yes
9	Thistle oil	0.14	0.12	0.05	2.2	0.2	0.5	2.1	0.1	0.3	Yes
10	Thistle oil	0.30	0.19	0.10	4.6	0.4	1.1	4.5	0.2	0.4	Yes
11	Thistle oil	0.30	0.11	0.16	6.1	0.7	1.8	6.1	0.2	0.4	Yes
12	Peanut oil	0.20	0.05	0.05	2.2	0.2	0.6	2.2	0.1	0.3	Yes
13	Peanut oil	0.20	0.05	0.05	2.0	0.2	0.5	2.2	0.1	0.3	Yes
14	Peanut oil	0.23	0.06	0.13	4.7	0.6	1.4	3.0	0.2	0.3	Yes
15	Peanut oil	0.12	0.00	0.05	1.8	0.2	0.6	2.1	0.1	0.3	Yes
16	Peanut oil	0.17	0.05	0.06	2.5	0.3	0.7	2.6	0.1	0.3	Yes
17	Peanut oil	0.15	0.04	0.05	2.0	0.2	0.6	2.6	0.1	0.3	Yes
18	Peanut oil	0.17	0.06	0.05	2.0	0.2	0.5	2.6	0.1	0.3	Yes

No.	Oil variety	$c_{alkanal}$ / mmol/mol	$c_{alkenal}$ / mmol/mol	$c_{alkadienal}$ / mmol/mol	ANV_{NMR}	$\sigma(ANV_{NMR})$	CI (95 %)	ANV	$\sigma(ANV)$	CI (95 %)	compliant
19	Peanut oil	0.24	0.06	0.08	3.1	0.4	0.9	2.9	0.1	0.3	Yes
20	Hazelnut oil	0.47	0.23	0.16	6.7	0.7	1.7	8.8	0.2	0.5	Yes
21	Hazelnut oil	0.49	0.11	0.08	3.5	0.4	0.9	4.7	0.2	0.4	Yes
22	Walnut oil	0.20	0.08	0.06	2.6	0.3	0.7	3.9	0.2	0.3	No
23	Walnut oil	0.17	0.09	0.06	2.7	0.3	0.7	2.6	0.1	0.3	Yes
24	Walnut oil	0.25	0.05	0.08	3.0	0.3	0.8	2.9	0.1	0.3	Yes
25	Walnut oil	0.17	0.06	0.05	2.2	0.2	0.6	2.0	0.1	0.3	Yes
26	Walnut oil	0.14	0.09	0.06	2.7	0.3	0.7	3.1	0.2	0.3	Yes
27	Walnut oil	0.27	0.07	0.07	2.7	0.3	0.7	2.2	0.1	0.3	Yes
28	Walnut oil	0.23	0.06	0.04	1.9	0.2	0.5	1.9	0.1	0.3	Yes
29	Walnut oil	0.17	0.06	0.07	2.6	0.3	0.7	3.1	0.2	0.3	Yes
30	Walnut oil	0.19	0.08	0.04	1.7	0.2	0.4	2.7	0.1	0.3	No
31	Walnut oil	0.18	0.22	0.00	1.5	0.0	0.0	2.2	0.1	0.3	No
32	Almond oil	0.06	0.00	0.00	0.0	0.0	0.0	0.3	0.1	0.3	No
33	Almond oil	0.00	0.00	0.00	0.0	0.0	0.0	0.4	0.1	0.3	No
34	Linseed oil	0.19	0.00	0.01	0.5	0.1	0.1	0.5	0.1	0.3	Yes
35	Linseed oil	0.24	0.00	0.01	0.3	0.0	0.1	0.6	0.1	0.3	Yes
36	Linseed oil	0.10	0.00	0.00	0.1	0.0	0.0	0.6	0.1	0.3	No
37	Linseed oil	0.33	0.06	0.00	0.5	0.0	0.0	0.8	0.1	0.3	Yes

No.	Oil variety	$c_{alkanal}$ / mmol/mol	$c_{alkenal}$ / mmol/mol	$c_{alkadienal}$ / mmol/mol	ANV_{NMR}	$\sigma(ANV_{NMR})$	CI (95 %)	ANV	$\sigma(ANV)$	CI (95 %)	compliant
38	Argan oil	0.05	0.05	0.00	0.3	0.0	0.0	0.5	0.1	0.3	Yes
39	Argan oil	0.06	0.00	0.00	0.0	0.0	0.0	1.1	0.1	0.3	No
40	Rapeseed oil	0.09	0.05	0.05	1.8	0.2	0.5	2.4	0.1	0.3	Yes
41	Rapeseed oil	0.00	0.00	0.00	0.0	0.0	0.0	0.0	0.1	0.2	Yes
42	Rapeseed oil	0.21	0.08	0.13	4.9	0.6	1.4	4.9	0.2	0.4	Yes
43	Rapeseed oil	0.08	0.04	0.05	1.9	0.2	0.5	1.8	0.1	0.3	Yes
44	Rapeseed oil	0.17	0.08	0.00	0.6	0.0	0.0	2.6	0.1	0.3	No
45	Rapeseed oil	0.00	0.00	0.00	0.0	0.0	0.0	0.3	0.1	0.3	No
46	Rapeseed oil	0.00	0.00	0.00	0.0	0.0	0.0	0.4	0.1	0.3	No
47	Rapeseed oil	0.00	0.00	0.00	0.0	0.0	0.0	0.3	0.1	0.3	No
48	Rapeseed oil	0.00	0.00	0.00	0.0	0.0	0.0	0.3	0.1	0.3	No
49	Rapeseed oil	0.05	0.00	0.00	0.0	0.0	0.0	0.5	0.1	0.3	No
50	Rapeseed oil	0.12	0.04	0.00	0.3	0.0	0.0	1.3	0.1	0.3	No
51	Rapeseed oil	0.08	0.02	0.06	1.9	0.2	0.6	2.9	0.1	0.3	No
52	Rapeseed oil	0.00	0.04	0.04	1.7	0.2	0.5	1.1	0.1	0.3	Yes
53	Sunflower oil	0.11	0.00	0.00	0.1	0.0	0.0	0.5	0.1	0.3	No
54	Sunflower oil	0.65	0.50	0.04	4.6	0.2	0.4	4.7	0.2	0.4	Yes
55	Sunflower oil	0.13	0.11	0.04	2.1	0.2	0.5	2.2	0.1	0.3	Yes
56	Sunflower oil	0.13	0.00	0.06	1.9	0.3	0.6	2.2	0.1	0.3	Yes

No.	Oil variety	$c_{alkanal}$ / mmol/mol	$c_{alkenal}$ / mmol/mol	$c_{alkadienal}$ / mmol/mol	ANV_{NMR}	$\sigma(ANV_{NMR})$	CI (95 %)	ANV	$\sigma(ANV)$	CI (95 %)	compliant
57	Sunflower oil	0.67	0.22	0.49	17.4	2.2	5.3	15.8	0.3	0.6	Yes
58	Sunflower oil	0.38	0.20	0.26	9.7	1.1	2.8	8.2	0.2	0.5	Yes
59	Sunflower oil	0.12	0.02	0.00	0.2	0.0	0.0	0.7	0.1	0.3	No
60	Sunflower oil	0.41	0.14	0.15	6.0	0.7	1.6	6.4	0.2	0.4	Yes
61	Sunflower oil	0.25	0.10	0.18	6.4	0.8	1.9	6.5	0.2	0.4	Yes
62	Sunflower oil	0.00	0.00	0.00	0.0	0.0	0.0	0.3	0.1	0.3	No
63	Sunflower oil	0.14	0.00	0.00	0.1	0.0	0.0	0.6	0.1	0.3	No
64	Sunflower oil	0.15	0.05	0.31	10.1	1.3	3.3	11.1	0.2	0.5	Yes
65	Sunflower oil	0.20	0.07	0.22	7.6	1.0	2.4	6.6	0.2	0.4	Yes
66	Grape seed oil	0.55	0.35	0.12	6.3	0.5	1.3	6.9	0.2	0.4	Yes
67	Grape seed oil	0.58	0.34	0.30	11.9	1.3	3.2	11.3	0.2	0.5	Yes
68	Grape seed oil	0.51	0.22	0.12	5.5	0.5	1.3	5.6	0.2	0.4	Yes
69	Grape seed oil	0.52	0.30	0.09	5.0	0.4	1.0	6.8	0.2	0.4	No
70	Grape seed oil	0.63	0.25	0.26	10.2	1.1	2.8	9.4	0.2	0.5	Yes
71	Grape seed oil	0.43	0.34	0.11	5.9	0.5	1.2	6.9	0.2	0.4	Yes
72	Grape seed oil	0.34	0.00	0.00	0.2	0.0	0.0	0.6	0.1	0.3	No
73	Grape seed oil	0.55	0.20	0.23	8.9	1.0	2.5	9.9	0.2	0.5	Yes
74	Soya bean oil	0.31	0.12	0.07	3.2	0.3	0.8	3.4	0.2	0.3	Yes
75	Sesame oil	0.00	0.00	0.00	0.0	0.0	0.0	0.4	0.1	0.3	No

No.	Oil variety	$c_{alkanal}$ / mmol/mol	$c_{alkenal}$ / mmol/mol	$c_{alkadienal}$ / mmol/mol	ANV_{NMR}	$\sigma(ANV_{NMR})$	CI (95 %)	ANV	$\sigma(ANV)$	CI (95 %)	compliant
76	Pistachio oil	0.12	0.09	0.05	2.2	0.2	0.5	2.7	0.1	0.3	Yes
77	Plant oil	0.22	0.03	0.14	4.8	0.6	1.5	4.7	0.2	0.4	Yes
78	Plant oil	0.19	0.07	0.30	10.1	1.3	3.2	9.8	0.2	0.5	Yes
79	Plant oil	0.06	0.00	0.02	0.6	0.1	0.2	0.9	0.1	0.3	Yes

11.4 ^{1}H NMR spectra of fats and oils

Rapeseed oil

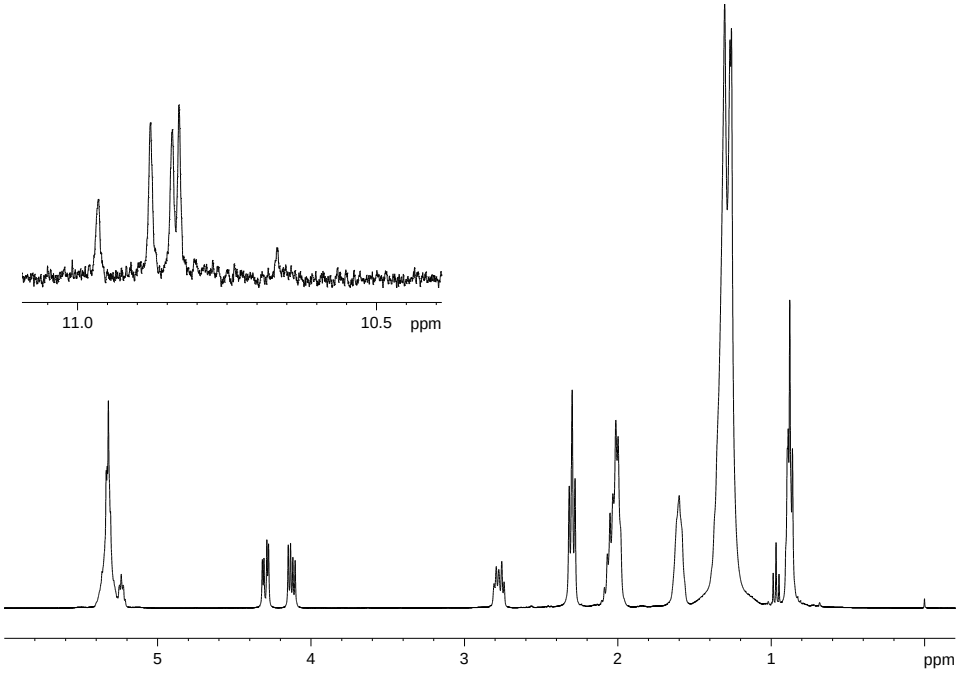

Sunflower oil

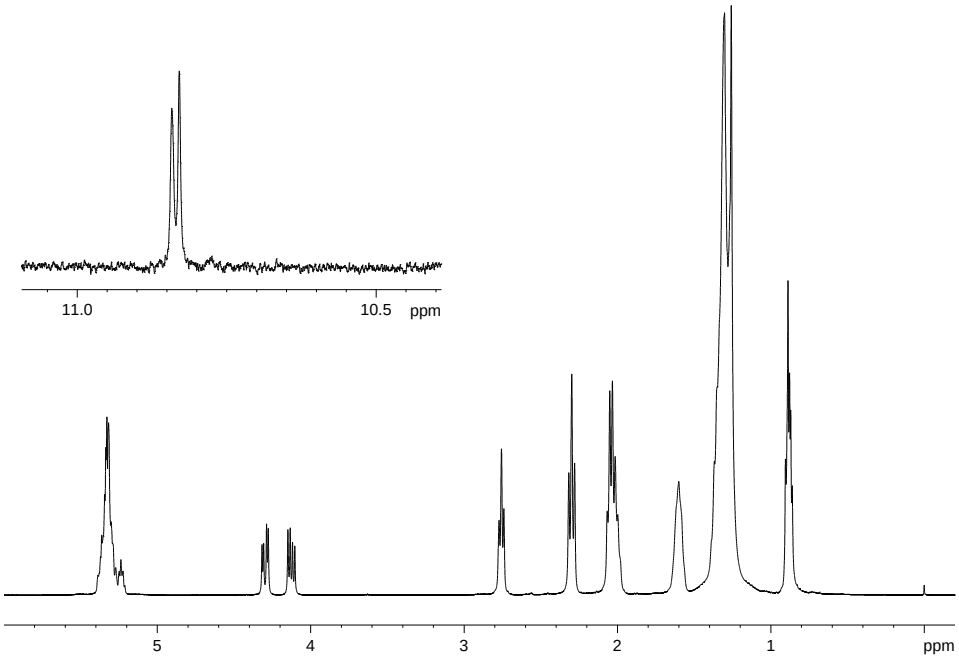

Olive oil

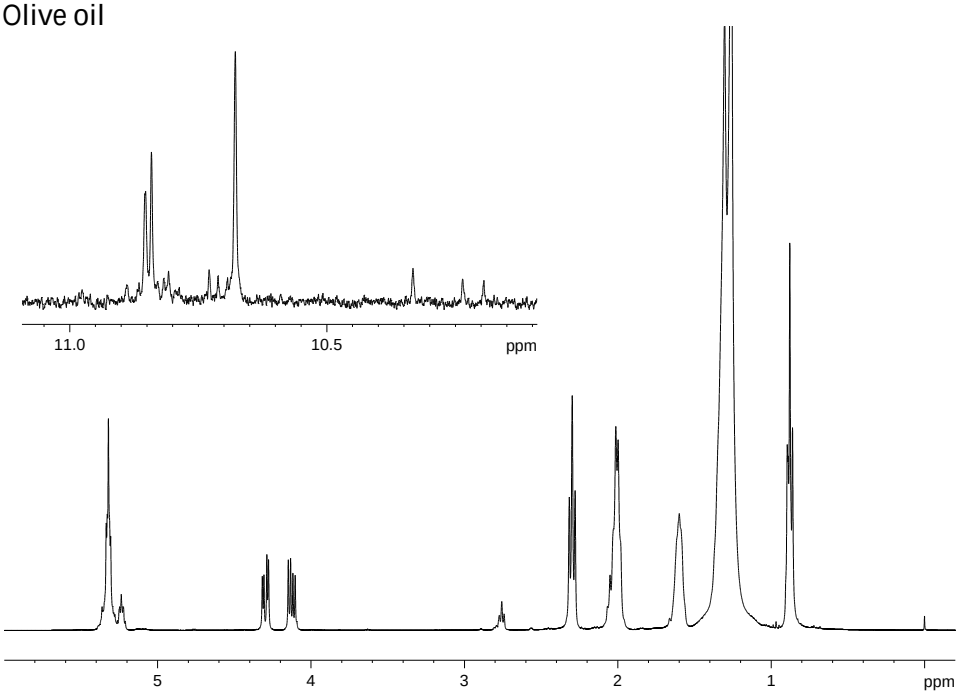

Peanut oil

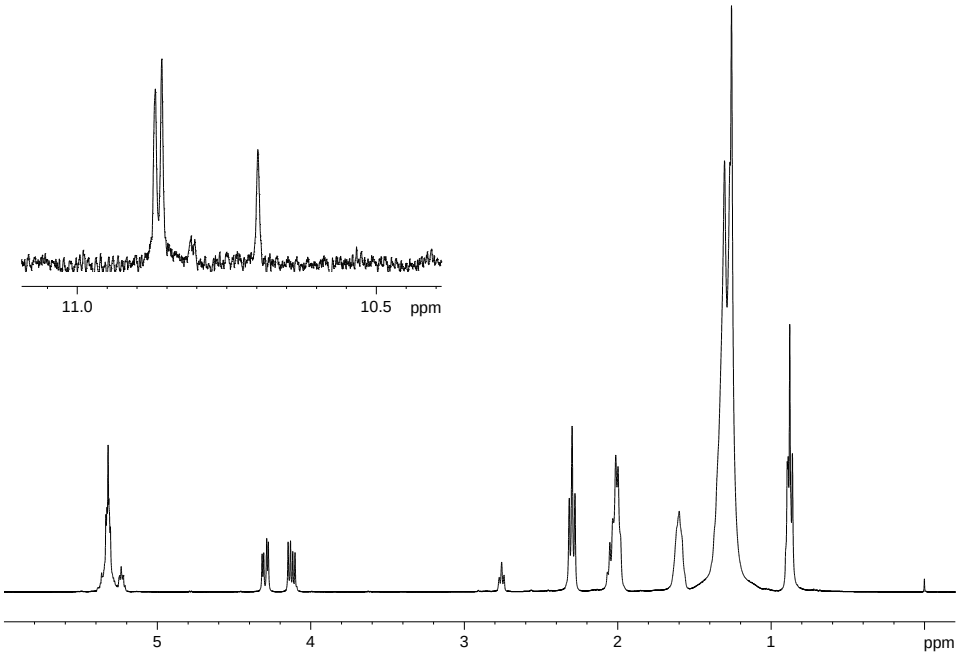

Almond oil

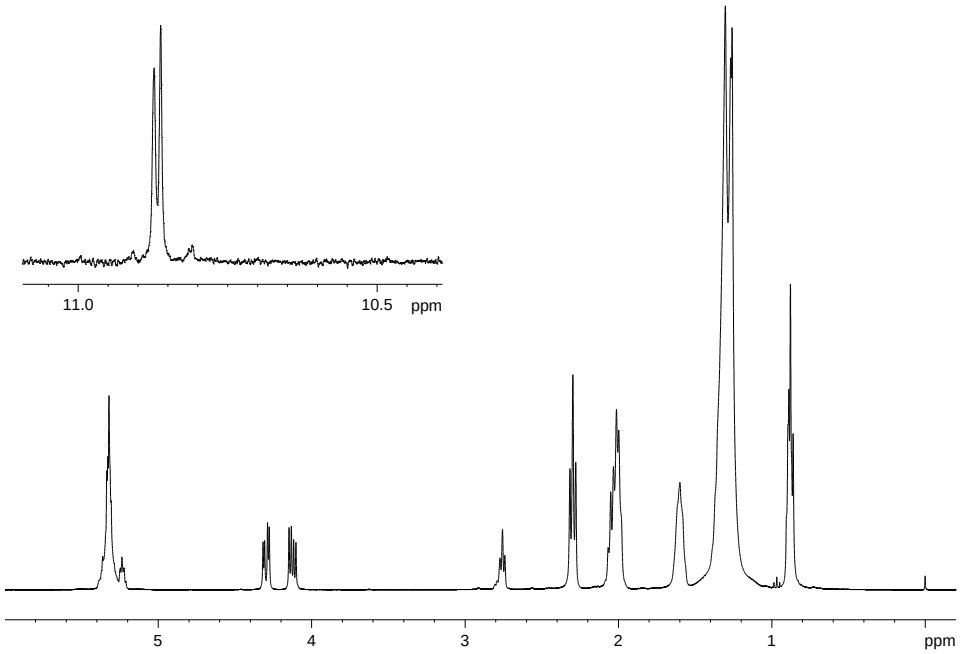

Hazelnut oil

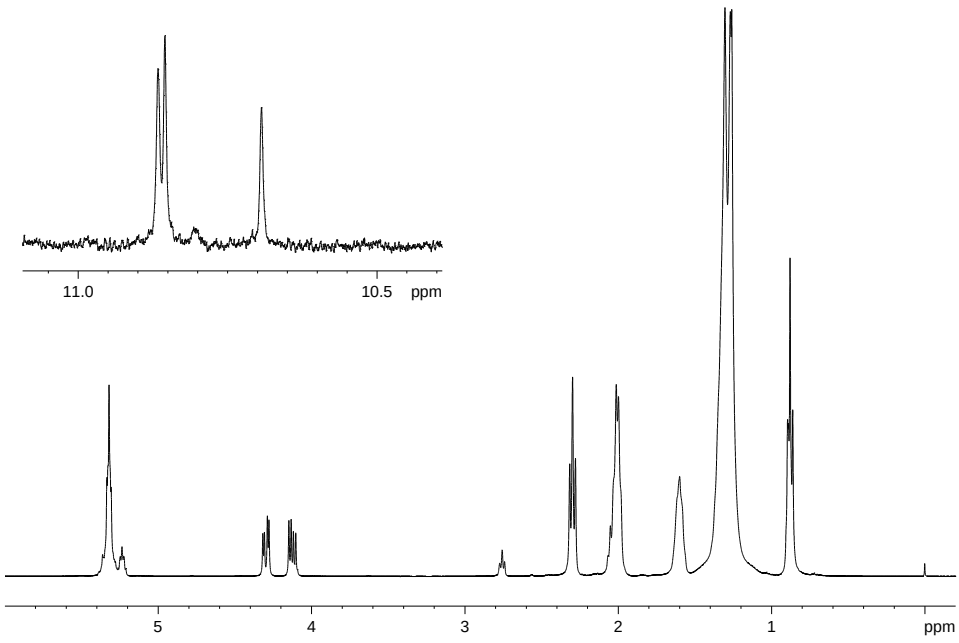

Pistachio oil

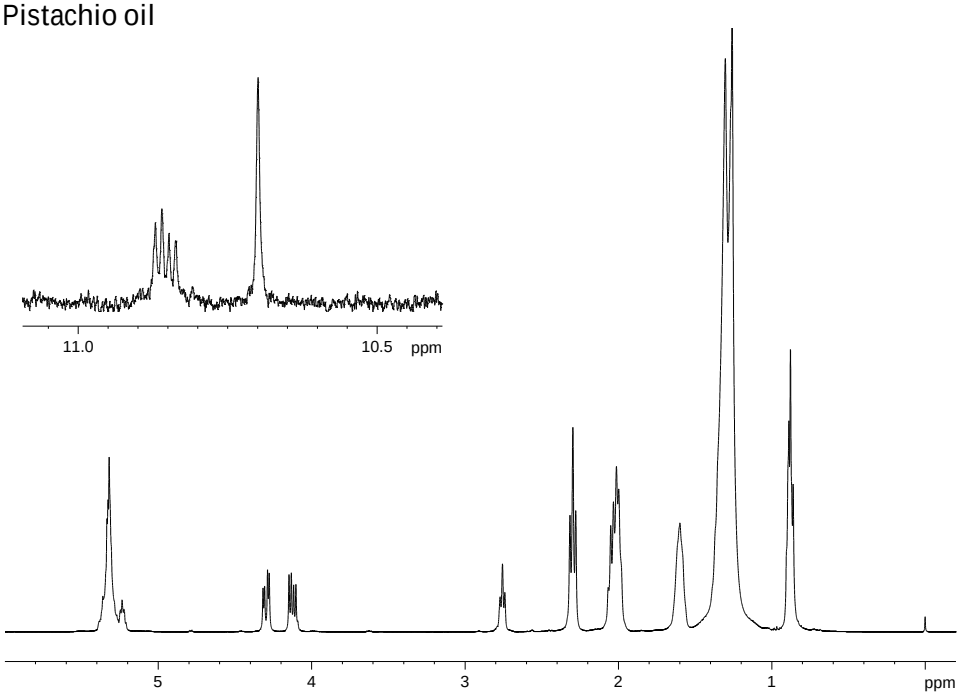

Pumpkin seed oil

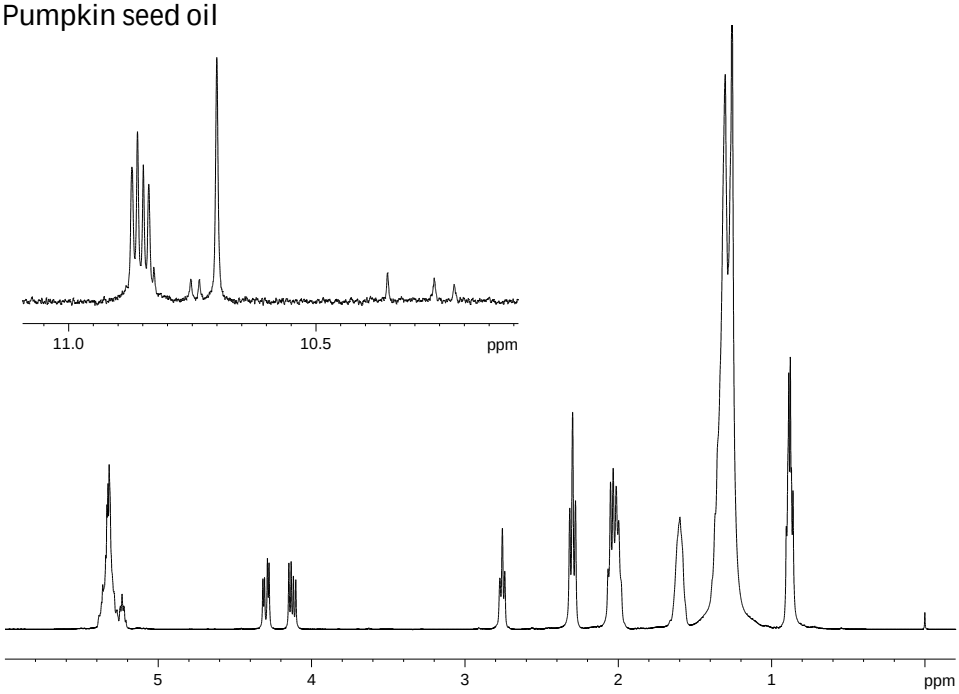

Grape seed oil

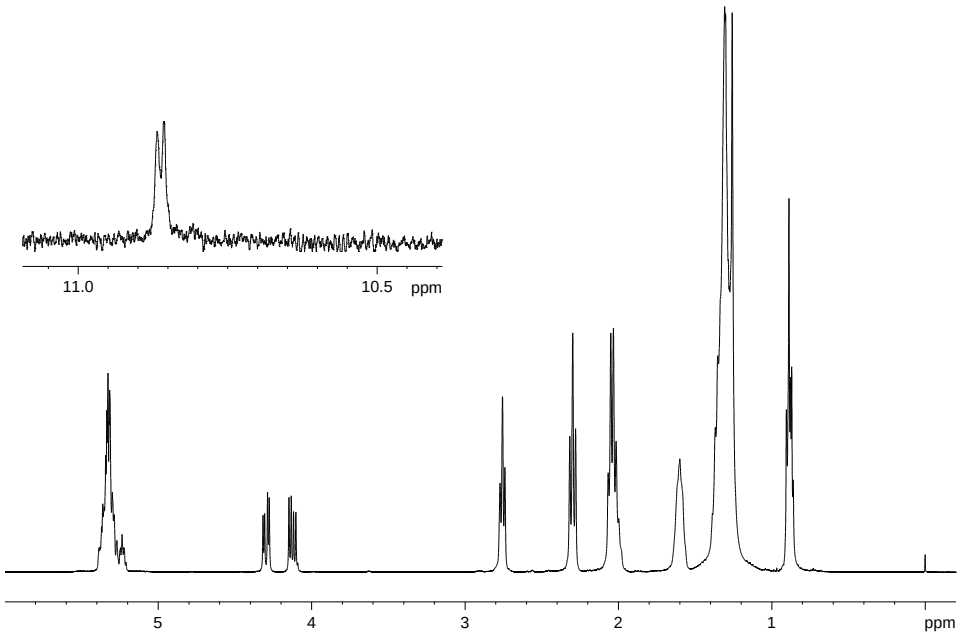

Linseed oil

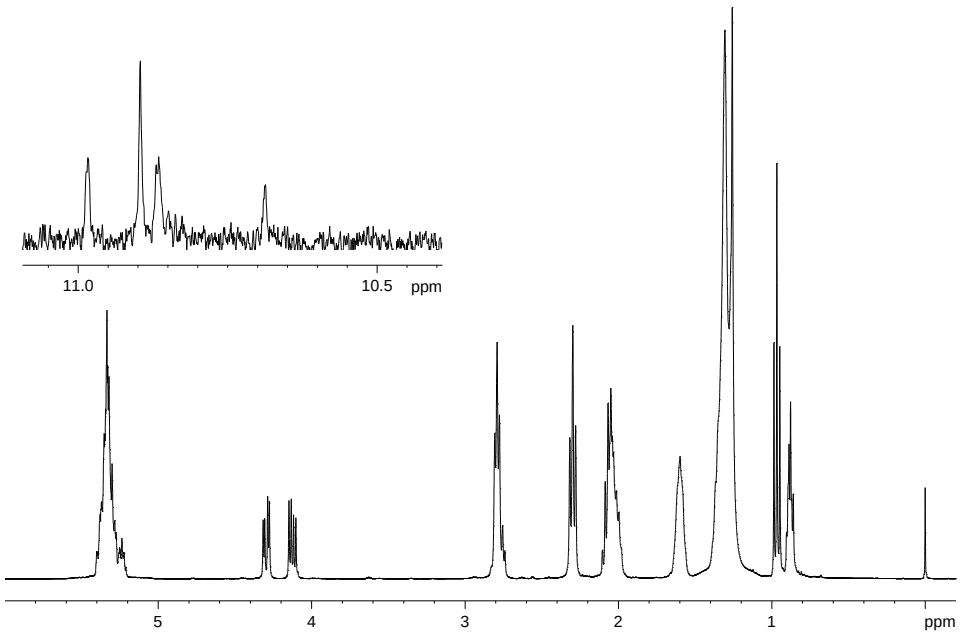

Walnut oil

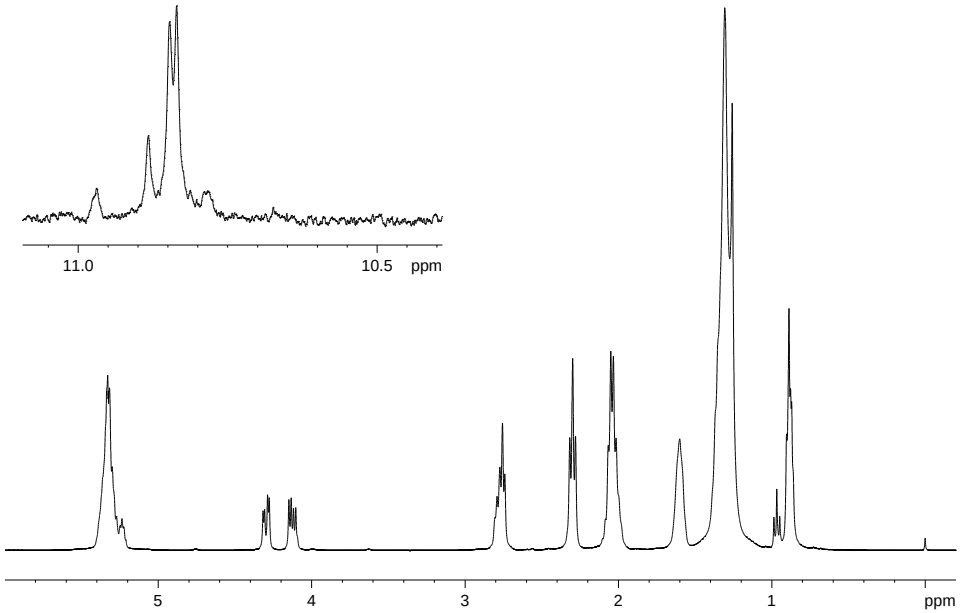

Thistle oil

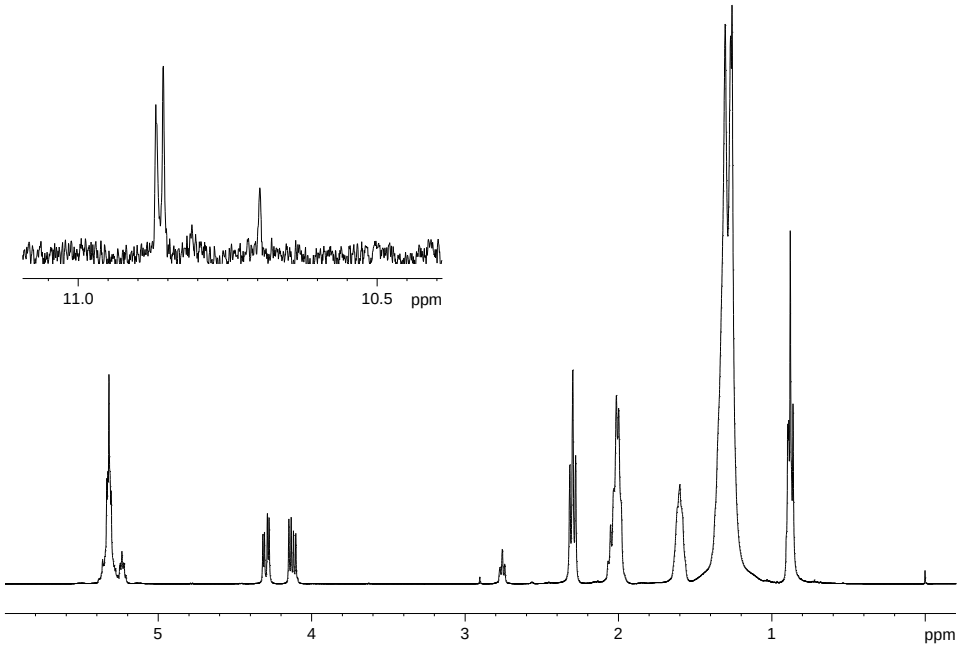

Black seed oil

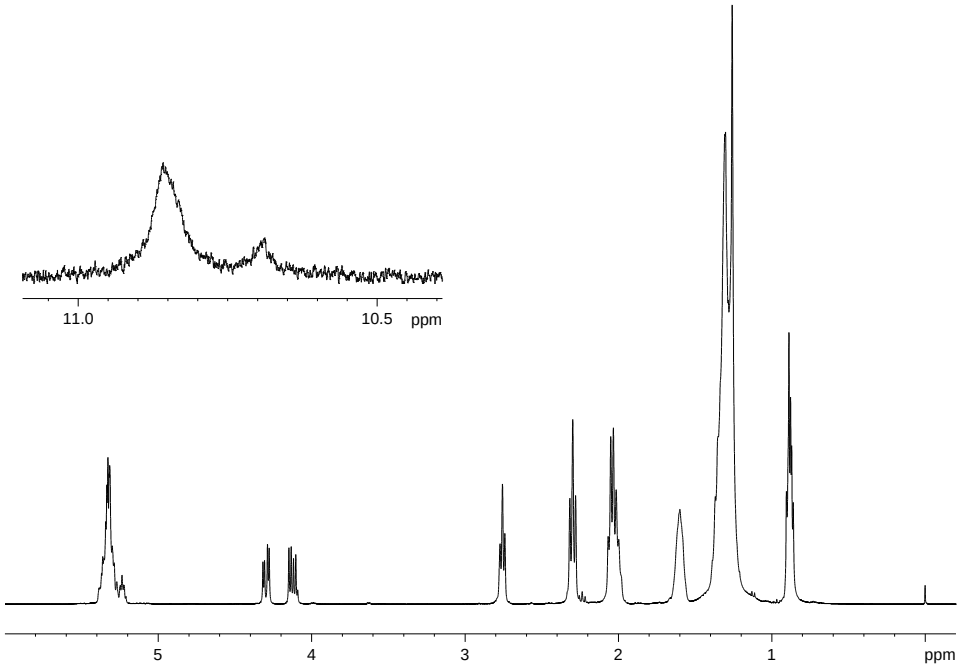

Maize oil

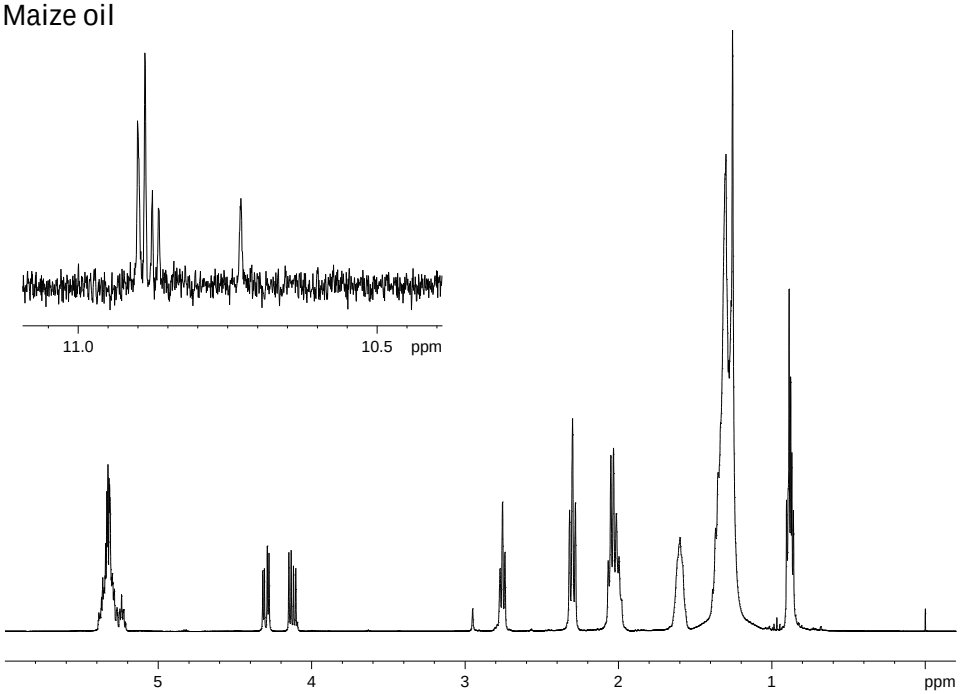

Argan oil

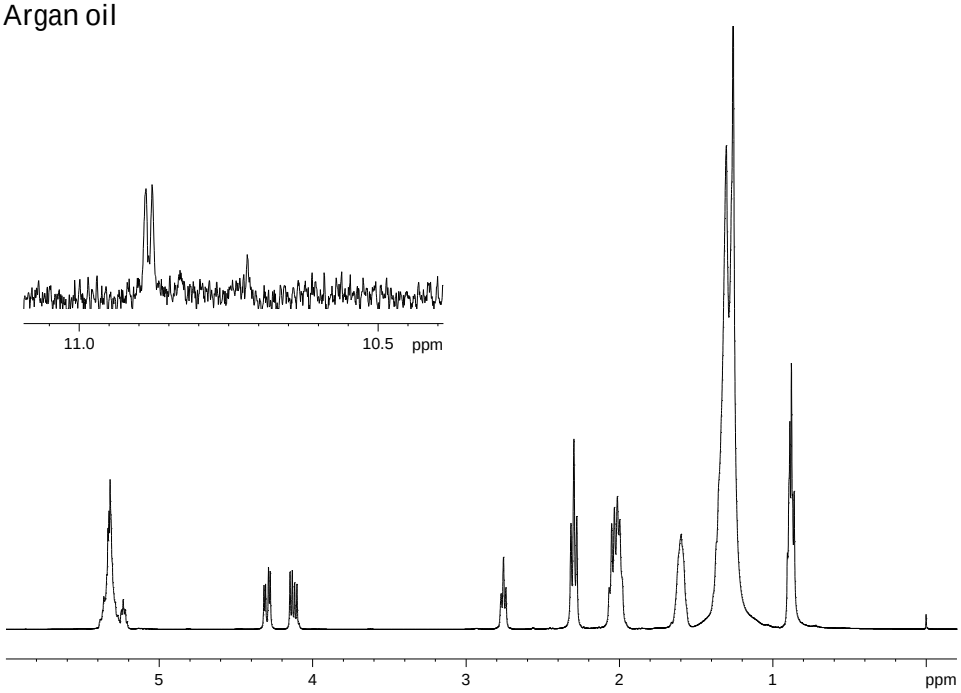

Soya oil

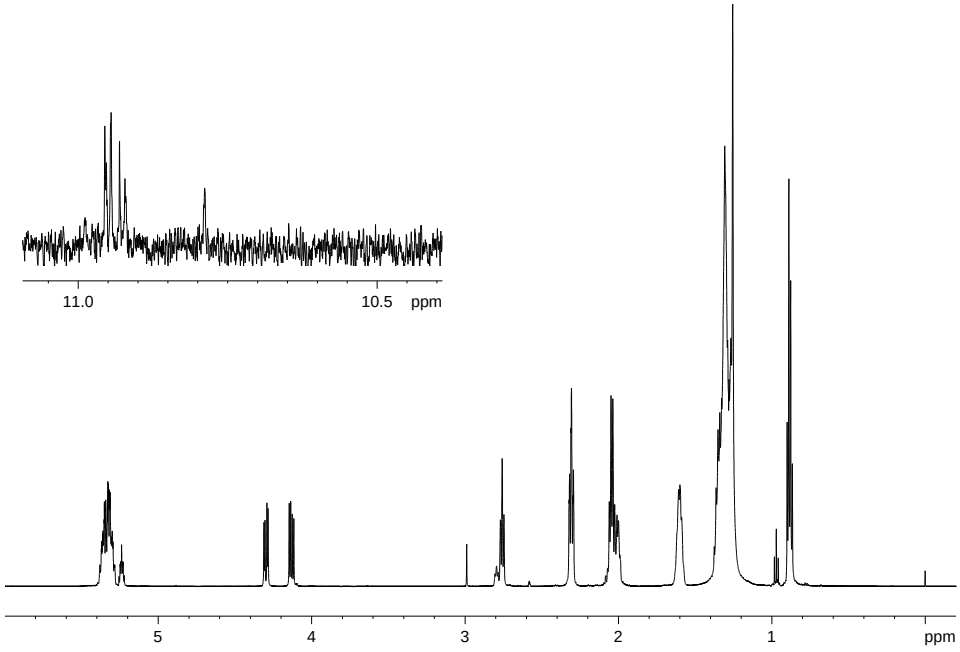

Coconut fat

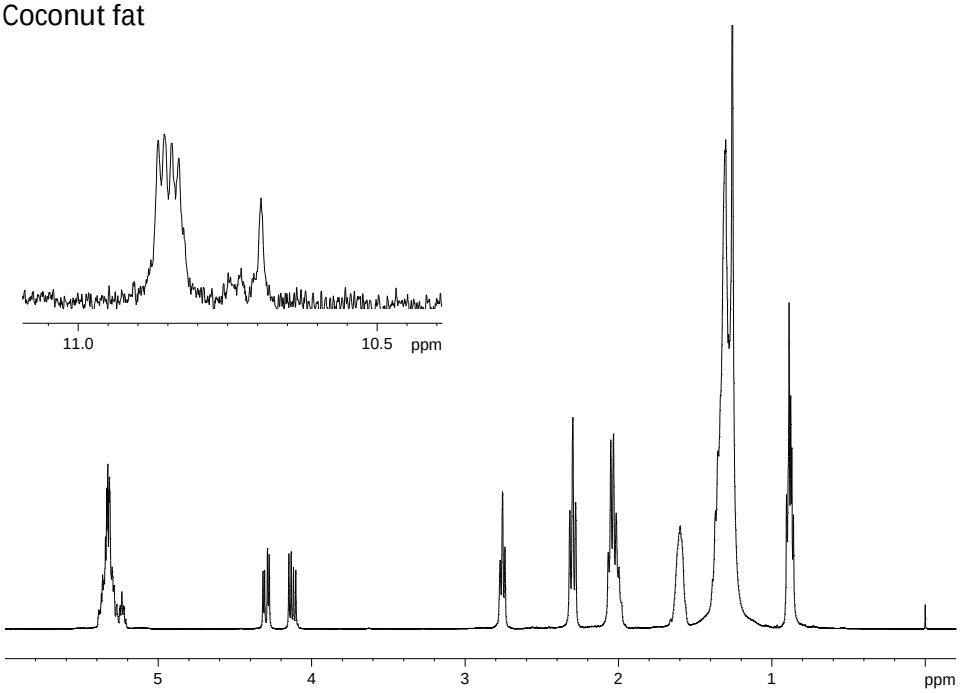

Macadamia nut oil

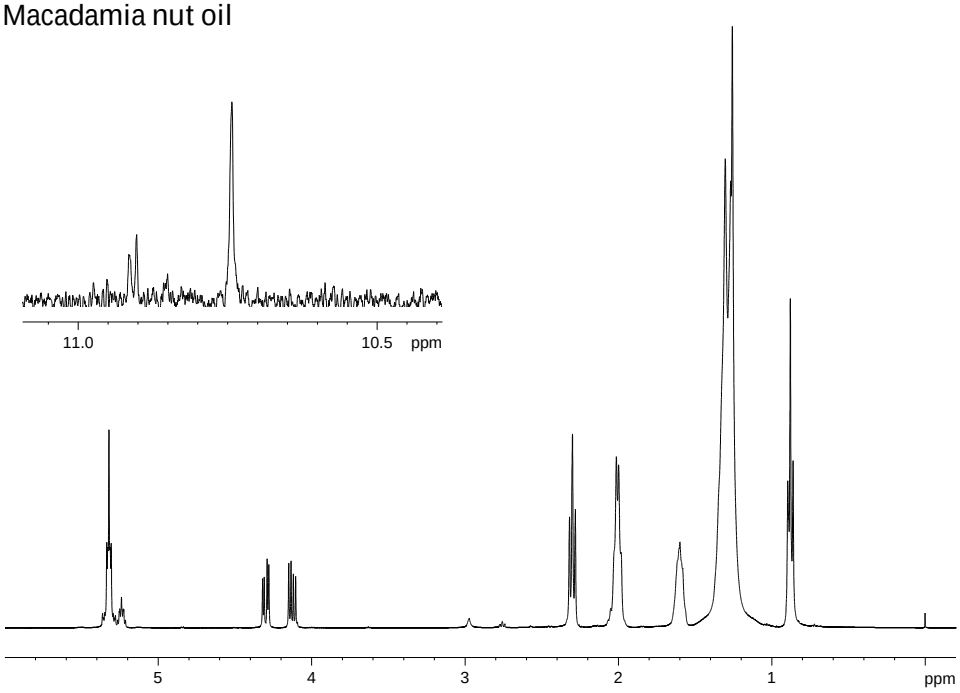

Rice oil

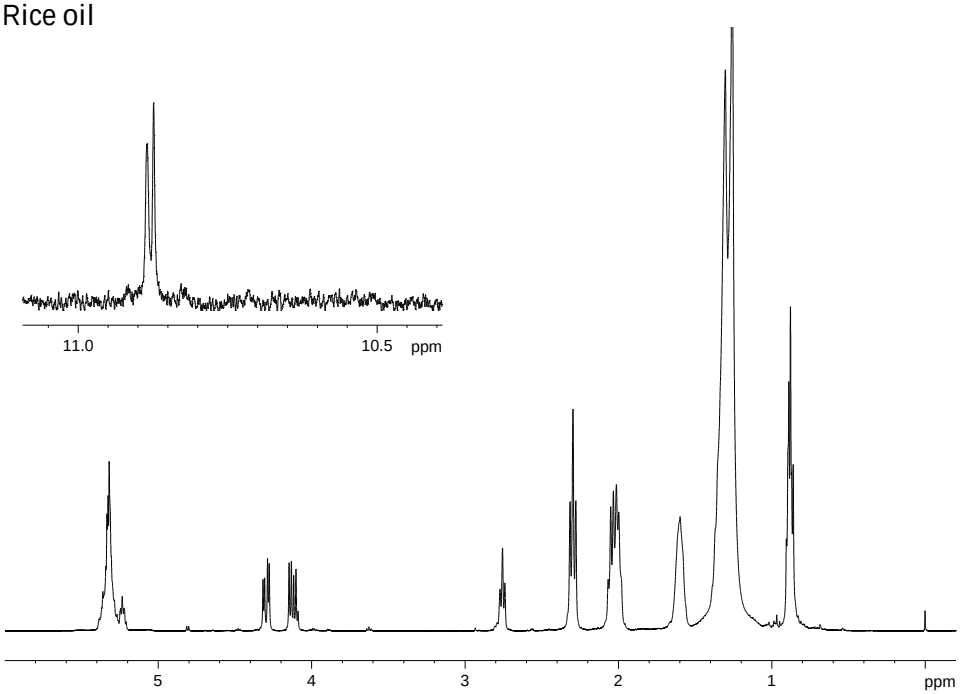

Palm oil (+ rapeseed oil)

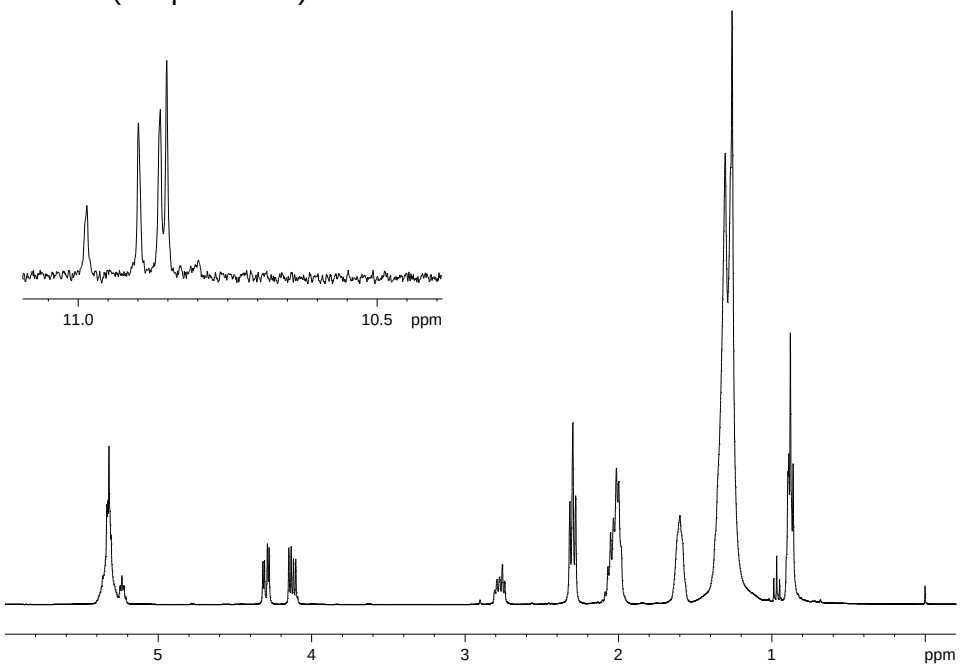

Hemp oil

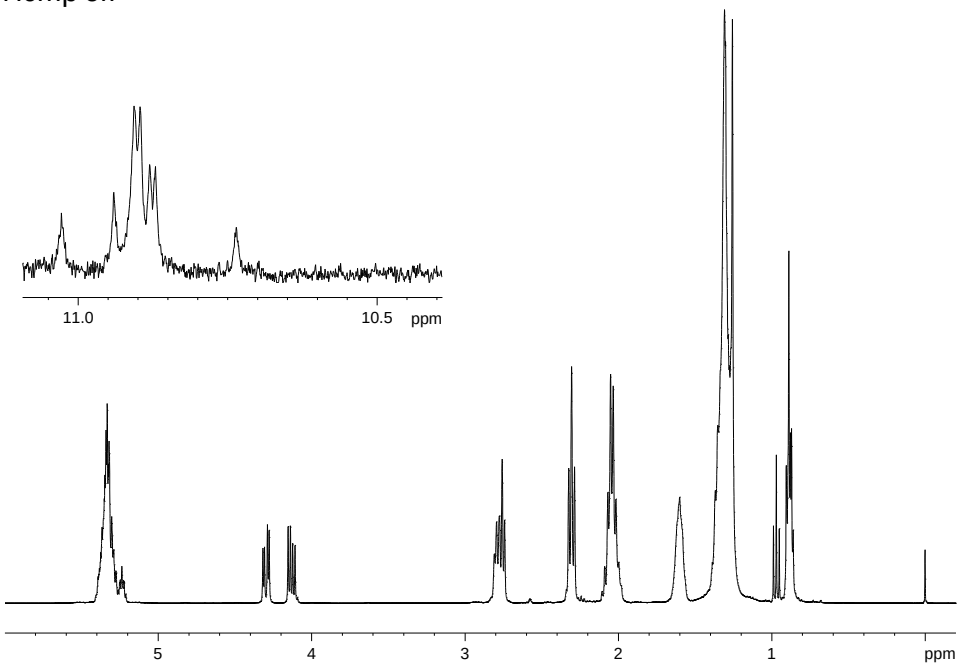

Alba oil

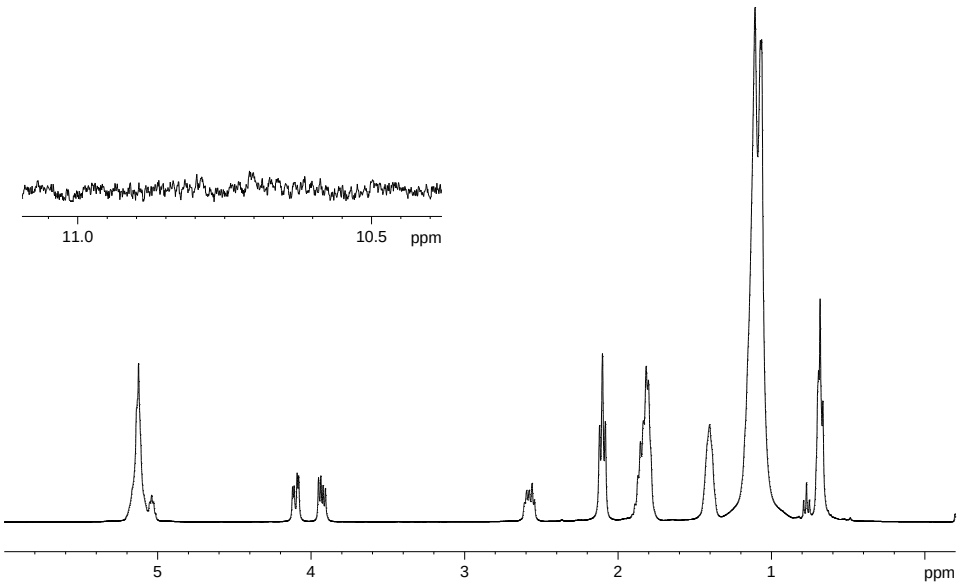

Sesame oil

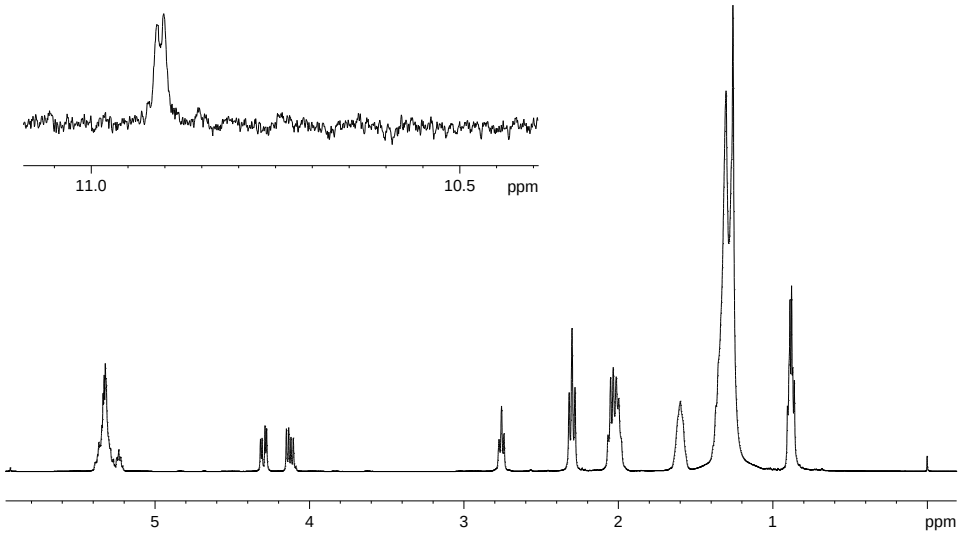

List of figures

Fig. 1: Structure of A) a TAG in Fischer projection and B) 1-palmitoyl-2-oleyl-3-stearyl-glycerol.

Fig. 2: Scheme of the mechanism of autoxidation.

Fig. 3: Autoxidation mechanism of oleic, linoleic and linolenic acid (Frankel 1998).

Fig. 4: Thermal or metal-catalysed decomposition of fatty acid monohydroperoxides.

Fig. 5: Spin angular momenta A) randomly directed, B) in a magnetic field with precession.

Fig. 6: Bulk magnetization vector in different NMR-relevant states.

Fig. 7: Detection of the NMR signal.

Fig. 8: Fourier transformation.

Fig. 9: ^{1}H NMR spectrum of a maize oil in $CDCl_3$.

Fig. 10: Downfield region of a rapeseed oil dissolved in A) mixtures of benzene-d_6 with $CDCl_3$, B) mixtures of DMSO-d_6 with $CDCl_3$, C) mixtures of acetone-d_6 with $CDCl_3$ and D) acetone-d_6 with addition of palmitic acid (oil concentration: 500 mg/1.2 ml).

Fig. 11: Downfield region of an oxidized sunflower oil dried for 0, 10, 20, 40, 60 and 120 min over a molecular sieve (oil concentration: 500 mg/1.2 ml).

Fig. 12: Downfield region of a rapeseed oil spiked at 2, 4, 8, 20 and 40 mg palmitic acid/g oil (oil concentration: 500 mg/1.2 ml).

Fig. 13: Downfield region of an oxidized sunflower oil with a sample weight of 400 mg, 500 mg, 600 mg, 800 mg, 1000 mg dissolved in 1.2 ml $CDCl_3$/DMSO-d_6 (5:1, v/v) and dried over a molecular sieve.

Fig. 14: OO*H* region A) of a high oleic, high linoleic and a high linolenic oil and B) of oxidized fatty acid methyl esters.

Fig. 15: OO*H* region of olive oil compared to that of oxidized squalene.

Fig. 16: OO*H* region of oxidized A) methyl oleate, B) methyl linoleate and C) methyl linolenate standards dissolved in $CDCl_3$.

Fig. 17: Chiral centres of a trioleate monohydroperoxide.

Fig. 18: Downfield region of the ^{1}H NMR spectrum of oxidized trilinoleate dissolved in $CDCl_3$.

Fig. 19: Downfield region of the ^{1}H NMR spectrum of oxidized trioleate dissolved in $CDCl_3$.

Fig. 20: Downfield region of the ^{1}H NMR spectrum of oxidized trioleate dissolved in $CDCl_3$. The spectrum is divided into six sections.

Fig. 21: Kinetics of the hydroperoxide formation of trioleate.

Fig. 22: *PV* in meq/kg versus the NMR-determined peroxide amount in mmol/kg (curve fitting by Deming regression).

Fig. 23: Plot of A) the NMR-determined hydroperoxide amount in mmol/kg versus the mixing ratio υ and B) the classical *PV* versus the mixing ratio υ.

Fig. 24: Plot of the *PV* versus the NMR-determined hydroperoxide amount for 444 oil samples.

Fig. 25: *PV* in meq/kg plotted versus the NMR-determined hydroperoxide amount in mmol/kg.

Fig. 26: ^{1}H NMR spectrum of a black seed oil containing thymoquinone as minor component.

Fig. 27: Formation of hydroxytyrosol in olive oils (Vissers et al. 2004).

Fig. 28: Downfield region of the ^{1}H NMR spectrum of a linseed oil dissolved in different mixtures of $CDCl_3$/DMSO-d_6 with 0 % to 25 % DMSO-d_6 (v/v).

Fig. 29: ^{1}H NMR spectrum of a rapeseed oil dissolved in $CDCl_3$/DMSO-d_6 (5:1, v/v).

Fig. 30: *AV* in mg KOH/g oil versus the NMR-determined FFA amount in mmol/mol TAG (curve fitted by Deming regression).

Fig. 31: Plot of the *AVs* versus the NMR-determined FFA amounts of 420 oil samples, overlaid by the straight line from equation 19.

Fig. 32: Downfield region of the ^{1}H NMR spectra of A) a thistle oil spiked with 0 %, 1 %, 2.5 %, 4.5 %, 10 % 3-pentanol in a mixture of $CDCl_3$/DMSO-d_6 (5:1, v/v); B) a rapeseed oil spiked with 0 %, 1 %, 10 %, 46 % ricinoleic acid methyl ester (RAME) in a mixture of $CDCl_3$/DMSO-d_6 (5:1, v/v); C) a castor oil with a sample weight of 250 mg, 125 mg, 63 mg, 31 mg, 16 mg dissolved in 0.6 ml of a mixture of $CDCl_3$/DMSO-d_6 (5:1, v/v); D) a castor oil dissolved in a mixture of $CDCl_3$/DMSO-d_6 with 17 % DMSO-d_6, 33 % DMSO-d_6, 50 % DMSO-d_6, 67 % DMSO-d_6, 83 % DMSO-d_6. The factors in brackets give the calculated excess of DMSO-d_6 molecules in comparison to hydroxyl groups in the sample solution.

Fig. 33: Aldehyde species in fats and oils (Guillén & Goicoechea 2009).

Fig. 34: Carbonyl region of the ^{1}H NMR spectrum of a mixture of n-hexanal (triplet), (*Z*,*E*)-2,4-hexadienal (doublet), (*E*,*E*)-2,4-hexadienal (doublet) and (*E*)-2-hexenal (doublet).

Fig. 35: Possible explanation of the observed shift differences of saturated and unsaturated aldehydes.

Fig. 36: ^{1}H NMR spectrum of a grape seed oil with zoomed downfield region.

Fig. 37: Reaction of saturated and unsaturated aldehydes with p-anisidine.

Fig. 38: Plots of the *ANV* versus the NMR-determined amount fraction for the aldehyde standards.

Fig. 39: Plot of the *ANVs* versus the NMR-determined *ANVs* of 79 oil samples.

Fig. 40: Water steam distillation apparatus according to Antonacopoulos (Antonacopoulos 1960).

List of tables

Tab. 1 Minor components of fats and oils.

Tab. 2 Quality requirements of the German guidelines for edible fats and oils.

Tab. 3 Dissociation energies of hydrogen atoms (Belitz et al. 2008).

Tab. 4 Proportions of hydroperoxide species of a) methyl oleate, b) methyl linoleate and c) methyl linolenate from autoxidation at 25 °C.

Tab. 5 Parameters of the exponential curves.

Tab. 6 Ratios of the hydroperoxide amounts in section 1 to 6.

Tab. 7 Comparison of AV_{NMR} and the classical *AV*.

Tab. 8 Comparison of AV_{NMR} and the classical *AV* of oleyl oleate.

Tab. 9 Comparison of AV_{NMR} and the classical *AV* of waxes.

Tab. 10 *SV* and SV_{NMR} of different lipid samples.

Tab. 11 Compound specific coefficients to model the *ANV*.

Tab. 12 Oxidation kinetics of trioleate: hydroperoxide amounts in mmol/mol.

Tab. 13 Analysis of Delios V spiked with different proportions of oxidized methyl linoleate.

Tab. 14 Results obtained from the analysis of 444 fats and oils by the NMR and the *PV* method.

Tab. 15 Analysis of a rapeseed oil spiked with different palmitic acid amounts.

Tab. 16 AV_{NMR}: Replicate measurements of oleyl oleate.

Tab. 17 Results obtained from the analysis of 420 fats and oils by the NMR and *AV* method.

Tab. 18 Analysis of mixtures of aldehyde standards and Delios V by the NMR and *ANV* method.

Tab. 19 Results of a round robin test on the *ANV* method: *ANVs* of dublicate measurements (mean values) of 8 different fats and oils with corresponding repeatability standard deviation $\hat{\sigma}_R$ and number of considered laboratories (L13.00-15 2008).

Tab. 20 Results obtained from the analysis of 79 fats and oils by the NMR and the *ANV* method.

List of abbreviations

Acetone-d_6	Hexadeuterioacetone
ANV	Anisidine value
AV	Acid value
Benzene-d_6	Hexadeuteriobenzene
α-carbonyl CH_2	CH_2 protons directly adjacent to the COOH of fatty acids
$CDCl_3$	Deuterated chloroform
C*H*O	Carbonyl group proton
CI	Confidence interval
COO*H*	Carboxyl group proton
DMSO-d_6	Hexadeuteriodimethylsulfoxide
Eq	Equivalent
FFA	Free fatty acid
FID	Free induction decay
Fig.	Figure
IV	Iodine value
NMR	Nuclear magnetic resonance
OO*H*	Hydroperoxide group proton
HV	Hydroxy value
Ph. Eur.	European Pharmacopoeia
PV	Peroxide value
qNMR	Quantitative NMR
$R^{\cdot}$	Alkyl radical
RAME	Ricinolic acid methyl ester
R.F.	Radiofrequency
$ROO^{\cdot}$	Peroxyl radical
Sn	Stereospecific numbering
SV	Saponification value
TAG	Triacylglyceride
TCNB	Tetrachlornitrobenzene
TMS	Tetramethylsilane
TOTOX value	Total oxidation product value
USM	Unsaponifiable matter
USP	United States Pharmacopoeia

List of variables

AV	Acid value
θ	Angle between the spin magnetic momentum and the field
a	Aldehyde specific coefficients
ANV	Anisidine value
δ_H	Chemical shift
c	Concentration
$\hat{\sigma}_R$	Empirical repeatability standard deviation
μ	Expectation value
γ	Gyromagnetic ratio
ω_0	Larmor frequency
T_1	Longitudinal relaxation time
B_0	Magnetic field
φ	Magnetic momentum
m	Mass
AV_{NMR}	Modelled acid value
ANV_{NMR}	Modelled anisidine value
M	Molecular weight
$\hat{S}$	Nuclear spin angular momentum
N	Number of protons
PV	Peroxide value
P	Purity
$t_{1-\propto,f}$	$1-\propto$ Quantile of the t-distribution with f degrees of freedom
k	Rate constant
RS	Relative sensitivity
τ	Repetition time
rsd	Residual standard deviation
$RS_{NMR/AV}$	RS of the NMR assay with respect to the *AV* method
$RS_{NMR/PV}$	RS of the NMR assay with respect to the *PV* method
I	Signal intensity (integrated signal area)
k_S	Spectrometer constant
I_s	Spin quantum number
t	Time

References

Antonacopoulos N (1960)
Verbesserte Apparatur zur quantitativen Destillation wasserdampfflüchtiger Stoffe. *Z. Lebensmitt.-Untersuch.* 113: 113-116

Belitz H-D, Grosch W, Schieberle P (2008)
Lehrbuch der Lebensmittelchemie, sixth ed., Springer-Verlag, Berlin, Heidelberg.

Belloque J, Ramos M (1999)
Application of NMR spectroscopy to milk and dairy products. *Trends Food Sci Technol* 10(10): 313-320

Bertram HC, Andersen HJ (2004)
Applications of NMR in meat science. *Annual Reports on NMR Spectroscopy* 53: 157-202

Beyer T, Schollmayer C, Holzgrabe U (2010)
The role of solvents in the signal separation for quantitative ^{1}H NMR spectroscopy. *J Pharm Biomed Anal* 52(1): 51-58

Bharti SK, Roy R (2012)
Quantitative ^{1}H NMR spectroscopy. *Trends Analyt Chem* 35: 5-26

Blaschek W, Ebel S, Hackenthal E, Holzgrabe U, Keller K, Reichling J, Schulz V (2012)
Hager ROM, Hagers Handbuch der Drogen und Arzneistoffe, Einträge: Hartfett, Oleyloleat, Springer-Verlag, Berlin, Heidelberg, New York

Bockisch M (2004)
Öle und Fette (außer Margarine), in: Heiss R (ed.) Lebensmitteltechnologie: Biotechnologische, chemische, mechanische und thermische Verfahren der Lebensmittelverarbeitung, sixth ed., Springer-Verlag, Berlin, Heidelberg

Bracher F, Heisig P, Langguth P, Mutschler E, Rücker G, Scriba G, Stahl-Biskup E, Troschütz R (2012)
Kommentar zum Europäischen Arzneibuch, 41. Aktualisierungslieferung, Monographie Pflanzliche Fette und Öle 1579, Monographie Unverseifbare Anteile 2.05.07.00 Wissenschaftliche Verlagsgesellschaft Stuttgart, Govi-Verlag, Pharmazeutischer Verlag GmbH Eschborn

Brash AR (2000)
Autoxidation of methyl linoleate: Identification of the bis-allylic 11-hydroperoxide. *Lipids* 35(9): 947-952

Burits M, Bucar F (2000)
Antioxidant activity of *Nigella sativa* essential oil. *Phytother Res* 14(5): 323-328

Butt MS, Sultan MT (2010)
Nigella sativa: reduces the risk of various maladies. *Crit Rev Food Sci Nutr* 50(7): 654-665

Chan HW-S, Levett G (1977a)
Autoxidation of methyl linoleate. Separation and analysis of isomeric mixtures of methyl linoleate hydroperoxides and methyl hydroxylinoleates. *Lipids* 12(1): 99-104

Chan, HW-S, Levett G (1977b)
Autoxidation of methyl linolenate: Analysis of methyl hydroxylinolenate isomers by high performance liquid chromatography. *Lipids* 12(10): 837-840

Claxson AW, Hawkes GE, Richardson DP, Naughton DP, Haywood RM, Chander CL, Atherton M, Lynch EJ, Grootveld MC (1994)
Generation of lipid peroxidation products in culinary oils and fats during episodes of thermal stressing: a high field ^{1}H NMR study. *FEBS Lett* 355(1): 81-90

CODEX STAN 19-1981
Codex standard for edible fats and oils not covered by individual standards, Rev. 2-1999, FAO/WHO Codex alimentarius commission, Rome

Commission Regulation (EEC) No 2568/91
on the characteristics of olive oil and olive-residue oil and on the relevant methods of analysis, OJ L 248 p 1 (5.09.1991), last change: Commission Regulation (EU) No. 229/2013 L 90 p 52 (26.03.2013)

Dayrit FM, Buenafe OE, Chainani ET, de Vera IM (2008)
Analysis of monoglycerides, diglycerides, sterols, and free fatty acids in coconut (Cocos nucifera, L.) oil by ^{31}P NMR spectroscopy. *J Agric Food Chem* 56(14): 5765-5769

De Levie R (2001)
How to use excel in analytical chemistry and in general scientific data analysis, Cambridge University Press, Cambridge

Dobarganes MC, Velasco J (2002)
Analysis of lipid hydroperoxides. *Eur J Lipid Sci Technol* 104(7): 420-428

Draper NR, Smith H (1998)
Applied regression analysis, third ed., Wiley, New York

Dubois J, van de Voort FR, Sedman J, Ismail AA, Ramaswamy HR (1996)
Quantitative Fourier transform infrared analysis for anisidine value and aldehydes in thermally stressed oils. *J Am Oil Chem Soc* 73(6): 787-794

Efron B, Tibshirani RJ (1993)
An introduction to the bootstrap, Chapman & Hall/CRC, Boca Raton, London

Ellison SLR, Williams A (2012)
EURACHEM/CITAC Guide: quantifying uncertainty in analytical measurement, third ed., ISBN 978-0-948926-30-3, www.eurachem.org.

Fauhl C, Reniero F, Guillou C (2000)
^{1}H NMR as a tool for the analysis of mixtures of virgin olive oil with oils of different botanical origin. *Magn Reson Chem* 2000(38): 436-443

Fishwick MJ, Swoboda PAT (1977)
Measurement of oxidation of polyunsaturated fatty acids by spectrophotometric assay of conjugated derivates. *J Sci Fd Agric* 28(4): 387-393

Frankel EN, Neff WE, Rohwedder WK, Khambay BPS, Garwood RF, Weedon BCL (1977)
Analysis of autoxidized fats by gas chromatography-mass spectrometry: III. methyl linolenate. *Lipids* 12(12): 1055-1061

Frankel EN, Garwood RF, Khambay BPS, Moss GP, Weedon BCL (1984)
Stereochemistry of olefin and fatty acid oxidation. Part 3 Allylic hydroperoxides from autoxidation of methyl oleate. *J Chem Soc Perkin 1* 0: 2233-2240

Frankel EN, Neff WE, Miyashita K (1990a)
Autoxidation of polyunsaturated triacylglycerols. II. Trilinolenoylglycerol. *Lipids* 25(1): 40-47

Frankel EN, Neff WE, Weisleder D (1990b)
Determination of methyl linoleate hydroperoxides by ^{13}C nuclear magnetic resonance spectroscopy. *Methods Enzymol* 186: 380-387

Frankel EN (1991)
Review. Recent advances in lipid oxidation. *J Sci Food Agric* 54(4): 495-511

Frankel EN (1998)
Lipid oxidation, The Oily Press ltd, Scotland

Fribolin H (2011)
Basic one- and two-dimensional NMR spectroscopy, fifth ed., Wiley-VCH, Weinheim

Gladovič **N, Zupančič**-Kralj L, Plavec J (1997)
Determination of primary oxidation products of linoleic acid and triacylglycerols. *J Chromatogr A* 767(1): 63-68

Gray JI (1978)
Measurement of lipid oxidation: A review. *J Am Oil Chem Soc* 55(6): 539-546

Günther H (1996)
NMR Spectroscopy, second ed., Wiley-VCH, Chichester

Guillén MD, Cabo N (2002)
Fourier transform infrared spectra data versus peroxide and anisidine values to determine oxidative stability of edible oils. *Food Chem* 77(4): 503-510

Guillén MD, Ruiz A (2004)
Formation of hydroperoxy- and hydroxyalkenals during thermal oxidative degradation of sesame oil monitored by proton NMR. *Eur J Lipid Sci Technol* 106(10): 680-687

Guillén MD, Ruiz A (2006)
Study by means of ^{1}H nuclear magnetic resonance of the oxidation process undergone by edible oils of different natures submitted to microwave action. *Food Chem* 96(4): 665-674

Guillén MD, Ruiz A (2008)
Monitoring of heat-induced degradation of edible oils by proton NMR. *Eur J Lipid Sci Technol* 110: 52-60

Guillén MD, Goicoechea E (2009)
Oxidation of corn oil at room temperature: primary and secondary oxidation products and determination of their concentration in the oil liquid matrix from ^{1}H nuclear magnetic resonance data. *Food Chem* 116: 183-192

Guillén MD, Uriate PS (2009)
Contribution to further understanding of the evolution of sunflower oil submitted to frying temperature in a domestic fryer: study by ^{1}H nuclear magnetic resonance. *J Agric Food Chem* 57(17): 7790-7799

Hämäläinen TI, Sundberg S, Mäkinen M, Kaltia S, Hase T, Hopia A (2001)
Hydroperoxide formation during autoxidation of conjugated linoleic acid methyl ester. *Eur J Lipid Sci Technol* 103(9): 588-593

Haywood RM, Claxon AWD, Hawkes GE, Richardson DP, Naughton DP, Coumbarides G, Hawkes J, Lynch EJ, Grootveld MC (1995)
Detection of aldehydes and their conjugated hydroperoxydiene precursors in thermally-stressed culinary oils and fats: investigations using high resolution proton NMR spectroscopy. *Free Radic Res* 22(5): 441-482

Hidalgo FJ, Zamora R (2003)
Edible oil analysis by high-resolution nuclear magnetic resonance spectroscopy: recent advances and future perspectives. *Trends Food Sci Technol* 14(12): 499-506

Holman RT, Elmer OC (1947)
The rates of oxidation of unsaturated fatty acids and esters. *J Am Oil Chem Soc* 24(4): 127-129

Holzgrabe U, Wawer I, Diehl B (2008)
NMR Spectroscopy in pharmaceutical analysis, Elsevier, Oxford

Holzgrabe U (2010)
Quantitative NMR spectroscopy in pharmaceutical applications. *Prog Nucl Magn Reson Spectrosc* 57(2): 229-240

ISO 660:2009
Animal and vegetable fats and oils - determination of acid value and acidity, third ed., International Organization for Standardization, Geneva

ISO 3657:2002
Animal and vegetable fats and oils - Determination of saponification value, third ed., International Organization for Standardization, Geneva

ISO 3960:2007
Animal and vegetable fats and oils - determination of peroxide value – iodometric (visual) endpoint determination, forth ed., International Organization for Standardization, Geneva

ISO 6885:2006
Animal and vegetable fats and oils - determination of anisidine value, third ed., International Organization for Standardization, Geneva

Kamal-Eldin A (2005)
Minor components of fats and oils, in: Shahidi F (ed.) Bailey´s industrial oil and fat products, sixth ed., John Wiley & Sons, Inc., New York

Kamal-Eldin A, Pocorny J (2005)
Analysis of lipid oxidation, first ed., AOCS Press, Champaign

Keeler J (2010)
Understanding NMR spectroscopy, second ed., Wiley, Chichester

Kidric J (2008)
NMR study of beverages. *Annual Reports on NMR Spectroscopy* 64: 161-171

Krist S, Buchbauer G, Klausberger C (2008)
Lexikon der pflanzlichen Öle und Fette, Springer, Vienna

L13.00-15 (2008)
Amtliche Sammlung der Untersuchungsverfahren nach §64 LFGB: Untersuchung von Lebensmitteln – Bestimmung der Anisidinzahl in tierischen und pflanzlichen Fetten und Ölen (Übernahme der gleichnamigen DIN EN ISO 6885, Ausgabe Oktober 2007)

Levitt MH (2009)
Spin dynamics – Basics of nuclear magnetic resonance, second ed., Wiley, Chichester

Liu J, Yeo HC, Doniger SJ, Ames BN (1997)
Assay of aldehydes from lipid peroxidation: Gas chromatography – mass – spectrometry compared to thiobarbituric acid. *Anal Biochem* 245(2): 161-166

LS Speisefette 2011
Leitsätze für Speiseöle und Speisefette des Deutschen Lebensmittelbuchs in der Neufassung vom 30.05.2011 (Beilage zum BAnz. Nr. 111 a vom 27.07.2011, GMBI Nr. 24 S 480 vom 27.07.2011)

Mandel J (1964)
The statistical analysis of experimental data, Wiley & Sons, Inc., New York

Mannina L, D'Imperio M, Capitani D, Rezzi S, Guillou C, Mavromoustakos T, Vilchez MDM, Fernández AH, Thomas F, Aparicio R (2009)
^{1}H NMR-based protocol for the detection of adulterations of refined olive oil with refined hazelnut oil *J. Agric. Food Chem.* 57(24): 11550-11556

Medina I, Sacchi R, Giudicianni I, Aubourg S (1998)
Oxidation in fish lipids during thermal stress as studied by ^{13}C nuclear magnetic resonance spectroscopy. *J Am Oil Chem Soc* 75(2): 147-154

Miyake Y, Yokomizo K, Matsuzaki N (1998)
Rapid determination of iodine value by ^{1}H nuclear magnetic resonance spectroscopy. *J Am Oil Chem Soc* 75(1): 15-19

Muik B, Lendl B, Molina-Díaz A, Ayora-Cãnada MJ (2005)
Direct monitoring of lipid oxidation in edible oils by Fourier transform Raman spectroscopy. *Chem Phys Lipids* 134(2): 173-182

Neff WE, Frankel EN, Miyashita K (1990)
Autoxidation of polyunsaturated triacylglycerols. I. trilinoleoylglycerol. *Lipids* 25(1): 33-39

Ng S (2000)
Quantitative analysis of partial acylglycerols and free fatty acids in palm oil by ^{13}C nuclear magnetic resonance spectroscopy. *J Am Oil Chem Soc* 77(7): 749-755

Pajunen TI, Koskela H, Hase T, Hopia A (2008)
NMR properties of conjugated linoleic acid (CLA) methyl ester hydroperoxides. *Chem Phys Lipids* 154(2): 105-114

Pardun H (1974)
Beurteilung des Präoxydationsgrades bzw. der Oxydationsstabilität pflanzlicher Öle aufgrund ihrer Benzidin- oder Anisidinzahl. *Fette Seifen Anstrichm* 76: 521-528

Ph. Eur. (2011)
European Pharmacopoeia, seventh ed., European Department for the Quality of Medicines, Strasbourg, France, www.pheur.eu

Porter NA, Dussault P, Breyer RA, Kaplan J, Morelli J (1990)
The resolution of racemic hydroperoxides: a chromatography-based separation of perketals derived from arachidonic, linoleic, and oleic acid hydroperoxides. *Chem Res Toxicol* 3(3): 236-243

Porter NA, Mills KA, Carter RL (1994)
A mechanistic study of oleate autoxidation: competing peroxyl H-atom abstraction and rearrangement. *J Am Chem Soc* 116(15): 6690-6696

Porter NA, Caldwell SE, Mills KA (1995)
Mechanisms of free radical oxidation of unsaturated lipids. *Lipids* 30 (4): 277-290

Russell GA (1957)
Deuterium-isotope effects in the autoxidation of aralkyl hydrocarbons. Mechanism of the interaction of peroxy radicals. *J Am Chem Soc* 79(14): 3871-3877

Saito H (1987)
Estimation of the oxidative deterioration of fish oils by measurements of nuclear magnetic resonance. *Agric Biol Chem* 51(12): 3433-3435

Satyarthi JK, Srinivas D, Ratnasamy P (2009)
Estimation of free fatty acid content in oils, fats, and biodiesel by ^{1}H NMR spectroscopy. *Energy Fuels* 23(4): 2273-2277

Servili M, Montedoro G (2002)
Contribution of phenolic compounds to virgin olive oil quality. *Eur J Lipid Sci Technol* 104(9-10): 602-613

Shahidi F, Wanasundra UN (1997)
Application of proton nuclear magnetic resonance (^{1}H NMR) spectroscopy for assessment of oxidative stability of fats and oils, in: Shahidi F (ed.) Natural antioxidants: chemistry, health effects, and applications, first ed., AOCS Press, Champaign, Illinois

Shahidi F, Zhong Y (2005)
Lipid oxidation: Measurement methods, in: Bailey´s industrial oil and fat products, Shahidi F (ed.), sixth ed., John Wiley & Sons Inc., New York

Sharma NK, Ahirwar D, Jhade D, Gupta S (2009)
Medicinal and pharmacological potential of *Nigella sativa*: A review. *Ethnobotancial Review* 13: 946-955

Silwood CJ, Grootveld M (1999)
Application of high-resolution, two-dimensional ^{1}H and ^{13}C nuclear magnetic resonance techniques to the characterization of lipid oxidation products in autoxidized linoleoyl/linolenoylglycerols. *Lipids* 34(7): 741-756

Skiera C, Steliopoulos P, Kuballa T, Holzgrabe U, Diehl B (2012a)
^{1}H NMR spectroscopy as a new tool in the assessment of the oxidative state in edible oils. *J Am Oil Chem Soc* 89(8): 1383-1391

Skiera C, Steliopoulos P, Kuballa T, Holzgrabe U, Diehl B (2012b)
^{1}H NMR approach as an alternative to the classical p-anisidine value method. *Eur Food Res Technol* 235(6): 1101-1105

Skiera C, Steliopoulos P, Kuballa T, Holzgrabe U, Diehl B (2012c)
Determination of free fatty acids in edible oils by ^{1}H NMR spectroscopy. *Lipid Technol* 24(12): 279-281

Skiera C, Steliopoulos P, Kuballa T, Diehl B, Holzgrabe U (2013)
Determination of free fatty acids in pharmaceutical lipids by ^{1}H NMR and comparison with the classical acid value. *JPBA*
http://dx.doi.org/10.1016/j.jpba.2013.04.010 -

Soler-Rivas C, Espín JC, Wichers HJ (2000)
Oleuropein and related compounds. *J Sci Food Agric* 80(7): 1013-1023

Steliopoulos P, Stickel E (2007)
Estimation of performance characteristics of a confirmation method for thyreostats in plasma by means of weighted least-squares approach. *Anal. Chim. Acta* 592(2): 181-186

Tur'yan YI, Berezin OY, Kuselman I, Shenhar A (1996)
PH-metric determination of acid values in vegetable oils without titration. *J Am Oil Chem Soc* 73(3): 295-301

van de Voort FR, Ismail AA, Sedman J, Dubois J, Nicodemo T (1994)
The determination of peroxide value by fourier transform infrared spectroscopy. *J Am Oil Chem Soc* 71(9): 921-926

Vissers MN, Zock PL, Katan MB (2004)
Bioavailability and antioxidant effects of olive oil phenols in humans: A review. *Eur J Clin Nutr* 58(6): 955-965

Wan PJ, Dowd MK, Thomas AE, Butler BH (2007)
Trimethylsilyl derivatization/gas chromatography as a method to determine the free fatty acid content of vegetable oils. *J Am Oil Chem Soc* 84(8): 701-708